COMPLEX ROLES OF MACROPHAGES IN LIPID METABOLISM AND METABOLIC DISEASE

A Dissertation Presented

By

Kimberly Anne Negrin

Submitted to the Faculty of the

University of Massachusetts Graduate School of Biomedical Sciences, Worcester

in partial fulfillment of the requirements for the degree of

DOCTOR OF PHILOSOPHY

(April 16, 2014)

PHD PROGRAM

Molecular Medicine

COMPLEX ROLES OF MACROPHAGES IN LIPID METABOLISM AND METABOLIC DISEASE

A Dissertation Presented
By
Kimberly A. Negrin

The signatures of the Dissertation Defense Committee signify completion and approval as to style and content of the Dissertation

_____

Michael P. Czech, Ph.D., Thesis Advisor

_____

Evelyn Kurt-Jones, Ph.D., Member of Committee

_____

Michael Brehm, Ph.D., Member of Committee

_____

Yong-Xu Wang, Ph.D., Member of Committee

_____

Steven E. Shoelson, M.D., Ph.D., Member of Committee

The signature of the Chair of the Committee signifies that the written dissertation meets the requirements of the Dissertation Committee

_____

Roger Davis, Ph.D., Chair of Committee

The signature of the Dean of the Graduate School of Biomedical Sciences signifies that the student has met all graduation requirements of the school.

_____

Anthony Carruthers, Ph.D.,

PhD Program

Acknowledgements

The most difficult task is to properly acknowledge all those who have encouraged and supported me throughout my studies. After all, I am a few years shy of turning thirty and have thus far spent all of my twenties studying. As a young woman with a thirst for growth and a zest for life, I hope to be fortunate enough to continue along my path of evolution. To do so, I must sincerely thank all who have been and continue to be active participants in my trials and tribulations as well as my triumphs and great successes.

First and foremost, I would like to express my deepest appreciation and thanks to my mentor, Michael Czech, for his scientific guidance and support in pursuing my interests during my PhD training. Michael is an extraordinarily inspiring mentor, professor and friend with the attitude and substance of a genius. He continuously showed a spirit of adventure in regards to my research and more times than not, I would leave his office ready to hit the ground running to tackle new endeavors. I am so very grateful for his generosity, patience, faith and most importantly his unwavering optimism that helped me through my difficult years of graduate school. His consistent emotional support and interest in not only my professional, but my personal growth and development has pushed me to succeed in all aspects of my life. Without his extraordinary mentorship, this dissertation would not have been possible.

I would also like to thank my ever-patient and encouraging dissertation committee. I would especially like to thank my committee chair, Roger Davis, for providing superb scientific advice, guidance and optimism during the course of my training. I sincerely thank Evelyn-Kurt Jones, Michael Brehm, and Yong-Xu Wang for

their encouragement, insightful comments and discussion as well as their excellent scientific and technical advice. Often times I found myself looking at a particular problem with a narrow perspective to only emerge from a TRAC meeting with a plethora of new ideas and approaches. Also, I would like to thank Stephen Shoelson for coming to UMASS Medical School for my defense and for providing his continuous mentorship, friendship and advice over the years, which have promoted both my personal and professional growth and development.

I would also like to thank past and present members of the Czech Laboratory for their help in the work presented herein and in their valuable insights during discussions. Rachel has been a great colleague, mentor and friend, and she has been instrumental in my successes achieved throughout my graduate career. In the midst of a long-time drought of negative data and failed experiments, it was always Rachel with her selfless time and care that kept me going when I had lost all perspective, confidence and belief in myself. I can't thank her enough for believing in me and providing her endless support and friendship. Myriam's reading of this dissertation and my manuscript, day-to-day advice regarding my various projects and encouragement during frustrating times was invaluable; I appreciate her mentorship and friendship throughout the years. Shinya kindly shared his expertise in flow cytometry and his friendship. Sarah provided a range of technical help throughout my graduate years as well as her friendship and support. Greg, Michaela, Adilson, Dave, and Tim have always provided advice, support and help with laboratory life. Joe, our one-of-a-kind lab manager, professor, mentor and friend gave his time to read and discuss my manuscript and dissertation, experiments and ideas.

I greatly appreciate his insight and time dedicated to enhancing the quality of my graduate work. I thank Marina, Anouch, Laura, Ozlem, Mengxi, Sophia, Joe and Jessica for their valued friendship, help and advice provided over the years in all of my crazy endeavors both in life and in the laboratory.

I would also like to thank my undergraduate mentor, Paul Birchkbichler. While a naïve undergraduate, Paul and his enthusiasm for Diabetes research sparked my love of science. His continuous commitment to my personal and professional growth is unparalleled and I am so sincerely thankful for each and every opportunity he presented me as an undergraduate research student. My success today is greatly reflective of his perseverance, commitment and optimism. I will be forever grateful for his mentorship and friendship.

Lastly, and most importantly, I would like to thank my family and friends for all of their love and encouragement. I struggle to find the words capable of expressing my sincerest appreciation and gratitude for the two most amazing influences that I am blessed to call my parents; Philip and Sherry Negrin. Thank you for raising me with unconditional love and support and for all of your guidance and encouragement in my many crazy pursuits. You are the driving force that has given me the confidence to follow my dreams and never settle for anything less than what I want and deserve. Without you, life just would not be what is today and I love you to the moon and back. I'd also like to thank my brother David and all of my aunts, uncles, and cousins who have always supported me from afar and given me endless love and support. My two best friends Carlee and Nikki for not only being the sisters I was never blessed with, but my

soul-mates. Thank you for sharing all of your laughter, hugs and smiles both near and far; I couldn't have done this without your unconditional love and support. Aldiana for her kind heart, words of wisdom and tough love and friendship that got me through some of my toughest moments; I can't thank you enough for all of your love and encouragement. And most of all, for my loving, supportive, encouraging, and patient boyfriend Jorge who kept a sense of humor when I had lost mine, encouraged me through every failed experiment and project and reminded me that I learned something from every negative experience. I certainly could not have done this without his endless supply of love, hugs, kisses and support.

In conclusion, I recognize that this research would not have been possible without the financial assistance of the Interdisciplinary Graduate Program and the Department of Molecular Medicine at the University of Massachusetts Medical School. These studies were supported by grants from the National Institutes of Health (DK085753, AI046629), a grant from the International Research Alliance at Novo Nordisk Foundation Center for Metabolic Research, a grant from the Juvenile Diabetes Research Foundation (17-2009-546), and by Core Facilities in the University of Massachusetts Diabetes and Endocrinology Research Center also funded by the National Institutes of Health (DK325220).

Abstract

The worldwide prevalence of obesity and metabolic disease is increasing at an exponential rate and current projections provide no indication of relief. This growing burden of obesity-related metabolic disorders, including type 2 diabetes mellitus (T2DM), highlights the importance of identifying how lifestyle choices, genetics and physiology play a role in metabolic disease and place obese individuals at a greater risk for obesity-related complications including insulin resistance (IR). This increased risk of IR, which is characterized by a decreased response to insulin in peripheral tissues including adipose tissue (AT) and liver, is associated with a chronic, low grade inflammatory state; however, the causative connections between obesity and inflammation remains in question. Experimental evidence suggests that adipocytes and macrophages can profoundly influence obesity-induced IR because adipocyte dysfunction leads to ectopic lipid deposition in peripheral insulin sensitive tissues, and obese AT is characterized by increased local inflammation and macrophage and other immune cell populations. Attempts to delineate the individual roles of macrophage-derived pro-inflammatory cytokines, like tumor necrosis factor alpha (TNF-α) and interleukin-1 beta (IL-1β), have demonstrated causative roles in impaired systemic insulin sensitivity, adipocyte function and hepatic glucose and lipid metabolism in obese animal models. Thus, the attenuation of macrophage-derived inflammation is an evolving area of interest to provide insight into the underlying mechanism(s) leading to obesity-induced IR.

Thus, in the first chapter of this thesis, I describe experiments to refine the current paradigm of obesity-induced AT inflammation by combining gene expression profiling

with computational analysis of two anatomically distinct AT depots, visceral adipose tissue (VAT) and subcutaneous adipose tissue (SAT) to address whether the inflammatory signature of AT is influenced by diet-induced obesity (DIO). Microarray and qRT-PCR analysis data revealed that DIO mouse SAT is resistant to high fat diet (HFD)-induced inflammation and macrophage infiltration, and our data support the current model of obesity-induced visceral adipose tissue macrophage (VATM) enrichment. Our data demonstrated robust increases in VAT pro-inflammatory cytokine expression, which are consistent with the significant increases in macrophage-specific gene expression and consistent with previous reports in which VAT inflammation is enhanced and attributed to classically activated (M1) macrophage infiltration. However, these data are only observed relative to the expression of invariant housekeeping gene expression. When M1-specific genes are expressed relative to macrophage-specific standards like F4/80 expression, these inflammatory makers are unchanged. These data indicate that the changes in the overall inflammatory profile of DIO mouse VAT is because of quantitative changes in adipose tissue macrophage (ATM) number and not qualitative changes in activation state. These observations are consistent with the idea that infiltrating ATMs may have roles other than the previously described role in mediating inflammation in obese adipose tissue

Hepatic IR occurs partly as a consequence of adipocyte dysfunction because the liver becomes a reservoir for AT-derived fatty acids (FAs), which leads to obesity-related non-alcoholic fatty liver disease (NAFLD). In the second part of my thesis, I used clodronate liposome-mediated macrophage depletion to define the role of macrophages in

hepatic lipid metabolism regulation. We discovered that i.p. administration of clodronate liposomes depletes Kupffer cells (KCs) in *ob/ob* mice without affecting VATM content, whereas clodronate liposomes depletes both KCs and VATMs in DIO mice. To this end, we established that clodronate liposome-mediated KC depletion, regardless of VATM content in obese mice, abrogated hepatic steatosis by reducing hepatic *de novo* lipogenic gene expression. The observed reductions in hepatic inflammation in macrophage-depleted obese mice led to the hypothesis that IL-1β may be responsible for obesity-induced increased hepatic triglyceride (TG) accumulation. We determined that IL-1β treatment increases fatty acid synthase (Fas) protein expression and TG accumulation in primary mouse hepatocytes. Pharmacological inhibition of interleukin-1 (IL-1) signaling by interleukin-1 receptor antagonist (IL-1Ra) administration recapitulated these results by reducing hepatic TG accumulation and lipogenic gene expression in DIO mice. Thus, these data highlight the importance of the inflammatory cytokine IL-1β in obesity-driven hepatic steatosis and suggests that liver inflammation controls hepatic lipogenesis in obesity.

To this end, the studies described herein provide new insight and appreciation to the multi-functional nature of macrophages and clinical implications for anti-inflammatory therapy in obesity and NAFLD treatment. We demonstrate the complexities of macrophage-mediated functions in insulin sensitive tissues and a role for obesity-induced inflammatory cytokine IL-1β in hepatic lipid metabolism modulation, which is reversed via IL-1Ra intervention. The use of anti-inflammatory therapy to ameliorate obesity-associated NAFLD was perhaps the most important contribution to

this body of work and is full of promise for future clinical application. It is likely that the future of therapeutics will be multi-faceted and combine therapeutic approaches to enhance glucose tolerance and overall health in obese, IR and T2DM patients.

Table of Contents

List of Tables

Chapter III

List of Figures

Chapter I

Chapter II

Chapter III

List of Frequently Used Abbreviations

AKT/PKB	Serine/threonine protein kinase B
Acc	Acetyl CoA carboxylase ½
Acyl	ATP citrate lyase
AT	Adipose tissue
ATM	Adipose tissue macrophage
Atgl	Adipose triglyceride lipase
BAT	Brown adipose tissue
BMI	Body mass index
ChREBP	Carbohydrate response element binding protein
Cidea	Cell death-inducing DFFA-like effector a
CCL4	Chemokine (C-C motif) ligand 4
CRP	C-reactive protein
CLS	Crown-like Structure
CVD	Cardiovascular disease
Dag	Diacylglycerol
Dgat	Diacylglycerol acyltransferase
DIO	Diet-induced obesity
DNL	De novo lipogenesis
DTR	Diphtheria toxin receptor
Elovl6	ELOVL family member fatty acid elongase 6
ER	Endoplasmic reticulum
EE	Energy expenditure
ERK	Extracellular signal regulated kinase 1 and 2
FA	Fatty acid

Fasn/Fas	Fatty acid synthase gene/protein
FACs	Fluorescence activated cell sorting
FBG	Fasting blood glucose
FFA	Free fatty acid
Foxo	Forkhead box O-class family
GeRP	Glucan encapsulated siRNA particle
G6P	Glucose-6-phosphate
G6Pase	Glucose-6-phosphatase
GLUT2	Glucose transporter 2
GLUT4	Glucose transporter 4
G3K3	Glycogen synthase kinase 3
GTT	Glucose Tolerance Test
GRB2	Growth factor receptor bound protein 2
GK	Glucokinase
GS	Glycogen synthase
HFD	High fat diet
HSL	Hormone sensitive lipase
IKKβ	Inhibitor of kappa B kinase β
T_H	Innate helper type cell
IL-1β	Interleukin-1 beta
IL-1α	Interleukin-1 alpha
IL-1Ra	Interleukin-1 receptor antagonist
IL-10	Interleukin-10
IL-6	Interleukin-6
IPGTT	Intraperitoneal Glucose Tolerance Test

IRS-1	Insulin receptor substrate 1
IR	Insulin resistance/resistant
IS	Insulin sensitivity/sensitive
IFNγ	Interferon gamma
iNKT	Invariant natural killer T cells
JNK	c-Jun n-terminal activated kinases 1/2
KC	Kupffer cell
KO	Knockout
LD	Lipid droplet
LPL	Lipoprotein lipase
M1	Pro-inflammatory macrophage
M2	Alternatively activated macrophage
MACE	Microarray computational environment
MAPK	Mitogen activated protein kinase
MCP-1/CCL2	Macrophage chemoattractant protein 1
MS	Metabolic Syndrome
NAFLD	Non-alcoholic fatty liver disease
NASH	Non-alcoholic steatohepatitis
ND	Normal diet
NF-κB	Nuclear factor kappa B
Pepck	Phosphoenolpyruvate carboxylase
PPARγ	Peroxisome proliferator activated receptor gamma
PGC-1α	Peroxisome proliferator activated receptor gamma co-activator 1-α
PI3K	Phosphatidylinositol 3-kinase
PKCΘ	Protein kinase C theta

PK	Pyruvate kinase
T_{reg}	Regulatory T-cell
RER	Respiratory exchange ratio
RMA	Robust multi-array average
SAT	Subcutaneous adipose tissue
Scd-1	Stearoyl-CoA Desaturase 1
Srebp-1C	Sterol regulatory element binding protein 1c
SVC	Stromal vascular cell
SVF	Stromal vascular fraction
T1DM	Type 1 diabetes mellitus
T2DM	Type 2 diabetes mellitus
TG	Triglyceride
TLR	Toll like receptor
TNF-α	Tumor necrosis factor alpha
TNFR	Tumor necrosis factor receptor
TZD	Thiazolidinedione
UCP-1	Uncoupling protein-1
WAT	White adipose tissue
WHO	World Health Organization
WT	Wild-type (C57bl6/J)
VAT	Visceral adipose tissue
VATM	Visceral adipose tissue macrophage
VLDL	Very low density lipoprotein

Preface

The work presented in this thesis was done in collaboration with the following individuals:

CHAPTER II

Chapter two was performed in conjunction with Timothy Fitzgibbons, M.D., Ph.D. Tim provided the mice for microarray analysis and performed experiments for Figures 2.1-2.5. The histology in Figure 2.3 was performed by the DERC Morphology Core and the microarray chips were scanned by the Genomics Core of the Diabetes and Endocrine Research Center (DK-32520). Juerg Straubhaar uploaded the microarray data to MACE and performed detailed statistical analyses.

CHAPTER III

Rachel Roth Flach assisted in the experimental design and completion, data analysis and revised the manuscript for publication. Marina T. DiStefano and Anouch Matevossian assisted in the mouse tissue and/or primary cell isolations. The DERC Morphology Core assisted in the liver immunohistochemical staining. DaeYoung Jung, Randall Friedline and Jason K. Kim performed Metabolic Cage and data analysis at the Mouse Metabolic Phenotyping Core of the University of Massachusetts Medical School.

Copyright Information

Chapter I: Introduction

1.1. Obesity and Diabetes

Obesity has become a global epidemic that threatens to overwhelm both industrialized and developing countries. According to the World Health Organization (WHO), greater than 1 billion adults are overweight and more than 300 million are obese worldwide (214). Recent projections anticipate that 86.3% of all American adults will become overweight or obese by the year 2030 (249). This growing burden of obesity and its co-morbidities will overwhelm our nation's health care expenditure, with projections upwards of 900 billion dollars in the year 2030, which accounts for 15-20% of the total health care costs (249). This expenditure is related to the imposing cost of treatment of obesity and co-morbidities, coined the metabolic syndrome (MS). MS most commonly consists of four pathogenic states: T2DM, cardiovascular disease (CVD), dyslipidemia and hypertension (77, 175, 214, 243). The growing body of evidence clustering these pathologies together suggests obesity as a common pathogenic link that acts as both a principal and causative component of the MS (246). It is also important to highlight the intimate association of obesity with IR, which is characterized by a decreased response to insulin in peripheral tissues including AT, liver and muscle. Interestingly, not all obese individuals are IR, which is a long-time conundrum in metabolic disease research (82). Thus, to control the rise in T2DM, we must first understand its causes at the molecular level, highlighting the importance of identifying how environmental factors, lifestyle choices, genetics and physiology play a role in metabolic disease and place obese individuals at a greater risk for obesity-related complications including IR.

The ever growing fast-food industry and a reduced need for physical labor in Westernized countries has given rise to obesity, partially because of increased accessibility to more energy-dense, nutrient poor food. The Western diet is primarily composed of calorically dense food with a relatively high carbohydrate and saturated fat content. This diet combined with a sedentary lifestyle creates an imbalance between energy intake and energy expenditure (EE), thus leading to increased adiposity. Excess energy from increased food consumption is stored within AT, which is an essential and metabolically active endocrine organ that can store and release energy to coordinate important biological processes (discussed in section 1.6.).

The postprandial state is a significant contributing factor to the MS and diabetic complications. Upon carbohydrate load, blood glucose levels rise and pancreatic β-cells release copious amounts of insulin into circulation to reduce blood glucose levels. This function of insulin is mediated primarily on 3 major insulin target tissues: liver, muscle and AT. In muscle and AT, insulin promotes the facilitated uptake of glucose and its conversion to glycogen and TGs for storage. However, in the liver, the function of insulin is to suppress hepatic glucose production by inhibiting select pathways that control glycogenolysis and gluconeogenesis while stimulating glucose storage as hepatic glycogen. The failure of insulin to elicit a response on these peripheral and vital target tissues results in the disruption of stable blood glucose levels, leading to IR and ultimately T2DM. These and other topics will be discussed in the sections below.

1.2. The Discovery of Insulin

One of the greatest biomedical advances of the twentieth century was the discovery of insulin in 1921 (32). The discovery of insulin has revolutionized our ability to maintain glucose homeostasis in Type 1 diabetics (T1DM) and has driven molecular investigations into the insulin signaling pathway, which has led to the development of therapeutics to prevent and treat T2DM. The molecular mechanisms and processes that are responsible for insulin action as well as its resistance in different organ systems have been investigated at both the molecular and physiological level. These molecular processes provide a foundation for the data herein and will be described in detail below.

Insulin is a small peptide hormone produced and secreted by pancreatic β-cells that is best known for its function to regulate blood glucose concentrations by signaling to its target tissues: muscle, liver and AT. Insulin suppresses hepatic glucose production (gluconeogenesis) and promotes glycogen synthesis (glycogenesis) and storage in both liver and muscle. These glucose metabolism and homeostasis pathways are described in section 1.4. Insulin also mediates TG synthesis and storage in the liver and AT while promoting amino acid storage in muscle (257). Therefore, in healthy individuals, the ability of insulin to balance glucose influx and output to and from the circulation by stimulating glucose uptake, utilization, and liberation for biological processes is essential.

Diabetes, commonly associated with obesity, is a disruption in the ability of insulin to reduce blood glucose concentrations and is clinically defined by the WHO as a fasting blood glucose levels >126 mg/dL. Although diabetes pathophysiology is diverse, it presents primarily as T1DM and T2DM, which both share insulin action as a common

denominator. T1DM is caused by an auto-immune-mediated destruction of insulin-producing pancreatic β-cells, which subsequently causes absolute insulin deficiency (257). Thus, T1DM patients are characterized by high blood glucose levels and are dependent on supplemental insulin to reach normoglycemia. In the setting of IR and T2DM, individuals are characteristically hyperinsulinemic, as insulin production and secretion by pancreatic β-cells fails to compensate for peripheral IR that typically occurs due to excess body weight. Thus, at least in its early stages, T2DM is characterized not by insulin deficiency, but by the failure of insulin to act efficiently upon target tissues. However, a long-time conundrum in the field of T2DM and IR is whether hyperinsulinemia precedes IR or vice versa. Transgenic mice that overexpress the human insulin gene developed IR subsequent to hyperinsulinemia, supporting the hypothesis that hyperinsulinemia might be a primary event leading to increased hepatic lipogenesis (described in section 1.7.2.) and the secondary development of IR (143, 151).

While innovative treatments for insulin management in T1DM patients are available, the only true treatment to restore physiological glucose metabolism is by pancreatic β-cell or isolated pancreatic islet transplantation (184). However, T2DM patients may require one or more anti-diabetic drugs such as Thiazolidinedione (TZDs) or exogenous insulin, and these patients can often reverse IR with these treatments and healthy lifestyle intervention. Thus, our understanding of the complexities of insulin signaling are critical, and enhancing this knowledge will significantly limit the expansion of the current obesity epidemic and the consequent rise in T2DM.

1.3. Insulin Signaling

For insulin action to occur, insulin must bind to the insulin receptor, which is a tyrosine kinase that undergoes a conformational change and autophosphorylation at multiple tyrosine residues upon stimulation (10, 127, 182). Autophosphorylation increases the catalytic activity of the receptor, and the phosphorylated tyrosines recruit scaffolding proteins including a protein family known as insulin receptor substrates or IRS proteins (231, 257). Docking of IRS proteins allows for their tyrosine phosphorylation by the insulin receptor and the subsequent formation of binding sites for Src-homology-2 (SH2) domain-containing proteins, which serves as a complex binding platform to initiate downstream signaling (256). These scaffolding proteins are required for a complete insulin signal and serve as a docking platform for the SH2 domain-containing regulatory subunits of phosphatidylinositol 3-kinase (PI3K) and the growth factor receptor bound protein 2 (GRB2) (256-257). These two adaptor molecules regulate the two main conduits of insulin action: PI3K and serine/threonine protein kinase B (AKT/PKB) and GRB2 and the mitogen activated protein kinases (MAPKs) (231, 256). The PI3K/AKT pathway regulates the metabolic actions of insulin including glucose utilization, production and uptake, while MAPKs coordinate with PI3K to regulate cell growth, gene expression and differentiation (231). The effects of these pathways are summarized below and in Figure 1.1.

PI3K plays an important role in the regulation of glucose and lipid metabolism and the metabolic actions of insulin by mediating the phosphorylation of many substrates including glycogen synthase kinase 3 β (GSK3β), the Rab GTPase activating protein

(GAP) with a molecular weight of 160 kDal (AS160), and phosphodiesterase 3B (PDE3B) which are important for regulating glycogen synthesis, glucose uptake and lipid storage, respectively (203, 257). PI3K via AKT activation also regulates the Forkhead box O-class (FOXO) family of transcription factors that requires phosphorylation and translocation to and from the nucleus to either activate transcription of target genes within the nucleus or inhibit gluconeogenesis and adipocyte differentiation when excluded from the nucleus (154, 190). Insulin also activates extracellular-signal regulated kinases (ERKs) via the GRB2 arm of insulin action which are involved in mitogenesis (203). Importantly, insulin also promotes lipid storage and inhibits AT lipolysis by promoting fatty acid re-esterification and TG synthesis as well as inhibiting fatty acid transport. These mechanisms of insulin-mediated lipid metabolism are relevant to Chapter 3 and will be described in detail in sections 1.5.1. and 1.7.2. in regards to AT and hepatic lipid metabolism, respectively (203).

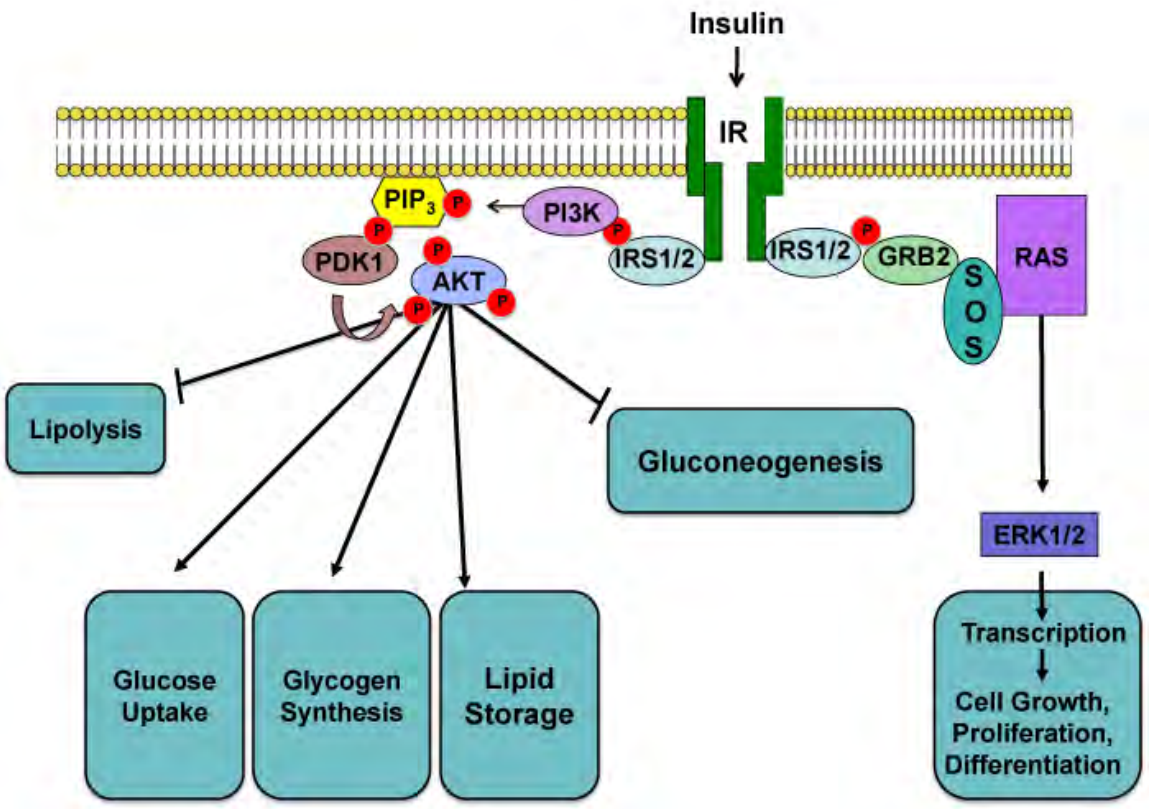

Figure 1.1 Nodes of insulin signaling. The metabolic pathways regulated by insulin action require insulin binding to the insulin receptor (IR) which activates its receptor tyrosine kinase activity and stimulates insulin receptor substrate adaptor protein 1 (IRS1/2) tyrosine phosphorylation. Tyrosine phosphorylated IRS1 serves as a docking substrate for phosphatidylinositol 3-kinase (PI3K) and growth factor receptor bound protein 2 (GRB2) to activate the protein kinase B (AKT) and extracellular-signal regulated kinase (ERK1/2) branches of insulin-mediated metabolic signaling. AKT and ERK activation regulates the processes indicated in the diagram. Some of these processes are cell type specific such as the stimulation of glycogen synthesis in muscle, TG synthesis in AT, glucose uptake in AT and muscle and the inhibition of hepatic gluconeogenesis.

1.4. Regulation of Glucose Homeostasis

A primary survival mechanism of mammals is maintaining blood glucose concentration homeostasis because glucose is utilized as a primary fuel source for all eukaryotic cells and is required to generate energy for physiological functions. Blood glucose concentrations must be tightly controlled by balancing the rate of glucose entry and removal from the circulation (119). The distribution of circulating glucose is complex and requires various tissues to uptake, process and store glucose to ensure adequate glycogen pools when energy is in demand. These processes are under strict hormonal control by the glucoregulatory hormones glucagon and insulin, which are hormones derived from pancreatic α- and β-cells, respectively (illustrated in Figure 1.2). These hormones have opposing functions as glucagon is a potent stimulator of hepatic glucose production whereas insulin both inhibits glucose production and facilitates glucose uptake into skeletal muscle and AT by stimulating the translocation of glucose transporter 4 (GLUT4), a transport protein that shuttles glucose across the cell surface, thus reducing plasma glucose concentrations (17, 97, 171). Other pancreatic and incretin hormones from the gut including amylin, glucagon-like peptide 1 (GLP-1) and other glucocorticoids also regulate circulating glucose concentrations (246).

In normal physiology, circulating glucose comes from intestinal food absorption and hepatic glycogenolysis and gluconeogenesis. After feeding, the most readily available circulating glucose is derived from intestinal absorption and is utilized by peripheral tissues such as skeletal muscle, brain, red blood cells and AT (171). The major cellular mechanism to remove exogenous circulating glucose is insulin-stimulated

glucose transport into skeletal muscle via GLUT4, where it can be stored as glycogen, a polymerized storage form of glucose, or oxidized to produce energy immediately upon transport into the muscle (97, 193). Insulin-stimulated glucose transport into AT via GLUT4 also occurs upon glucose load, although to a much lesser degree than skeletal muscle. However, downregulation of GLUT4 expression in obese mouse AT as well as humans has a profound impact on glucose homeostasis and IS (68, 104). Excess glucose is also transported through the portal vein into the liver by non-insulin-dependent glucose uptake via glucose transporter 2 (GLUT2). This uptake can initiate a number of processes including glycogenesis, which is the process of glycogen synthesis (171). Other sources of circulating glucose come from hepatic processes, which maintain blood glucose levels during periods of prolonged fasting and are stimulated by glucagon. During the first 8-12 hours of a fast, glucose is primarily produced by glycogenolysis, or the breakdown of glycogen to release glucose (119). During periods of prolonged fasting, the liver produces glucose via gluconeogenesis, which is the metabolic process by which the liver synthesizes glucose *de novo* from non-carbohydrate sources such as pyruvate, lactate, glycerol, and amino acids (119, 171).

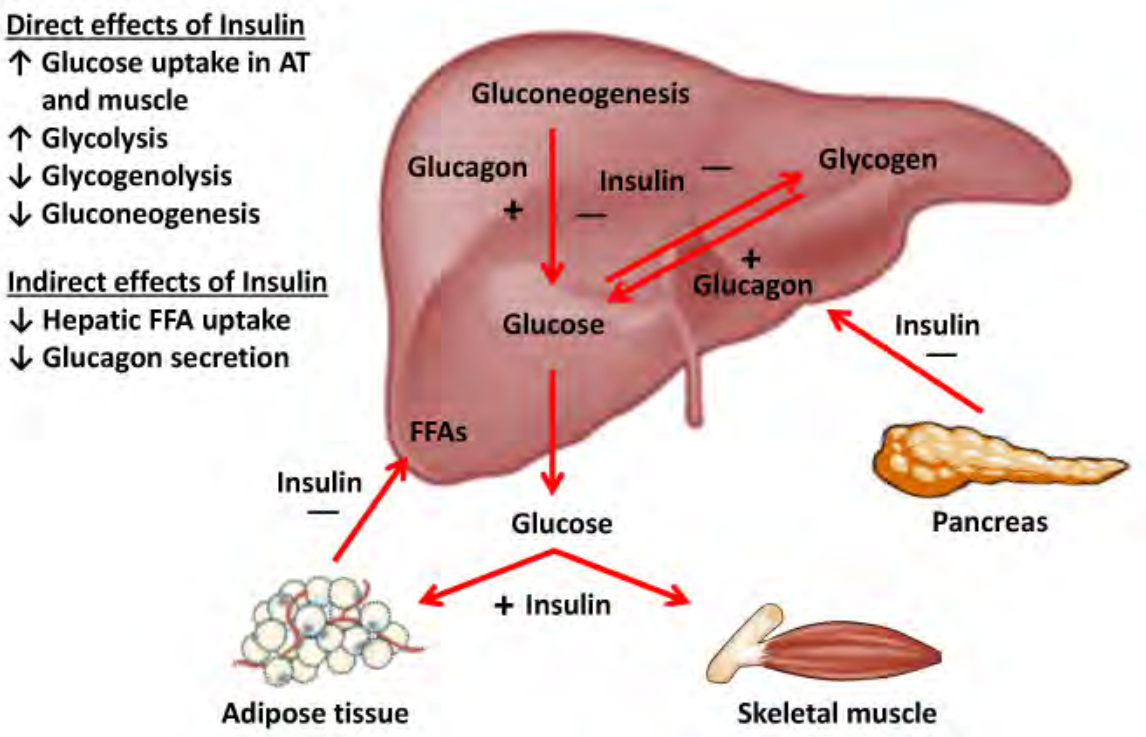

Figure 1.2. Insulin suppresses hepatic glucose production by direct and indirect mechanisms. Hepatic glucose metabolism is under strict hormonal control by the glucoregulatory hormones glucagon and insulin. These hormones have opposing functions as glucagon is a potent stimulator of hepatic glucose production (HGP), whereas insulin both inhibits HGP and facilitates glucose uptake into skeletal muscle and AT. Insulin stimulates glycolysis and represses gluconeogenesis and glycogenolysis pathways where as glucagon is a potent stimulator of gluconeogenesis and glycogenolysis in fasted conditions. In IR, insulin has impaired ability to suppress AT lipolysis and glucagon secretion by pancreatic α-cells causing increased gluconeogenesis. Insulin inhibition of glycogenolysis is also impaired. Thus, both hepatic and peripheral IR results in abnormal glucose production by the liver.

The inhibition of *de novo* glucose synthesis in the fed state is critical to avoid a circulatory glucose overload. The insulin-mediated inhibition of the hepatic glucose production and release is accomplished by blocking gluconeogenesis and glycogenolysis pathways. Insulin directly regulates the expression of genes encoding hepatic enzymes required for gluconeogenesis and glycolysis, which is the energy releasing process of converting glucose to ATP and pyruvic acid. Insulin accomplishes this inhibition by post-translational modifications to the enzymes, thus controlling their activity (183, 202). Insulin also inhibits the transcription of the gene encoding phosphoenolpyruvate carboxylase (PEPCK), the enzyme required for the rate limiting step in gluconeogenesis, as well as other enzymes fructose-1,6-bisphosphatase ($F6P^2$) and glucose-6-phosphatase (G6Pase) by the liver (228). Insulin also upregulates the transcription of the genes that are necessary for glycolysis including glucokinase (GK) and pyruvate kinase (PK) (202).

Insulin mediates its regulation of lipid metabolism mainly via the promotion of lipid storage within adipocyte lipid droplets (LDs) and lipolysis inhibition. However, actions of insulin must be coordinated in both AT and liver to enhance the synthesis of TGs, which are the primary source and storage form of lipid in humans that allow energy to be stored until times of caloric or energy demand (33). It is within the adipocyte LD that TGs are stored in healthy individuals; however, this storage capability is upregulated in DIO mice and humans. Although AT has the capability to expand to store excess nutrients within LDs without molecular repercussions, excessive nutrient overload subsequently leads to dysregulation of the lipolysis-lipogenesis balance in adipocytes, thus increasing ectopic lipid stores in the liver and other peripheral tissues (33, 207). In

the liver, hepatocytes are a major site of *de novo* lipogenesis (DNL) or FA synthesis as well as the overall lipogenesis pathway involving FA esterification with glycerol 3-phosphate (G3P) to form triacylglycerol, or TGs (discussed in section 1.7.2.) (33, 35). Studies using non-metabolizeable glucose analogues in hepatocytes, adipocytes, and even pancreatic β-cell lines have provided evidence that glucose must be actively metabolized to affect the transcription of genes involved in these glucose-responsive pathways, including lipogenesis (69).

Major impact was made in T2DM therapeutics with the discovery of novel anti-diabetic drugs that improve systemic IS by reducing circulating blood glucose concentrations. One such class of drugs is the TZDs, including rosiglitazone and pioglitazone, which function to enhance glucose disposal in skeletal muscle as well as insulin-mediated hepatic gluconeogenesis inhibition (192, 209). Thus, TZDs successfully improve glycemic control via insulin sensitization in humans undergoing treatment. These drugs target the peroxisome proliferator-activated receptor (PPAR) family of nuclear receptors, specifically the PPARγ isoform, which is most highly expressed in adipocytes. PPARγ is the master regulator of adipogenesis, or the development of fat cells from preadipocytes otherwise known as adipocyte differentiation. Importantly, PPARγ is intimately involved in energy homeostasis and is required to regulate essential glucoregulatory and lipogenic genes (GK, GLUT4, lipoprotein lipase (LPL), adipocyte fatty acid transporter protein, and fatty acid synthase (Fasn)), supporting the increased IS in TZD-treated T2DM humans and mice (156, 209). However, because these drugs promote adipogenesis, a side effect of treatment is weight gain from increased AT mass,

fluid retention and edema, which is a possible complication with obese patients that are also suffering from CVD (209). Other therapeutic options are the use of high doses of salicylates or aspirin, or non-steroidal anti-inflammatory drugs (NSAIDs), which have been used in obese IR rodents such as the Zucker *fa/fa* rat or the *ob/ob* leptin-deficient mouse (described in section 1.5.2.) (266). These drugs reduce fasting blood glucose with significant improvements in glucose tolerance and insulin signaling (266). Salsalate, an NSAID in the class of salicylates, lowers fasting blood glucose in humans with impaired glucose tolerance (71). The mechanism whereby salsalate mediates its metabolic effects on IS remains elusive, although it is likely due to alterations in hepatic IS by regulating glucose production or insulin clearance and it's affects on NFkB activity (discussed in section 1.10.2.) (71).

1.5. The Role of Adipose Tissue

In humans and rodents, there are two distinct types of AT: brown adipose tissue (BAT) and white adipose tissue (WAT). BAT is a thermogenic organ that is comprised of many mitochondria and functions to maintain thermal homeostasis by oxidizing FAs to generate heat (244). BAT has significant control over the body's total energy expenditure (EE) and metabolic rate, and expressing uncoupling protein-1 (UCP-1). UCP-1 uncouples proton pumping and ATP production from oxidative phosphorylation by creating a proton leak to produce heat by the process of nonshivering thermogenesis (72-73). Thus, dysfunctional BAT can profoundly impact metabolism and play a role in obesity and the MS by reducing EE. WAT, a considerable focus of this thesis and will herein be referred to as AT, functions as the primary reservoir of the human body for energy and plays a central role in the development of IR in obesity.

AT is highly responsive to insulin and exerts profound control over whole body glucose metabolism (77, 214). The ability to sequester FAs from circulation and synthesize TGs *de novo* from glucose is a significant contribution of adipocytes within AT to maintaining metabolic homeostasis. The significance of AT plasticity and storage capability is reinforced by the observation that a lack of normal and functioning AT, a medical condition known as lipodystrophy, increases circulating TGs and free fatty acid (FFA) concentrations, which are both causal for IR in mice and humans (discussed in section 1.10.2.) (77, 88, 150). Considering that both obese and lipodystrophic humans and mice both exhibit severe IR and dyslipidemia, it is a lucid fact that excess fat

contributes to the pathology of the MS and that normal AT is required for the maintenance of systemic glucose and lipid homeostasis.

1.5.1. Lipid Metabolism in AT

AT functions as a lipid sink to buffer energy imbalances by storing energy in the form of TGs, which are highly concentrated neutral lipids that are comprised of a glycerol backbone and 3 FA moieties, in times of excess energy intake. TGs are stored within adipocyte LDs, which are a single intracellular, hydrophobic organelle. Contained within this dynamic structure are the building blocks for membranes and substrates for energy metabolism, and they thus serve as a reservoir of energy stores for times of caloric need (74, 247). LDs associate with unique protein complexes that enable lipid synthesis into TGs via lipogenesis, which requires multiple mechanisms including fatty acid uptake, *de novo* FA synthesis and esterification into TGs (33, 201). Although a fraction of whole-body TG synthesis is observed in AT, the process of lipogenesis is primarily executed in the liver during very low-density lipoprotein (VLDL) production (discussed in section 1.7.2.). However, FA mobilization via breakdown of these TGs that are stored within the LD is a process unique to adipocytes and is known as lipolysis (201). One hypothesis in obesity, is dysregulation of the lipogenesis-lipolysis balance in AT stemming from AT expansion and the subsequent immune cell infiltration and cytokine production and secretion results in the observed metabolic and cardiovascular complications (discussed in section 1.6.) (201).

Excess FAs and other circulating lipids are a driving force for inflammation and are toxic to cells, however, lipolysis-mediated FA mobilization when glucose is limited is important to deliver energy to peripheral tissues (14, 197). Adipocytes liberate FAs by activating adipose triglyceride lipase (ATGL), hormone-sensitive lipase (HSL) and monoglyceride lipase (MGL) within adipocytes in a stepwise fashion to sequentially hydrolyze TGs into diacylglycerol (DAG), monoacylglycerol, and glycerol, releasing a FA moiety at each step (116). HSL and ATGL are key enzymes that are required for normal AT function, which has been verified by knockout (KO) mouse studies. HSL KO mice have reduced AT mass, and these mice as well as ATGL KO mice both have a decreased lipolytic response to catecholamines *in vivo* and *in vitro* (78-79, 248). Classically, the canonical pathway to activate lipolysis is the interaction of catecholamines with β-adrenergic receptors on adipocytes, which activates adenylate cyclase to increase cellular cAMP levels and ultimately stimulate lipolytic FA breakdown (270). Alternatively, lipolysis can be activated by the ERK signaling cascade, natiuretic peptide, growth hormone, and in the context of obesity and IR, cytokine signaling plays an important role in FA mobilization (described in section 1.10.1.) (24, 270).

1.5.2. Adipokine and Cytokine Secretion

Functional AT is necessary for the synthesis and secretion of endocrine hormones called adipokines, such as leptin and adiponectin, which enhance IS and display impaired expression in lipodystrophic humans and mice (88, 110). Leptin is a hormone that is secreted by adipocytes and acts in the brain to decrease food intake and promote EE (120,

147). Leptin stimulates FA oxidation and prevents lipid accumulation in non-adipose tissues, including muscle, liver and pancreas (146-147). The role of leptin in energy homeostasis is demonstrated by the extreme obesity and hyperphagia (over-eating) of the *ob/ob* mouse, which lacks leptin (269). The *db/db* mouse has a mutation within the leptin receptor resulting in an absence of activity and has an obese phenotype with hyperphagia, similar to the *ob/ob* mouse (126). The key site of leptin action in regulating energy balance is the central nervous system (CNS) via regulation of Janus kinase (JAK)-signal transducers and activators of transcription (STAT) intracellular signaling pathway by STAT3 phosphorylation (120). The positive correlation of increased adiposity and elevated leptin suggests that obesity not only to leads to IR, but also leptin resistance (152). Another adipokine that is exclusively secreted from AT is adiponectin, which functions to regulate whole body IS and circulating levels are decreased in both obese and IR humans and mice (95-96). Adiponectin KO mice present with reduced hepatic IS (156). Interestingly, transgenic mice overexpressing adiponectin on the *ob/ob* background results in increased IS despite massive obesity, which may be explained by increased adipogenesis and enhanced ability to expand subcutaneous AT (SAT) by redistributing TG deposition from hepatocytes and muscle cells to adipocytes as well as increased expression of PPARγ target genes in AT (113).

In obesity and IR, AT is also a potent source of pro-inflammatory cytokines such as tumor necrosis factor-α (TNF-α), interleukin-1β (IL-1β) and monocyte chemoattractant protein 1 (MCP-1), all of which are upregulated in obese humans and mice (41, 108, 237). These cytokines contribute to increased immune cell trafficking and AT infiltration

and are hypothesized to be causal to the adipocyte dysfunction observed in obesity (24, 41). TNF-α, IL-1β and other important cytokines will be discussed further in section 1.10.1., but the role of MCP-1 in AT is quite paradoxical. With increasing obesity and adipocyte enlargement (hypertrophy), MCP-1 expression and secretion in AT is increased (204). As a potent chemoattractant, MCP-1 secretion increases macrophage infiltration into AT, thus contributing to the chronic state of low-grade inflammation in obesity. In agreement with this, studies from our laboratory demonstrate MCP-1 treatment of *ob/ob* mouse VAT explants induces macrophage cell division and decreases in ATM proliferation within the VAT of MCP-1 KO mice, independently of monocyte recruitment (1). Surprisingly, other studies report that MCP-1 KO mice are IR when fed a high fat diet (HFD), and adoptive transfer experiments with MCP-1 KO monocytes reveal insignificant reductions in immune cell trafficking (100, 170). However, mice deficient in the receptor for MCP-1, the C-C motif chemokine receptor-2 (CCR2) show significant improvements in AT inflammation, glucose homeostasis and IS, suggesting it is the receptor that is responsible for the inflammatory phenotype and that other factors impact immune cell trafficking into obese AT (166, 251). Together, these observations provide evidence that functional AT is necessary and required to maintain normal IS and glucose homeostasis.

1.5.3. AT distribution

AT contains adipocytes as well as the stromal vascular fraction (SVF), which is comprised of immune cells, endothelial cells, fibroblasts, preadipocytes and other non-

adipocyte cells. Although cross-talk among these cells facilitates the function of AT, the anatomical location of AT depots plays an important role in whole-body metabolism. It is well known that AT distribution is essential to regulating the metabolic state of humans and rodents. In human obesity, body type and specific differences in fat distribution reveal differential inflammatory profiles. Visceral AT (VAT) is associated with more adverse risk factors than SAT for the MS because its anatomical location within the peritoneal cavity allows for the release of adipokines, FFAs, cytokines, and other endocrine hormones directly into the portal vein, which affects hepatic metabolic functions and ultimately systemic IS (61). Unlike the VAT depot, evidence from both human and animal studies has suggested a protective role for SAT. In humans, increased subcutaneous fat in the lower extremities is associated with a decreased risk of disturbed glucose metabolism and dyslipidemia independent of VAT expansion (218). In both humans and rodents, TZD treatment increases total fat mass, mostly in subcutaneous fat stores, resulting in significant improvements in IS (149). SAT transplantation into visceral compartments in mice reduces body weight and total fat mass and improves glucose metabolism, suggesting that SAT may be intrinsically different from VAT in beneficial ways (235).

1.6. Adipose Tissue Expandability Theory and Insulin Resistance

Although AT functions primarily as a storage depot, the expandability hypothesis states that AT has a defined expansion limit (243). AT can expand by hyperplasia (increased cell number), but it is adipocyte hypertrophy that protects other tissues from circulating lipids and is key to maintaining IS. As described above, the hormonal regulation of the lipolytic-lipogenic balance in AT is pertinent to IS. Thus, the uptake of substrates for storage coupled with the timed release of FAs to non-adipose organs for oxidization as an energy source must be tightly controlled to avoid the molecular repercussions caused by dysregulated expansion (77). The effects of nutrient overload on AT expansion and systemic IS are described below and are illustrated in Figure 1.3.

In lean, healthy individuals, insulin-stimulated glucose uptake is normal and AT can expand to buffer excess nutrients. However, in a state of over nutrition and dietary excess, the AT is under high metabolic stress and once the cell 'expansion limit' is exceeded, hypertrophic adipocytes "spillover" releasing copious amounts of FFAs into the circulation. This rise in circulating FFAs and subsequent ectopic lipid deposition within IS and insulin-producing tissues in the periphery leads to a systemic disruption of glucose metabolism and cardiac function (77, 207). This phenomenon, known as lipotoxicity, adversely affects non-adipose tissues leading to cellular dysfunction and apoptosis (207). The lipotoxic hypothesis, first proposed by Robert Unger in 1995, illustrates that in obesity-dependent T2DM, the IR of peripheral tissues and glucose incompetence of β-cells are both caused by an increase in FFA delivery to both insulin target tissues and the islets of Langerhans within the pancreas (236). This theory

parallels the expandability theory of AT in that they both present causal evidence for ectopic FA deposition being responsible for the IR observed in obesity (243). Lipid deposition in the pancreas and islet TG accumulation results in dysregulated insulin secretion, pancreatic inflammation and β-cell apoptosis (207, 212). Although skeletal muscle and heart are tissues with high FFA turnover and metabolism, excess intramyocellular accumulation of FAs and their metabolites disrupt insulin receptor tyrosine phosphorylation and prevent insulin-stimulated GLUT4 translocation to the plasma membrane (75, 207). In the liver, lipids accumulate within hepatocytes, which impairs FA β-oxidation and the ability of insulin to suppress hepatic gluconeogenesis, thus increasing circulating glucose concentrations (171). Hepatic TG and FFA accumulation also leads to NAFLD and progression to non-alcoholic steatohepatisis (NASH), which is characterized by the increased inflammatory response of lipid-laden resident liver macrophages (KCs) and hepatocyte cell death (described in section 1.7.3.) (129). Thus, the adverse effects of ectopic lipids in non-adipose tissues and the pathogenesis of IR is partially attributed to dysregulated adipocyte metabolism and lipotoxicity in IS/producing tissues.

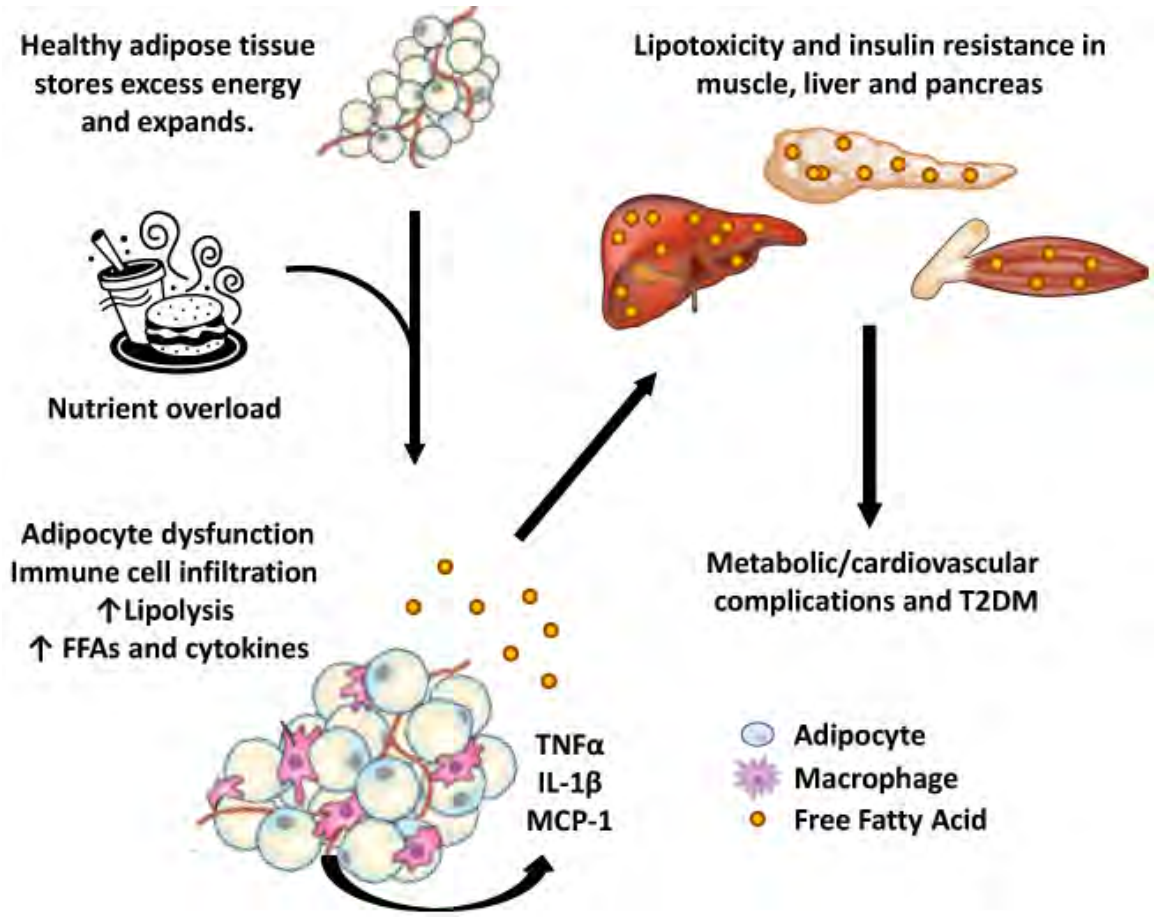

Figure 1.3. Nutrient overload leads to inflammation and insulin resistance in adipose and peripheral tissues. In the lean state, healthy AT efficiently stores excess energy as TG and expands with properly regulated insulin-stimulated glucose uptake. In a state of dietary excess, the AT is under high metabolic stress and the adipocyte expansion limit is reached whereby TG storage is dysregulated. Resident and recruited macrophages and other immune cells are activated and hypertrophic adipocytes release copious amounts of inflammatory cytokines and FFAs into the circulation causing ectopic lipid deposition in insulin sensitive/producing tissues muscle, liver and pancreas. This lipotoxicity causes pancreatic β-cell failure and IR in insulin sensitive tissues in the periphery. The increasing glucose, inflammatory cytokine and FA levels in the circulation causes the metabolic and cardiovascular complications associated with obesity and ultimately T2DM.

1.7. The Role of the Liver

As the main detoxifying organ of the body, the liver also plays a unique role in metabolic homeostasis by controlling both systemic carbohydrate and lipid metabolism. The liver is the major site for uptake, synthesis, storage, secretion, and catabolism of FAs and TGs, and other important functions including glycogen storage, plasma protein synthesis and hormone production. These pathways are controlled through the coordinated actions of hormones circulating from the portal vein to the liver where they can bind their respective receptors located on the plasma membrane of hepatocytes, the primary cell type within the liver (217). Other cell types are present within the lining of the hepatic sinusoidal walls including Kupffer cells, endothelial cells, stellate cells, lymphocytes and other immune cells (2, 217). Notably, it is the hepatocyte that is responsible for the many functions of the liver and the two major metabolic functions relevant to this thesis, glucose and lipid metabolism, are intimately connected and critical to the understanding of the work described herein. The molecular details of these metabolic functions are described in detail below and illustrated in Figures 1.4.-1.5.

1.7.1. Hepatocyte glucose uptake and processing

As described in section 1.4., the liver produces glucose by two mechanisms: glycogenolysis, or the breakdown of glycogen stores and gluconeogenesis, the *de novo* synthesis of glucose from non-carbohydrate precursors. In contrast to GLUT4, which is expressed in muscle and AT, insulin-independent expression and activity of GLUT2 is essential in the post-prandial state for hepatocytes to take up glucose for metabolic processes (12). Once taken up by hepatocytes, glucose is immediately phosphorylated by

GK, creating G6P, a critical intermediate of hepatic glucose metabolism, trapping glucose inside the cell to be metabolized (Figure 1.4) (185). The rate limiting activities of the enzymes PEPCK, G6Pase, and GK are required to generate G6P (185). PEPCK catalyzes the conversion of oxaloacetic acid to phosphoenolpyruvate (PEP), the metabolite necessary to begin the conversion of (PEP) to glucose. G6Pase however, catalyzes the final reaction of gluconeogenesis by dephosphorylating G6P to generate free glucose. This final step is shared both by gluconeogenesis and glycogenolysis as glucose must be phosphorylated by GK, the rate limiting enzyme for glucose utilization and the first step in generating G6P for the glycogen production for storage within the liver (185). Intracellular G6P concentrations also act within a feedback loop as an allosteric activator of glycogen synthase (GS), the rate-limiting enzyme of glycogen synthesis (12, 185). In hepatocytes, the balance of GK and G6Pase as well as the expression levels of other enzymes are tightly controlled at the transcriptional level by hormones, mainly insulin, glucagon and glucocorticoids to maintain normoglycemia (119, 185). Transcription factors including the hepatocyte nuclear factor-4α (HNF-4α), PPARα, cAMP response element-binding protein (CREB) and the peroxisome proliferative activated receptor-γ co-activator-1α (PGC-1α) all regulate enzymes involved glucose metabolism, including PEPCK and G6Pase (12). PGC-1α alters gluconeogenic gene expression by directly binding to HNF-4α and to other transcription factors including Foxo1, the activation of which is dependent upon the PI3K/AKT arm of insulin action (185). GSK3 is a multifunctional kinase downstream of the PI3K/AKT arm of insulin action that is responsible for phosphorylating GS for activating glycogen synthesis and also

phosphorylates sterol response element-binding protein 1c (SREBP-1c), a critical transcription factor involved in hepatic lipid metabolism and described in the next section 1.7.2.

As described above, the metabolic state of the body dictates the fate of glucose utilization. G6P is not only metabolized for glycogen synthesis in the fed state, but G6P is also processed by glycolysis, the ten-step energy-releasing process that metabolizes glucose to pyruvate with a net gain of two ATP and two NADH molecules per glucose molecule (12). When ATP is in abundance and the cell no longer requires the energy from this process, this pathway is inhibited by a feedback loop dependent upon ATP concentrations (12). The end product pyruvate is further decarboxylized to acetyl-CoA, which enters the intramitochondrial tricarboxylic acid cycle or acts as a substrate for *de novo* lipogenesis (DNL). This pathway is regulated by the PI3K/AKT arm of insulin action and is controlled hormonally by insulin, epinephrine, and glucagon (185). NADH, however, is a co-substrate for DNL and cholesterol synthesis that is provided by alternative G6P degradation via diversion to the pentose phosphate shunt pathway. This alternative glucose metabolism links intracellular glucose and lipid metabolism providing evidence that any alteration in hepatic glucose uptake and processing not only affects hepatic and systemic glucose homeostasis, but affects hepatic and ultimately systemic lipid metabolism, described in the next section (1.7.2.).

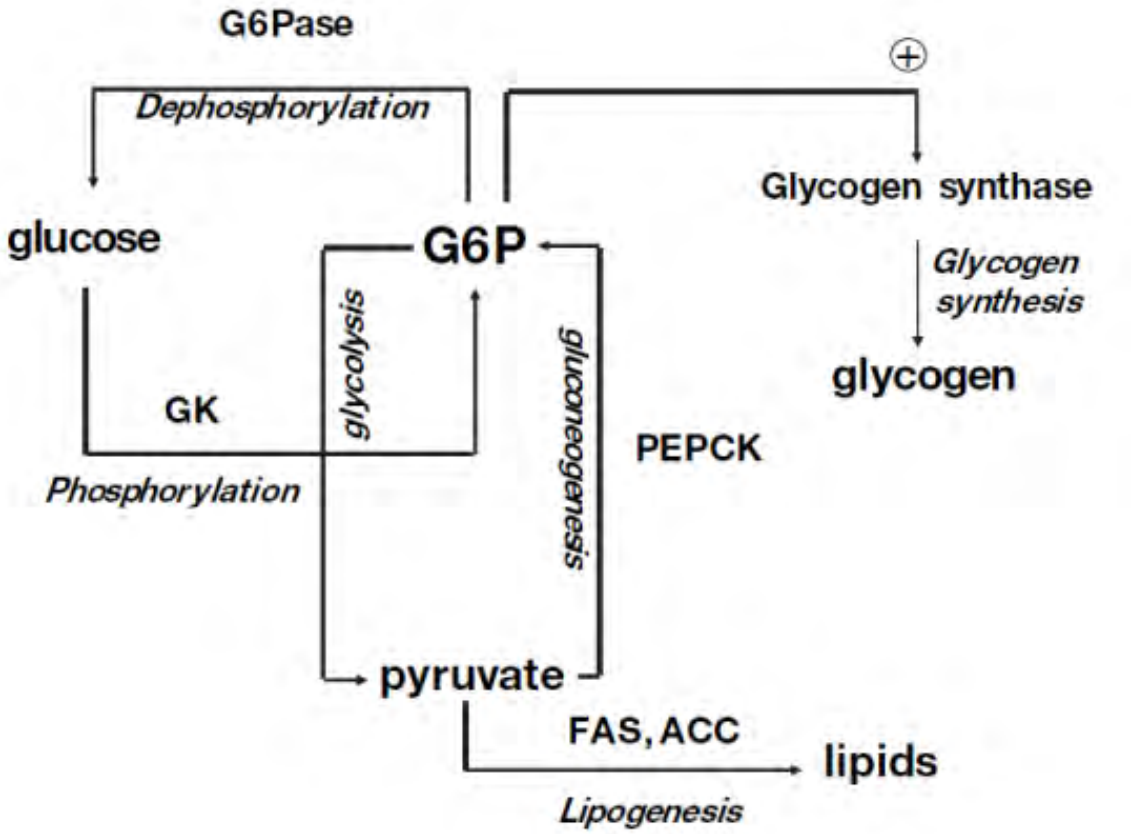

Figure 1.4. Glucose 6-phosphate is a metabolite that is shared by several hepatic pathways. Hepatic glucokinase (GK) allows for the rapid and efficient phosphorylation of glucose to yield glucose 6-phosphate (G6P), a key substrate in glucose metabolism. In hepatocytes, G6P concentrations are determined by the balance between G6Pase and GK activities. G6P is an allosteric activator of glycogen synthase (GS), but is also a key metabolite that can enter glycolysis. Additionally, because the major function of hepatic glycolysis is to provide carbons from glucose for *de novo* lipogenesis (DNL), G6P is also a determinant for this pathway and for fatty acid synthase (FAS) and acetyl CoA carboxylase (ACC) induction. Adapted from Postic, et al. *Diabetes Metab* 30: 398-408, 2004.

1.7.2. Hepatic lipid metabolism

Hepatic lipid metabolism is composed of a number of pathways including fatty acid uptake, lipogenesis, fatty acid oxidation, VLDL synthesis and secretion. The metabolic breakdown of lipids begins with the ingestion of dietary carbohydrates and fats. Once fats are ingested, they are emulsified by bile acids that are synthesized and secreted by hepatocytes and hydrolyzed by pancreatic lipases in the intestines (12). Intestinal enterocytes absorb, re-synthesize and package these lipids into intestinal TG-containing chylomicrons to enter circulation through the lymphatic system (12, 217). These chylomicrons express lipoproteins on their surface that are crucial for the lipase-mediated breakdown of TGs into their FA and glycerol components (12). These FAs are then taken up by adipocytes for storage via FA transport proteins (FATPs), while the chylomicron remnants re-enter the blood stream. In the postprandial state, these FAs are transported into the liver, elongated and esterified into TGs within the LD of the hepatocyte cytoplasm. In fasted conditions they are rapidly metabolized via β-oxidation to provide energy (12). This oxidation occurs within the mitochondria, peroxisomes and endoplasmic reticulum (ER) and is required to generate electrons to drive ATP synthesis by the electron transport chain (12). β-oxidation, however, is inhibited in the fed state and DNL is promoted, thus allowing for lipid storage and distribution. This hepatic lipid storage may arise from two major routes: the uptake of circulating FAs by hepatocytes as described above or via DNL from non-lipid precursors including dietary carbohydrates (i.e., glucose) (121). Once FAs are esterified into TGs they can either be stored within

the hepatocyte LD or they can be secreted as TG-enriched lipoproteins (VLDLs) into circulation (57).

The results herein are highly dependent upon the understanding of hepatic lipogenesis, which includes the *de novo* synthesis of FAs by glycolytic conversion of glucose to acetyl-CoA and malonyl-CoA, and further elongation and esterification of FAs to generate hepatic TGs (111). Lipogenesis is both insulin and glucose-dependent and under strict transcriptional control by SREBP-1c and carbohydrate response element binding protein (ChREBP). These transcription factors are activated by insulin and carbohydrates, respectively, eliciting changes in the expression of lipogenic genes that catalyze the rate limiting steps of FA synthesis; acetyl-CoA carboxylase (Acc) and fatty acid synthase (Fasn) (84, 111). Although originally discovered as a transcription factor involved in cholesterol biosynthesis, SREBP-1c is a major mediator of insulin action on GK and many other lipogenic genes including ATP citrate lyase (Acyl), ELOVL family member fatty acid elongase 6 (Elovl6), glycerol-3-phosphate acyltransferase (Gpat), diacylglycerol acyltransferase (Dgat), and stearoyl-coenzyme A desaturase 1 (Scd1) by binding to the sterol regulatory element (SRE) present in the promoters of these genes (33, 35). Transgenic over-expression of hepatic SREBP-1c in mice increases hepatic TG accumulation (steatosis) and increased mRNA expression of most lipogenic genes (213). Consistent with this, SREBP-1c KO mice have impaired lipogenic gene expression after high carbohydrate feeding, which is known to rapidly induce hepatic Fas mRNA expression (35, 131). Additionally, SREBP-1c is elevated in the livers of IR rodents, suggesting its involvement in the pathogenesis of hepatic IR (35). Taken together, these

results indicate that hepatic carbohydrate and lipid metabolism are intimately connected and dysregulation of one or more of these pathways will perturb metabolic control and ultimately lead to IR and T2DM.

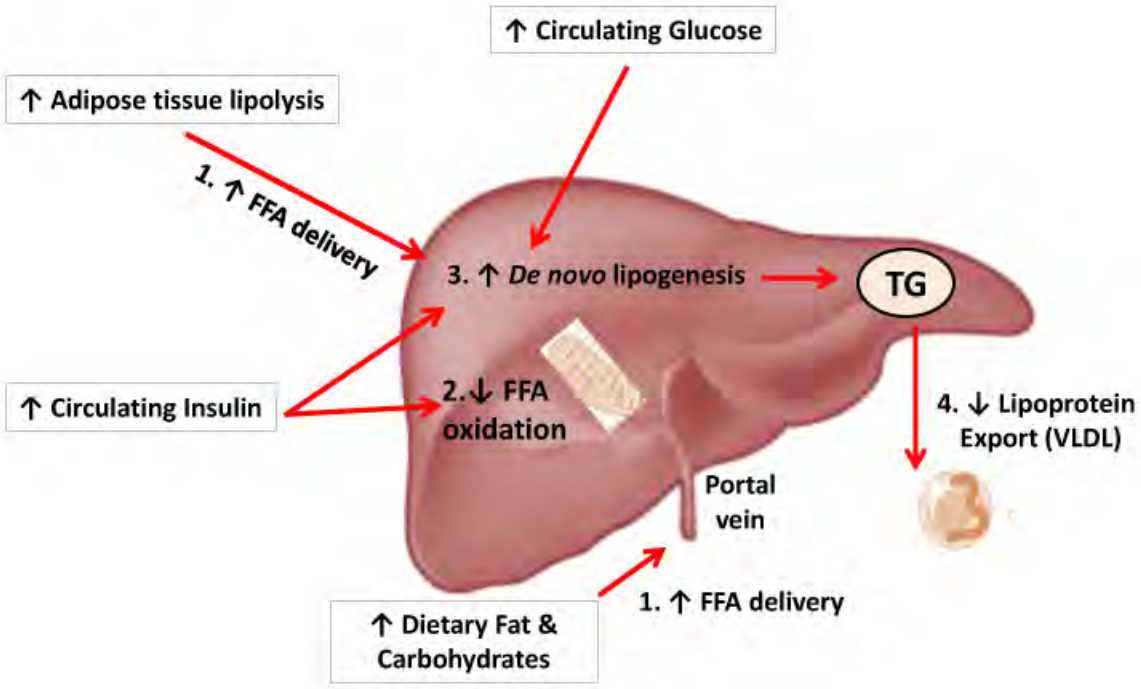

Figure 1.5. Mechanisms contributing to hepatic lipid accumulation. In the context of obesity, a disruption of 1 or more of the pathways of hepatic lipid metabolism contribute to hepatic fat accumulation. (1) Increased delivery of FFAs as the result of over nutrition and the increased release of FFAs from AT as a result of increased lipolysis. (2) Decreased hepatic FFA oxidation. (3) Increased hepatic *de novo* lipogenesis caused by hyperinsulinemia, hyperglycemia and increased FFA delivery. (4) Decreased export of TG-rich lipoproteins in the form of VLDL secretion into circulation.

1.7.3. Hepatic Steatosis and NAFLD

NAFLD represents the most prevalent liver disease in Westernized countries. NAFLD is the hepatic manifestation of the MS and IR, and it frequently occurs as part of the metabolic changes that accompany obesity, T2DM and dyslipidemia (4). In obese humans, steatosis prevalence is approximately 75% and nearly 35% of these individuals progress to developing NASH, a condition that occurs when steatosis is accompanied by inflammation (2). NASH can further progress to fibrosis with an increased risk to develop end-stage liver disease or hepatocellular carcinoma (12).

Hepatic steatosis is characterized by intracellular TG accumulation and the subsequent formation of LDs in hepatocytes causing liver enlargement. Hepatic steatosis in the context of obesity and IR occurs when there is an imbalance in hepatic lipid metabolism (summarized in Figure 1.4.): (1) An excess supply of FAs coming from dietary intake or increased lipolysis from obese AT, (2) decreased FA β-oxidation, (3) increased DNL and (4) decreased VLDL export. Quantitative analysis using labeled isotopes in patients with NAFLD revealed that 59% of the labeled hepatic TGs were derived from circulating FAs from increased AT lipolysis, 26% were from hepatic DNL and 15% were from the dietary sources (46). Isotope tracing of VLDL in normal subjects versus obese subjects reveals a significant increase in export from 2-5% to 25-30%, indicating that NAFLD patients may have impaired export and thus display hepatic TG accumulation (42, 46).

Although TGs are relatively inert, intracellular FA accumulation within hepatocytes and KCs can activate resident immune cells within the liver causing the

progression of steatosis to NASH. This progression is inevitably linked to the paracrine effect of increased pro-inflammatory cytokine secretion including TNF-α and IL-1β from AT and KCs within the liver, thus upregulating inflammatory signaling, oxidative stress, imbalanced circulating insulin-sensitizing adipokine levels and mitochondrial defects leading to decreased FA oxidation and hepatic lipotoxicity (2, 5, 12). These cytokines derived from activated KCs exacerbate liver inflammation and increase hepatic lipid synthesis and TG accumulation (53, 76, 129). Because of the significant association of NAFLD with obesity and IR, a common treatment for these patients is lifestyle intervention by the prescription of exercise and nutritional programs to achieve diet- or surgically-induced weight loss. Diet-induced weight loss and laparoscopic adjustable gastric banding improve liver histology, however, the characteristic inflammation of NASH may be exacerbated by bariatric surgical techniques because malabsorption and gut diversion confound the effects of weight loss (3, 43). TZDs also improve liver function by histologically decreasing necrosis, serum ALT, and improving fasting insulin, glucose and HOMA IR in NAFLD patients (20, 158). Recently, anti-cytokine therapy has been utilized to treat alcoholic liver disease (ALD), the onset of which is caused by excess alcohol consumption. Results in mice indicate that that pharmacological inhibition of IL-1 signaling by recombinant interleukin-1 receptor antagonist (IL-1Ra) treatment had protective effects in various stages of ALD, including development and progression of steatosis to steatohepatitis and fibrosis (181). Chapter 3 of this dissertation demonstrates that IL-1Ra administration in DIO mice to attenuate

hepatic steatosis, illustrating a therapeutic approach to NALFD treatment in the context of IR and obesity.

1.8. Inflammation and Metabolic Disease

The association between inflammation and metabolic disease was discovered well over 100 years ago in studies using anti-inflammatory agents to normalize glycemia. The earliest reports in presumed T2DM and IR patients noted decreased glycosuria, or glucose in the urine, after treatment with high doses of sodium salicylate, the primary metabolite of aspirin (11, 215, 258). A resurgence regarding the effects of salicylates occurred 50 years later when a T1DM patient no longer required daily insulin injections after being given high-dose aspirin to treat the arthritis that was associated with rheumatic fever (11). However, when additional patients were treated with salicylates, it was recognized that maintenance of normoglycemia required continuous high-dose treatment and these patients suffered from salicylate toxicity (11). These data demonstrate the importance in our understanding of the mechanistic link between inflammation and systemic glucose regulation.

Case studies conducted in IR and non-disease control subjects revealed increased secretion of inflammatory mediators (TNF-α, IL-1β, IL-6) and circulating acute phase proteins including C-reactive protein (CRP) and serum amyloid A (SAA) in IR patients (195, 222). Additional increases in serum levels of IL-1Ra, an anti-inflammatory acute phase protein, are also observed in obesity-induced IR patients (66, 103). Surgically induced weight loss by gastric bypass reduces circulating IL-1Ra levels, thus illustrating the immune effects induced by obesity (145). However, it was the discovery in 1971 by Vane and colleagues, who were awarded the Nobel Prize, that revealed the anti-inflammatory effects of aspirin is via the inhibition of prostaglandin synthesis, and

further research has found the effects to be partially mediated by nuclear factor kappa b (NF-kB) inhibition (described in section 1.10.2.) (117, 240). More recently it was discovered that salicylates mediate their effects on insulin sensitivity by inhibiting the inhibitor of kappaB kinase β (IKKβ) to improve hyperglycemia, hyperinsulinemia, and dyslipidemia in obese rodents (264, 266). Although the role of immune activation in IR and T2DM progression remains incompletely defined, the emerging study of immunometabolism has enhanced our understanding of the mediators and signaling mechanisms involved (56).

1.9. The Immune Response in Adipose Tissue

The endocrine and metabolic functions of AT and the subsequent changes in systemic physiology are intimately controlled by changes in insulin sensitizing and inflammatory adipokine secretion. In recent years, much effort has been devoted to understanding the immune response that ensues in AT in obesity. Though many hypotheses have been brought forth to explain why this immune response occurs, it is clear that the metabolic complications along with increased immune cell infiltration and secretion of pro-inflammatory cytokines are directly related the chronic state of low-grade inflammation within the AT of obese humans and mice. This is determined by the increased expression of pro-inflammatory mediators TNF-α, IL-6, IL-1β, iNOS, CRP, MCP-1 and others (62, 245, 252). Adipocytes express the receptors for several of these cytokines supporting the hypothesis that adipocytes are both the source and the target of these pro-inflammatory signals (252). However, data suggests that in AT, the pro-inflammatory molecules including IL-1β, PG-E2, TNF-α, and IL-6, are primarily produced by the growing stromal vascular cell population (SVC) (198, 252). The SVC fraction is comprised of pre-adipocytes, fibroblasts, mast, endothelial and immune cells; the most abundant and well-studied of these cells are adipose tissue macrophages (ATMs). The inflammatory processes by these ATMs are also mimicked by KCs, or resident liver macrophages that drive the obesity-induced hepatic inflammatory response secondary to AT inflammation.

1.9.1. Hypotheses of Adipose Tissue Inflammation

The homeostatic program of AT is maintained in a complex manner through the paracrine and autocrine interactions of adipocytes, endothelial cells, immune cells, and others. Changes within the expanding AT perturb this local environment and elicit microenvironmetal cues and signals to other cells, thus evoking a chronic immune response. Recent studies suggest that this immune response in obese AT is causal to the increased basal lipolysis and circulating lipids that are associated with obesity and IR (discussed in section 10.1.1) (118). Disruptions in the vascularization of expanding AT cause local hypoxia, which is also suggested to cause the dysregulation of adipokine secretion, pro-inflammatory macrophage recruitment and local AT inflammation in obesity (48, 90). Another hypothesis of AT inflammation identifies that hypertrophic adipocyte necrosis is an important modulator of macrophage responses by the appearance of crown like structures (CLS) surrounding dying adipocytes in expanding AT (30). Importantly, attenuation of this immune response and subsequent inflammation improves IR and it is without question that ATMs are the primary source of this local AT inflammation in obesity (9, 216, 220, 237, 252). However, the complete immune program and involvement of other immune cell types remains incompletely defined.

1.9.2. Immune Cells in Adipose Tissue

The metabolic state of AT modulates both the quantities and proportions of immune cells as illustrated by the increasing shift in immune cell populations with increasing adiposity (55, 252). Of the immune cells, ATMs represent the largest and

most well-studied within obese AT and are the primary source of inflammatory cytokines. Immune cells, however, are not selective to obese AT; macrophages, mast cells and T and B lymphocytes also accumulate in the AT depots of lipodystrophic mice confirming their contribution to inflammation and IR (88). ATMs are discussed extensively in the following sections and throughout chapter 2 and therefore this section will be devoted to the analysis of other immune cells and their contribution to local AT inflammation.

Recent studies suggest that included in the first wave of cells to respond to acute infection or tissue injury are neutrophils, which are mononuclear cells that facilitate the recruitment of macrophages, dendritic cells and lymphocytes, thus initiating the immune response (55). A recent study demonstrated that short term HFD in mice causes a significant recruitment of neutrophils to the VAT, peaking at 3-7 days and preceding macrophage accumulation in AT (47). It has also been demonstrated that β3-adrenergic stimulation by catecholamines in vivo, used to mimic the increased AT lipolysis in obesity, causes rapid infiltration of neutrophils into AT depots of mice, specifically VAT (199). In contrast, the elevation of inflammatory gene expression and macrophage infiltration are significant in AT after 3 days of HFD, although to a lesser extent than induced by chronic feeding (128). Thus, the immune cells responsible for initiating local AT inflammation still remains elusive and contributing cell types continue to be accounted for.

While the immune response responsible for AT inflammation is causal to the IR in obesity, not all immune cells within the AT cause inflammation. Studies have reported

the presence of anti-inflammatory cytokines within AT, including interleukin 4 (IL-4), interleukin 10 (IL-10), interleukin 13 (IL-13) and transforming growth factor β (TGF-β) (63, 136). In lean mice, eosinophils are a large portion of the SVCs and inversely correlate with increasing adiposity (260). Identified by the expression of surface marker sialic acid–binding immunoglobulin receptor (SiglecF), eosinophils can modulate macrophage activation to an anti-inflammatory state (M2) with insulin sensitizing affects in AT by IL-4 secretion (260). The remaining SVCs in lean mice are made up of lymphocytes including $CD4^+$ and $CD8^+$ T cells, innate helper type cells (T_H), invariant natural killer T cells (iNKT), B cells and others.

Regulatory T cells (T_{regs}) promote the anti-inflammatory activities of cells of the innate immune system including T_H cells and macrophages (115). T_{regs} are $CD4^+$ and decrease with obesity like eosinophils, but T_{regs} are only a subset of $CD4^+$ lymphocytes found in AT (58). Other $CD4^+$ and $CD8^+$ T cells increase in parallel with increasing adiposity including $CD4^+$ T_H1 cells that promote inflammatory cues by secreting interferon γ (IFNγ) (115, 259). Interestingly, $CD8^+$ T cells have recently been demonstrated to play a role IR pathogenesis because genetic depletion of $CD8^+$ T cells reduces macrophage infiltration into the AT of obese mice and ameliorates systemic IR (162). Like neutrophils, these $CD8^+$ T cells precede macrophage accumulation into the AT of mice challenged by HFD and are necessary for AT inflammation (162). Additionally, genetic deletion of iNKT cells ameliorates the development of AT inflammation and glucose intolerance in DIO, however, studies evaluating the number of these cells in obese AT are conflicting (23, 172). Furthermore, a small population of

lymphocytes (B cells) is present within the AT, and much like T cells are divided into distinct B cell populations. B cells secrete antibodies to assist in the destruction of pathogens by phagocytes including macrophages, however, a distinct subset of B_{regs} inhabit the AT and secrete IL-10 to restrain AT inflammation and maintain metabolic homeostasis in DIO mice (163). Lastly, the inflammatory mast cell is increased in the AT from obese subjects compared with that from lean donors and their deficiency improves glucose tolerance and insulin sensitivity in obese mice (132). Taken together, these data suggest that many subtypes of immune cells are responsible for AT inflammation and are required to control both the macrophage content and polarization state within obese AT.

1.9.3. Adipose Tissue Macrophages

Obesity-induced AT inflammation is primarily mediated by both innate and adaptive immune cells residing in the SVC fraction as described above. Characterization of these cells by Weisberg and colleagues piloted the emergence of immunometabolism with evidence that macrophage activation within AT drives the obesity-related immune response and IR (252). Because adiposity does not predict IR, studies in our laboratory combining expression profiling with computational approaches determined that elevated inflammatory gene expression can distinguish the omental AT of IR obese patients from that of IS obese individuals, even though they are matched for body mass index (BMI) (82). When analyzed by fluorescence activated cell sorting (FACs), ATMs within omental and VAT of obese humans and mice increase in parallel with increasing

adiposity (252). In agreement, approximately 5% of cells in the lean AT are F4/80^{+} macrophages (described below), whereas this number increases to approximately 40% of cells in obese individuals and to upwards of 50% in obese mice illustrating a drastic shift in macrophage proportions within AT (252). In agreement, histological analysis of omental AT from obese IS and IR patients determined that increased adipocyte size and macrophage infiltration into AT is a better predictor of IR than clinical measures of adiposity; highlighting the significance of understanding macrophage populations within obese AT, specifically the VAT/omental depot (82).

Macrophages are identified by the characteristic expression of surface markers F4/80 (EMR1), CD68 and CD11b (Itgam), and represent the most functionally and numerically dominant immune cell (leukocyte) in the SVC fraction. Encompassed within F4/80^{+} macrophages are a heterogeneous hematopoietic cell population with different immunophenotypes based on surface marker protein expression. Sorting cells with specific surface marker combinations using flow cytometry has provided mechanistic details on the functional role of macrophages within AT and how their activation contributes to obesity-induced IR. Importantly, ATMs in lean mice are phenotypically distinct from those in obese mice by exhibiting different inflammatory potentials and are classified in an activation spectrum of polarization states.

There is a dichotomous, yet simplistic classification of ATMs categorizing them as anti-inflammatory alternatively activated (M2) macrophages, which express specific genes including Arginase 1 (Arg1), CD206 (Mrc1) and CD301 (Mgl1). These resident ATMs secrete anti-inflammatory cytokines IL-4 and IL-13, which are essential to the

homeostatic functions of AT including tissue repair and remodeling (167). In contrast, ATMs in a classical pro-inflammatory (M1) activation state express CD11c (Itgax) and can drive inflammatory signaling cascades by releasing TNF-α, IL-1β and MCP-1. Resident ATMs of lean mice are not $CD11c^+$, but a phenotypic switch occurs with increasing adiposity connecting the M1 macrophage to obese AT (136). In addition to infiltration, in situ proliferation driven by MCP-1 is an important process by which macrophages accumulate in obese VAT (1). It is important to note that $CD11c^+$ ATMs correlate with IR in obesity (167-168). A more comprehensive subdivision of macrophage activation exists and illustrates the plasticity, versatility and antigenic diversity of ATMs. For the extent and purposes of discussing the projects herein, the concept that ATM content is closely correlated with IR is most important. Therefore, we sought to investigate the inflammatory potential of ATMs within the AT by combining a computational approach and gene expression profiling in hypertrophic, IR DIO mouse AT. These results are described in Chapter 2.

Recently, much effort has been taken to alter AT macrophage content to determine whether AT macrophage content can in fact alter IS in obese mice and humans. Lifestyle and/or surgical intervention to induce substantial weight loss in obese subjects both decrease ATM content and inflammatory gene expression (16, 21). The use of insulin sensitizing TZDs, specifically rosiglitazone, in genetically obese *ob/ob* mice yields significant reductions in macrophage marker gene expression in AT (261). These methods demonstrate a correlation of reduced ATM content with improved systemic IS. In agreement, recent studies using conditional macrophage ablation techniques have

obtained similar results. One such method is based on transgenic diphtheria toxin receptor (DTR) expression under the control of the CD11c promoter to conditionally and globally ablate $CD11c^+$ cells. A marked reduction in $CD11c^+$ macrophages in AT along with local and systemic decreases in pro-inflammatory cytokines and a normalization of IS was observed in DTR-BM DIO mice (179). Additionally, selective macrophage depletion *in vivo* can be executed using the liposome-mediated intracellular delivery of dichloromethylene-bisphosphonate (clodronate) (239). This method selectively targets phagocytes by inducing apoptosis as intracellular clodronate concentrations increase. The success of this method is dependent upon the concentration of clodronate incorporated into the liposome preparation, timeline and injection strategy. Feng and colleagues report that intraperitoneal (i.p.) clodronate liposomes injection in DIO mice markedly reduces ATM and KC content, improves systemic glucose tolerance and IS, and alleviates obesity-induced steatosis (54). Conversely, Clemente, et al reported significant increases in VATM content in DIO mice treated with clodronate liposomes i.p. demonstrating inconsistencies in the literature using this method. We sought to investigate these inconsistencies using clodronate in 2 models of mouse obesity and the results are discussed in Chapter 3. In contrast to depleting macrophages, investigators have also used transgenic approaches to drive macrophage accumulation by overexpressing MCP-1 in AT. These studies report robust increases in macrophage content in both lean and obese mice accompanied by decreased IS (107-108). Taken together, these studies highlight the importance in studying the molecular mechanisms

whereby macrophage-induced inflammatory processes contribute to systemic IR and inflammation.

1.10. Inflammatory Pathways and Insulin Resistance

Inflammation causes IR via a number of molecular mechanisms, and the affects of pro-inflammatory cytokines on insulin signaling in peripheral insulin-sensitive and producing tissues is profound. One mechanism whereby inflammatory signaling causes IR is via the inhibitory phosphorylation of serine residues on IRS-1 by stimuli such as TNF-α or FFAs (253). This phosphorylation reduces both insulin-stimulated IRS-1 tyrosine phosphorylation and the ability of IRS-1 to associate with the insulin receptor and thereby inhibits insulin action by preventing downstream signaling (180, 253). Inflammatory signaling pathways contributing to IR can also become activated by intracellular stress responses. The functional capacity of the ER is overwhelmed in obesity, which causes an ER stress response and consequent activation of inflammatory signaling pathways (176). Additionally, increased glucose metabolism in obesity drives production of reactive oxygen species (ROS) by the mitochondria, which is also responsible for activating inflammatory signaling cascades (64). Although these different areas of research provide mechanistic links between inflammation and IR, these findings have funneled into few primary signaling mechanisms responsible for inhibiting insulin action. These pathways are described below and are illustrated in Figure 1.6.

1.10.1. Cytokines and Insulin Resistance

The work of Gohkan Hotamisligil and Bruce Spiegelman discovered that TNF-α was overexpressed in obese rodents and humans gave insight to the mechanistic links between obesity and inflammation (56, 237). TNF-α is a pleiotropic cytokine that has a

beneficial involvement in wound healing and pathological mediation of cellular apoptosis and inflammation (85, 263). TNF-α promotes cellular inflammatory responses by tumor necrosis factor receptor 1 and 2 (TNFRI and TNFRII) activation (85). This causes recruitment of several intracellular adaptor proteins to activate multiple signal transduction pathways to alter gene expression through nuclear factor kappa B (NFκB) and activator protein-1 (AP-1) signaling. These pathways upregulate cytokine expression, and negatively regulate insulin receptor signaling by increasing serine phosphorylation of IRS-1, which directly interferes with insulin signaling (85, 93, 138, 160, 233). TNF-α also downregulates adiponectin secreted by adipocytes that sensitizes liver and muscle to insulin in rodents and humans, therefore decreasing insulin sensitivity (160). As described above, increased TNF-α expression also induces chronic lipolysis, which increases serum FFA levels and promotes ectopic lipid deposition and IR in muscle and liver (221). TNF-α also opposes the beneficial functions of PPARγ by inducing a rapid and potent reduction in adipocyte and macrophage PPARγ expression (168). These data were confirmed by the generation of TNF-α or TNF-α receptor KO mice, which displayed protection against DIO and IR (237, 241). TNF-α neutralization in obese rats also lowered plasma glucose and lipid levels, thus improving insulin sensitivity and providing the first evidence that inflammatory mediators can cause IR (92). However, this improved insulin sensitivity was not observed in obese, IR patients following recombinant TNF-α antagonist administration (178). Although TNF-α antagonists were not successful clinically, it remains important to understand the signaling mechanism(s) that require the action of TNF-α and other cytokines.

Investigators have since identified many other cytokines that modulate insulin action, and one such family of cytokines and a particular focus of this dissertation is the IL-1 family, which includes both the pro-inflammatory and anti-inflammatory, IL-1β and IL-1Ra, respectively. Blockading IL-1-induced inflammation in humans by administration of recombinant IL-1Ra or IL-1β antibodies has demonstrated a central role of IL-1β in a number of inflammatory diseases including rheumatoid and osteoarthritis and myeloma (40). In obesity, IL-1β expression increases in the pancreas, AT and liver and it impairs insulin secretion and induces β-cell apoptosis (103, 125). Similar to TNFα, IL-1β is produced by macrophages and correlates with IR (41, 122, 153). Interestingly, IL-1Ra expression is reduced in T2DM patients and administration of recombinant IL-1Ra in these patients improves glycemia and β-cell function and also reduces systemic inflammatory markers (CRP and IL-6) (125). β-cell production of IL-1β is enhanced by diet-derived FAs and high glucose levels, implicating its involvement in the pathogenesis of diabetes (41). IL-1β also decreases the ability of insulin to stimulate glucose transport in both human and mouse adipocytes (102). Like TNF-α, IL-1β can promote its own transcription by signaling through the IL-1 receptor complex to target IKKβ and NFκB to drive gene transcription. However, a caspase-dependent signaling mechanism is also required to promote its activation via the NLRP3 inflammasome; an innate immune response that involves the formation of a multiprotein caspase-1-activating complex containing cysteine-aspartate protease-1 (caspase-1), apoptosis-associated speck-like protein containing a CARD (ASC), and a Nod-like receptor (NOD) protein (NLRP) (39, 44). Formation of the inflammasome complex activates caspase-1, which proteolytically

cleaves the IL-1β precursor into the mature active form that is secreted (250). HFD-induced elevation of FAs activate the inflammasome, which result in IL-1β production and impaired glucose tolerance and insulin sensitivity (254). These data pioneered the studies designed to understand how the molecular effects of obesity activate the immune system, and how activation of inflammatory signaling influences the progression of IR.

1.10.2. Inflammatory Signaling Pathways in Insulin Resistance

The expansion of AT in obesity and the subsequent increase in inflammatory cytokines promotes cellular inflammatory responses by activating canonical pathways that mediate inflammatory signaling; the stress kinase, c-junN-terminal activated kinases 1 and 2 (JNK1/2), protein kinase C theta (PKCΘ) and the inhibitor of NFκB kinase IKK (89, 233, 266). The activities of both JNK and IKKβ/NFκB are increased with increasing adiposity and genetic or chemical inhibition of these pathways improves IR providing a link to their involvement in metabolic disease (242, 266). JNK and NFκB represent the most well studied and potent inflammatory signaling cascades in the context of regulating insulin signaling (38, 211, 268). Cytokines can stimulate a feedback loop via these pathways whereby they can exacerbate and drive their own production, however, other initiators of inflammatory activation include lipid metabolites, FAs and cellular stress responses including endoplasmic reticulum (ER) and oxidative stress. (64, 176, 211, 226). These ligands can also activate the p38 stress-activated protein kinase (p38 SAPK), extracellular signal-related kinases 1 and 2 (ERK1/2), toll-like receptors (TLRs) and others, and they also recruit adaptor proteins and signaling molecules to activate mitogen

activated protein kinase (MAPK) signaling and IKKβ to coordinate inflammatory responses through activation of NFκB to activate inflammatory gene transcription and ultimately promote the same inflammatory processes (133, 157). Once activated, the downstream consequences of these pathways include production of pro-inflammatory cytokines and cellular adhesion molecules that recruit and localize immune cells, including monocytes and macrophages to provoke the immune response (215).

JNK is a central metabolic regulator in the development of obesity-induced IR (242). In obesity, JNK activity is elevated in liver, muscle, and AT, and an absence of JNK1 results in decreased adiposity, improved insulin sensitivity and enhanced insulin receptor signaling in diet-induced and genetic mouse models of obesity (89, 242). JNK-mediated inhibitory phosphorylation of IRS1 may contribute to obesity-induced IR development, but IRS-independent mechanisms also play important roles as mediators of IR (200). Suppression of the JNK pathway can protect β-cells from glucose toxicity (109). Modulation of hepatic JNK1 by dominant negative over-expression in obese mice restores insulin sensitivity (155). Interestingly, JNK1 deficiency in hematopoietic cells by adoptive transfer in obese mice has no effect on adiposity, but protects against diet-induced IR by decreasing obesity-induced inflammation and macrophage accumulation in AT (219). In agreement, deletion of both JNK1/2 in macrophages protects against obesity-induced IR, and these mice display reduced hepatic TG accumulation and inflammatory gene expression (80). These data indicate that JNK signaling, specifically in macrophages, is required for both AT and liver macrophage accumulation and diet-induced IR.

Recently, the role of FAs derived from fat-enriched diets have emerged as key participants in obesity-induced inflammation. Intracellular lipid metabolites, specifically diacylglycerol (DAG), fatty acyl-CoAs and ceramide, play a large role in inhibiting insulin action by activating TLRs, IKK and PKC-θ (253). Circulating FFAs suppress insulin action by activating JNK and IKKβ in AT, liver and skeletal muscle (34, 159). Moreover, palmitate, a major FFA that is released from adipocytes, increases macrophage TNF-α production, which further augments FFA release and inflammatory changes in the AT (159, 225). This macrophage response is thought to be signaled through TLR4, which is highly expressed on the surface of macrophages and is blunted in the absence of TLR4 (34, 211). Mice heterozygous for IKKβ are partially protected against IR induced by lipid-infusion and diet- or genetically-induced obesity (112, 266). Importantly, as described above, inhibiting IKKβ in IR patients by high doses of aspirin improves insulin signaling (98). In agreement with the macrophage specific JNK deletion, macrophage IKKβ deletion protects against diet-induced IR. However, when IKKβ is conditionally deleted in the hepatocytes of IR mice, these mice develop IR in muscle and AT and remain insulin sensitive in the liver. Lastly, a more specific approach using an *in vivo* siRNA delivery system to target ATMs by glucan encapsulated siRNA particles (GeRPs) has been developed by our laboratory. Targeting inflammatory mediators TNF-α and osteopontin in VATMs of genetically obese mice by administration of GeRPs i.p. significantly improved systemic glucose tolerance (7). Taken together, these data are consistent with the hypothesis that cytokines produced by macrophages, specifically

ATMs, can exacerbate whole-body glucose intolerance, thus providing evidence that macrophages are excellent therapeutic targets for obesity and T2DM treatment.

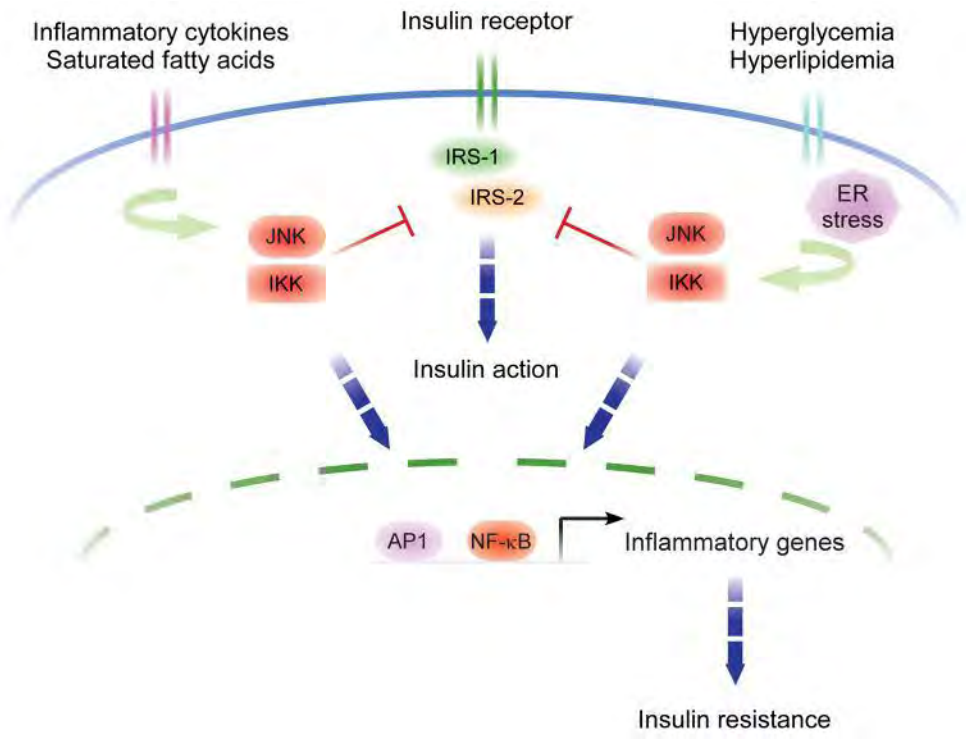

Figure 1.6. Inflammatory pathways of insulin resistance. Insulin action is transduced from the cell surface to cytoplasmic and nuclear responses via tyrosine phosphorylation of the insulin receptor substrates (IRS)-1/2. However, the inhibitory serine residue phosphorylation on these same substrates by JNK1 and IKKβ, the central mediators of stress and inflammatory responses, potently inhibits insulin action, thereby directly linking these responses to insulin resistance. In addition, the transcriptional activation of inflammatory genes by JNK1 and IKKβ induces insulin resistance in an autocrine and paracrine manner in insulin sensitive and insulin producing tissues. Moreover, in obesity, the JNK1 and IKKβ signaling pathways are also activated by increased influx of free fatty acids and glucose as well as other intracellular stress responses. Adapted from Chawla, et al. Annu Rev Pathol. 2011; 6: 275–297.

1.11. Specific Aims:

Since the discovery that macrophages infiltrate the AT of obese mice and humans, investigators have taken a more functional approach to determine the role of these macrophages in obesity-induced IR. The use of KO technology to remove mediators of systemic inflammation and alternative approaches to deplete macrophages has determined that macrophage-derived inflammation is pertinent to the development of IR; however, the causative connection remains in question. It is well established by studies comparing lean and obese AT histology and genome profiles that macrophages infiltrate obese AT, become M1-polarized and localize to necrotic adipocytes to phagocytose cell debris (137, 252). More recently, however, it was discovered that macrophages aid in the sequestration of FAs released from these dying cells and gives rise to foam cell formation within obese AT (118, 188, 252). This accumulation of lipid species and the proliferation of lipid droplets in ATMs induces gene-expression networks associated with lipid metabolism in the macrophage and provides evidence of an alternative role of macrophages in obese AT (188). Thus, the initial paradigm of macrophage-derived AT inflammation has evolved from the idea of macrophages solely causing inflammation to a more complex model in which ATMs might protect insulin sensitive tissues from lipotoxic events and subsequent immune cell activation. In the midst of this paradigm shift regarding the purpose and activation state of macrophages in obese AT, we used whole-genome transcription profiling to delineate whether increased AT inflammation is because of increased macrophage activation or recruitment in obese mice.

Furthermore, the obesity- and inflammation-induced increases in VAT lipolysis cause increased delivery of FFAs to the liver causing hepatic lipid deposition and lipotoxicity, KC activation and hepatic IR. Administration of recombinant IL-6, TNF-α or IL-1β can also cause acute hypertriglyceridemia by stimulating hepatic VLDL secretion and hepatic steatosis by stimulating hepatic DNL in obese mice (25, 28, 50, 52-53, 76, 164). To this end, it is essential in obesity-associated NAFLD treatment to understand the molecular events modulating hepatic lipid metabolism and IR, which are caused by both hepatic and systemic inflammation**.** Recently, macrophage depletion strategies have been used to determine the role of KCs in the development and progression of steatosis from a benign state to full-blown inflammation and fibrosis. One such strategy is the use of clodronate-encapsulated liposomes to study the effects of macrophage depletion on steatosis development and progression in obesity. However, this literature has diverged with growing contradictory phenotypes and hypotheses. Thus, to clarify this issue and elucidate the mechanism by which KC-derived pro-inflammatory cytokines regulate hepatic lipid metabolism in obesity, we targeted KCs *in vivo* by i.p. clodronate liposome administration in two animal models of obesity. Furthermore, pharmacological inhibition of IL-1 signaling was used to decifer the role of IL-1β in hepatic lipid metabolism modulation in DIO mice.

CHAPTER II: The Complex Roles of Adipose Tissue Macrophages: A Genomics Approach to Define the Inflammatory Signature of Obese Mouse Adipose Tissue

2.1. Abstract

Obesity is characterized by an expansion of AT and a chronic state of low-grade inflammation (77, 86, 91, 94, 252, 267). The gene expression profiles and functions of resident and recruited ATMs have been extensively studied, and established the concept that infiltrating ATMs are M1-polarized with upregulated inflammatory gene expression and localize around necrotic adipocytes to phagocytose cell debris (137, 252). More recently, however, it was discovered that ATMs have the ability to take up and sequester FAs released from these dying cells, giving rise to foam cell formation and indicating an alternative, non-inflammatory function of macrophage populations in obese AT (118, 188, 252). Thus, the initial paradigm of macrophage-derived AT inflammation has evolved from the idea of macrophages solely causing inflammation to a more complex model in which ATMs might protect insulin sensitive tissues from lipotoxic events and subsequent immune cell activation. Here we describe a genomics approach to determine whether ATMs in an obese animal model display inflammatory properties. We used whole-genome transcription profiling to determine the changes in inflammatory gene expression relative to macrophage-specific gene expression in both lean and DIO mouse AT. DIO mice displayed glucose intolerance and IR compared with lean control mice. AT inflammatory and macrophage-specific gene expression profiles were compared with microarray data that was performed on thioglycollate-elicited peritoneal macrophages (PECs) stimulated with lipopolysaccharide (LPS), which induces M1 polarization and cytokine release. We determined that common macrophage markers (CD68, F4/80, CD11b, and CD11c) were not affected by LPS treatment of PECS and these genes were

therefore used as a measure of the macrophage content within the AT. We determined that these markers were significantly increased as much as 35 fold in DIO mouse VAT, but not in SAT, consistent with an expansion of the macrophage population in VAT. Expression of inflammatory cytokines and chemokines (TNF-α, IL-1β, IL-6, and MCP-1) was also elevated in DIO mouse VAT and markedly elevated in LPS-activated control macrophages as expected, consistent with previous reports in which VAT inflammation was attributed to infiltration of M1 polarized macrophages. However, relative to macrophage-specific standards like F4/80, the expression of these inflammatory markers is unchanged. These data indicate that the changes in the overall inflammatory profile of DIO mouse VAT is because of quantitative changes in the ATM number and not qualitative changes in their activation state. These observations are consistent with the idea that infiltrating ATMs may have roles other than the previously described role in mediating inflammation in obese AT.

2.2. Introduction

Obesity and IR are associated with a complex immune program and chronic low-grade inflammation in AT where resident and recruited macrophages and other immune cells play a significant role in systemic insulin sensitivity (77, 91, 252, 267). Many hypotheses have been brought forth to explain why this immune response occurs including ER and oxidative stress, lipotoxicity and AT hypoxia (90, 176, 236). It is clear, however, that the metabolic complications along with increased immune cell infiltration and secretion of pro-inflammatory cytokines are directly related the chronic state of low-grade inflammation within the AT of obese humans and mice and potentiate IR (86, 91, 252, 267). Studies in our laboratory combining expression profiling with computational approaches discovered that the AT of IR obese patients exhibits higher expression of inflammatory genes than the AT of IS obese individuals matched for BMI (82). Additionally, when analyzed by flow cytometry, the omental AT of obese individuals demonstrates parallel increases in adiposity and macrophage accumulation. The significant accumulation of macrophages to become approximately 40% of cells within the AT illustrates a drastic shift in macrophage proportions in obesity (252). In agreement with these data, histological analysis of omental AT from obese IS and IR patients determined that increased adipocyte size and macrophage infiltration into the AT is a better predictor of IR than clinical measures of adiposity, highlighting the significance of understanding macrophage populations within obese AT, specifically the omental depot (82).

It has been extensively reported that both macrophages and adipocytes express inflammatory mediators, including TNF-α, IL-6, IL-1β, iNOS, MCP-1 and others; however, ATMs have been identified as the key regulators of the inflammatory phenotype displayed by obese AT (63, 134, 188, 252). ATMs are primarily increased in the omental AT depot of obese individuals and correlate with measures of obesity-induced IR (83). Although much effort has ensued to understand the recruitment or expansion of inflammatory macrophage populations within obese AT, resident tissue macrophages are also present within lean AT. The properties and functions of both resident and recruited ATMs are determined by their polarization toward an inflammatory or anti-inflammatory activation state. Macrophage polarization exists as a continuum characterized by specific gene expression profiles, but a simplistic differentiation between two activation phenotypes has been used to classify ATMs in obesity: classically activated (M1) or alternatively activated (M2) macrophages. This dichotomous classification of ATMs as either M1 or M2 does not fully capture both the diversity and functions of ATMs, but simplifies the nomenclature for defining macrophage populations within obese AT.

ATMs from lean individuals are predominately $CD11c^-$ and the first antigenically distinct subpopulation of ATMs to be discovered express the integrin CD11c (55). Although $CD11c^-$ and $CD11c^+$ ATM populations increase in obesity, $CD11c^+$ population expansion is much greater than $CD11c^-$ cells (55, 210). Originally characterized as M1 polarized, the $CD11c^+$ ATMs are thought to contribute disproportionately to the inflammatory phenotype and metabolic dysfunction of obese AT because M1

macrophages have enhanced production of inflammatory cytokines TNF-α and IL-1β, known to contribute to obesity-induced IR (63, 93, 136, 222). Functional studies in mice have demonstrated that ablation of CDllc^{+} macrophages and genetic deletion of molecules involved in inflammation (TNF-α, IKKβ, NLRP3, etc), results in improved glucose tolerance and insulin sensitivity, indicating their importance in metabolic disease pathogenesis (9, 237, 254). On the other hand, M2 ATMs, which are the major resident macrophages in lean AT, are characterized by the expression of arginase 1 (Ym-1), CD206, macrophage galactose N-acetyl-galactosamine specific lectin 1 (Mgl1), and IL-10, all known to be involved in tissue repair and remodeling (26, 63). Several groups have reported that CD11c^{+} ATMs are negative for these M2 markers of alternative activation, however, this has not been consistently found in rodents and humans (55, 208, 210, 255). Interestingly, the impairment of alternative macrophage activation by macrophage-specific PPARγ deletion results in DIO, IR, and glucose intolerance, highlighting the importance of M2 macrophages in maintaining systemic insulin sensitivity (168). Thus, ATM characterization is evolving away from the M1/M2 paradigm and toward a general understanding of the purpose, presence, and function of expanding ATM populations in obese AT. For simplicity, the macrophages referred to herein with be referenced as M1-like and M2-like to depict inflammatory or anti-inflammatory populations.

Evidence associating a phenotypic switch in ATM polarization from an anti-inflammatory M2-like state toward a pro-inflammatory M1-like state exists in DIO mouse models (136). The significance of this switch in polarization state is highlighted

by the random scattering of M2-like macrophages throughout the AT of lean mice versus the specific clustering of M1-like macrophages into CLS around necrotic adipocytes in obesity, demonstrating a change in ATM distribution that correlates with increasing adiposity (188, 252). At the time of this study, it was of particular interest to understand whether the increased M1-like:M2-like ATM ratio in obese AT was because of transdifferentiation or the expansion of M1-like macrophages in obese AT, even though the standard model of AT inflammation proposes that macrophages infiltrate obese AT and act as a conduit to initiate and exacerbate AT inflammation. Therefore, it was expected that macrophage infiltration into the AT would result in an increased inflammatory profile of DIO mouse AT. It is also known that resident tissue M2-like macrophages are at the junction of innate immunity and are responsible for inflammation resolution (167). Thus, we hypothesized that both resident and recruited ATMs may serve an alternative function and act in a non-inflammatory and perhaps protective role within the AT; a role that had not been reported at the initiation of this study.

To address this question, we compared the gene expression profiles of *ex vivo* activated macrophages to the genome wide expression in VAT and SAT from DIO mice to determine whether ATMs displayed similar elevation of inflammatory markers. We used this strategy to distinguish between two possible outcomes: increased activation or recruitment of M1 polarized macrophages should result in disproportionately higher expression of inflammatory markers (TNF-α, IL-6, IL-1β) compared to common macrophage markers like F4/80. On the other hand, if recruitment or expansion of the macrophage population occurs without activation, we would expect proportionate

increases in both categories of markers. In fact we observe the latter: as expected, VAT (but not SAT) from DIO mice show increased expression of inflammatory markers, however, this increase is proportional to the increase in general macrophage markers. This contrasts with the *ex vivo* M1 polarization model in which inflammatory marker expression is massively increased while general macrophage markers are unchanged. These data suggest that the changes in the overall inflammatory profile of DIO mouse VAT is mainly because of quantitative changes in ATM number and not qualitative changes in activation state. This is consistent with the idea that the expanded population of ATMs may include cells with alternative, possibly beneficial functions in obese AT.

2.3. Results

High fat feeding promotes macrophage accumulation into VAT but not SAT of DIO mice.

In human obesity, body type and fat distribution play an important role in the maintenance of systemic insulin sensitivity. The anatomical location of AT determines the inflammatory profile, with VAT being associated with a more adverse risk profile than SAT for the metabolic syndrome and T2DM (61). A number of studies have demonstrated that macrophages infiltrate the omental and VAT of obese humans and mice and a phenotypic switch from M2 to M1 activation state occurs, thus correlating M1 accumulation with the development of systemic IR (252, 261). Therefore, we wanted to confirm published data regarding the inflammatory signature of two anatomically distinct AT depots, VAT and SAT, and analyze whole AT by microarray analysis to determine macrophage-specific and inflammatory gene expression.

To assess the inflammatory changes within obese AT, WT mice were fed a high fat diet for 13 weeks. These DIO mice gained more weight than lean control mice beginning at 3 weeks and remained significantly more obese throughout the end of the study **(Figure 2.1 A; 30.9 ± 0.75 vs. 42.08 ± 0.78 g; $p \leq 0.001$)**. At the end of 13 weeks, DIO mice were more glucose intolerant as demonstrated by elevated fasting blood glucose concentrations **(Figure 2.1 B; $p \leq 0.02$)**, elevated fasting insulin levels **(Figure 2.1 C; $p < 0.02$)**, and increased area under the curve for the IPGTT (**Figure 2.1. B; (min*mg/dL) = 29352 ± 753 vs. 38983 ± 1928; $p \leq 0.01$)**.

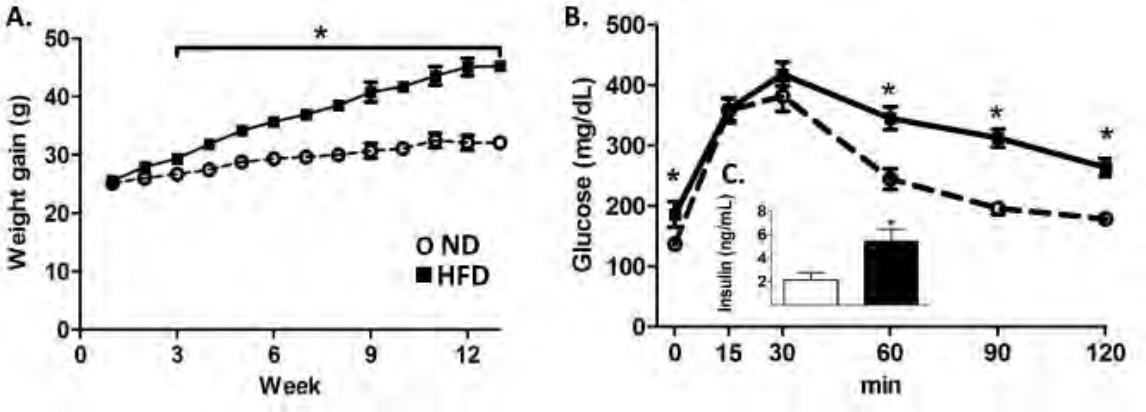

Figure 2.1. HFD mice displayed glucose intolerance and insulin resistance at the end of 13 weeks. WT mice were fed a ND or HFD for 13 weeks and glucose tolerance and insulin resistance were assessed by GTT. **A.)** Growth curves of C57BL6/J mice on ND (n = 12, dashed line) and HFD (n = 12, solid line). Weights were significantly different at all time points after 3 weeks (* $p < 0.001$). **B.)** IPGTT of ND (n = 12, dashed) and HFD (n = 12, solid line) at 13 weeks (AUC with baseline correction = 29352 ± 753 vs. 38983 ± 1928 (min*mg/dL); $p \leq 0.01$). **C.**) Fasting insulin levels of ND (n = 12, white) and HFD mice (n = 12, black) at 13 weeks (inside B. graph) (* $p < 0.02$). The values are represented as the mean ± SEM. An unpaired student's t-test was used for comparisons between groups. Figure from Fitzgibbons, et al. Am J Physiol Heart Circ Physiol. 2011.

We used gene expression profiling of macrophage-specific gene expression to examine macrophage presence within the tissue as well as the inflammatory profile of the AT of DIO mice. Our gene profiling experiment directly compared whole VAT and SAT explants to *ex vivo* activated peritoneal exudate cell macrophages (PECs) that were untreated or LPS-stimulated, which would drive an M1 gene expression profile to represent a classical M1-type macrophage as a control. Upon LPS stimulation, macrophage-specific marker gene expression (F4/80, CD68, CD11c, CD11b) was unchanged **(Figure 2.2 A)** and therefore, these genes served as standard macrophage markers to determine the presence of macrophages within the AT. Expression profiling was performed on total RNA preparations from whole AT, including adipocytes and the SVF which contains preadipocytes, fibroblasts, endothelial and immune cells. Our data is consistent with previous observations as we observed mRNAs of these standard macrophage-specific markers to be significantly increased by as much as 8-fold in the VAT of DIO mice compared with lean control mice **(Figure 2.2. A; $p \leq 0.01$)**. Interestingly, we did not observe this increase in SAT **(Figure 2.2. A)**. Confirmation of the microarray by qRT-PCR illustrated that macrophage-specific marker gene expression was significantly increased 8-35 fold in the VAT from DIO mice compared with lean control mice **(Figure 2.2. B; $p \leq 0.001$)**. No changes in macrophage marker genes are observed in the SAT of DIO mice compared with lean control animals **(Figure 2.2 C)**. In agreement with the genomics and qRT-PCR data, an enrichment of $F4/80^{+}$ macrophages was observed by histology in the VAT but not the SAT of DIO or the AT of lean control mice (**Figure 2.3 A-D**). These data illustrate that obesity drives increased macrophage

population into DIO mouse VAT without changes to the macrophage content in the SAT depot. This indicates that the SAT and VAT depots respond differently to high fat feeding and suggests a potential different microenvironment within the two AT depots.

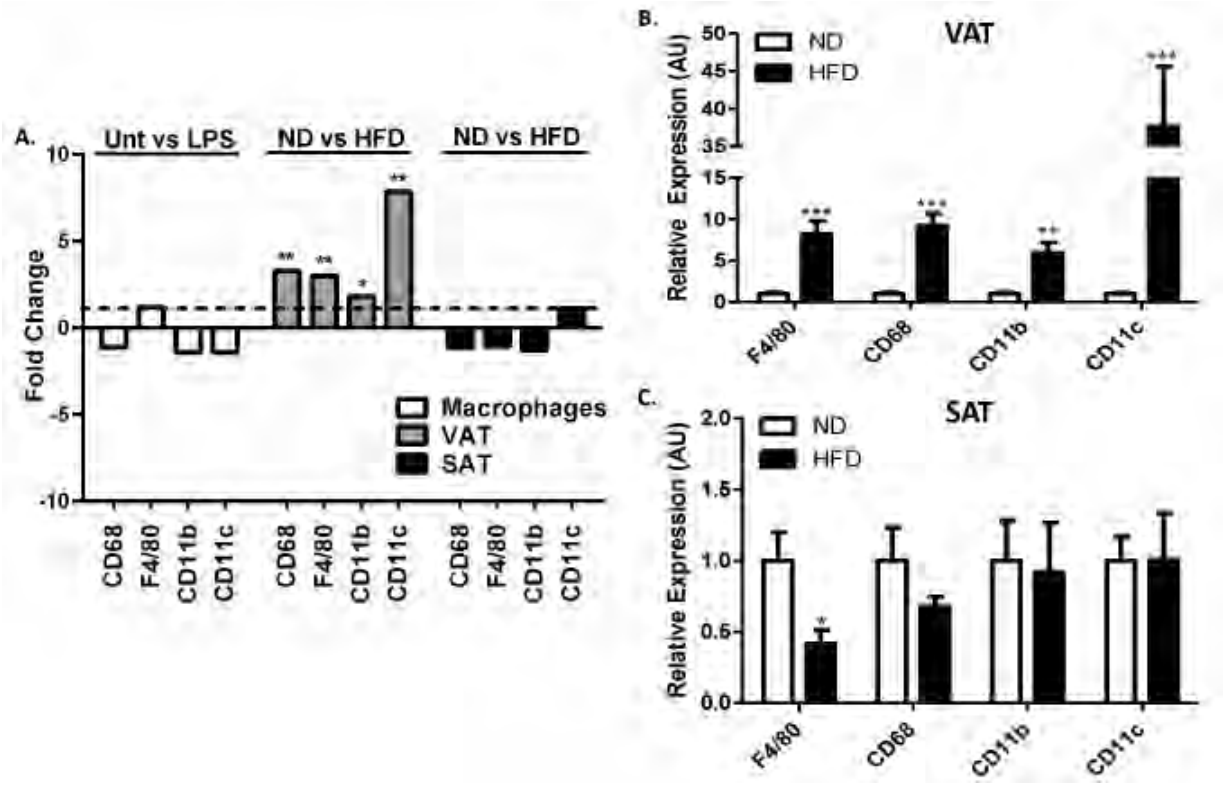

Figure 2.2. Standard macrophage marker genes were unaffected by LPS treatment but are significantly increased in obese VAT and unchanged in SAT. Thioglycollate-elicited PECs were isolated from 10-week old WT mice and stimulated *ex vivo* with LPS for 6 hours. WT mice were HFD-challenged for 13 weeks and whole VAT and SAT was harvested from ND and HFD fed mice. RNA was extracted from PECs and whole AT and microarray analysis was performed. The data are representative of 12 DIO, 12 lean mice and 3 experimental replicates *ex vivo*. A) The data represent the average fold change of macrophage-specific surface marker mRNAs, which were not affected after LPS treatment in PECs (white bars) or the presence of these genes in VAT (grey bars) and SAT (black bars) of obese mice compared with lean controls. RNA was subjected to quantitative RT-PCR for macrophage-specific gene expression (CD68, F4/80, CD11b, and CD11c) to confirm the microarray data in B.) VAT and C.) SAT. The values represent the mean ± SEM. An unpaired student's t-test was used for comparisons between groups. * $p < 0.01$, ** $p < 0.001$.

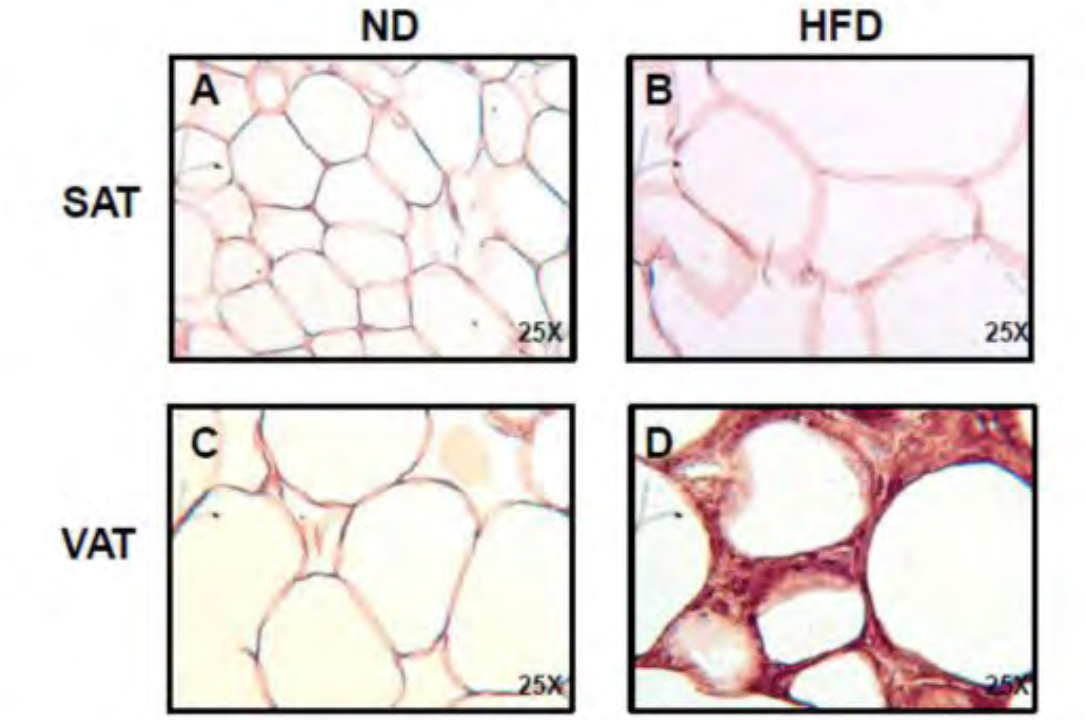

Figure 2.3. SAT is resistant to diet-induced inflammation, but VAT is enriched with F4/80 positive macrophages in DIO mice. C57Bl6/J mice were HFD-challenged for 13 weeks and whole VAT and SAT was harvested from ND and HFD fed mice (n = 3 per group). Samples were fixed in 4% formalin, sectioned, and stained with rat anti-mouse F4/80 primary antibodies (ABd Serotec). Staining was visualized with HRP-linked rabbit anti-rat secondary antibodies. Minimal staining was observed in the **A.**) SAT of lean control mice **B.**) SAT of DIO mice or in the **C.**) VAT of lean control mice. Abundant macrophages were seen predominantly in the **D.**) VAT of DIO mice, forming crown like structures surrounding adipocytes. Figure from Fitzgibbons, et al. Am J Physiol Heart Circ Physiol. 2011.

Markers of inflammation show minimal or no change in obese VAT relative to macrophage-specific genes.

ATMs produce pro-inflammatory cytokines and chemokines such as TNFα, IL-6 and MCP-1/CCL2, which may contribute to the induction of IR (173). The production of these canonical markers of inflammation increase in whole AT from obese mice, which is attributed to the presence of classically activated M1 macrophages (26, 262). Because we observed significant increases in macrophage-specific marker genes in the DIO mouse VAT **(Figure 2.2 A-B)**, we expected to find parallel increases in the mRNAs of classical gene products of inflammation. These genes were markedly elevated, upwards of 60 fold in LPS-stimulated macrophages, an *ex vivo* model of macrophage activation (**Figure 2.4 A; $p < 0.001$**). Though common macrophage markers are increased in VAT, the expression levels of inflammatory cytokine microarray data (TNFα, IL-1β, IL-6) are unchanged in the DIO mouse SAT or VAT when compared with lean control mice; inconsistent with the current belief that macrophages exacerbate inflammation within the AT of obese mice (**Figure 2.4 A-B)**. However, as expected, chemoattractant proteins MCP-1/CCL2 and MIP-1β/CCL4 were both significantly increased in DIO mouse VAT, with the latter also significantly increased in SAT (**Figure 2.4 A; $p \leq 0.05$)**. These data encouraged the question of whether macrophages in obese mouse AT are in a classical M1 activation state. Increased activation or recruitment of M1 polarized macrophages should result in disproportionately higher expression of inflammatory markers (TNF-α, IL-6, IL-1β) compared to common M1/M2 markers like F4/80. However, we observed no elevation in the inflammatory signature of the DIO mouse AT compared with lean

control mice **(Figure 2.5).** This suggests that the recruitment or expansion of the macrophage population in obese mouse VAT occurs without activation because the inflammatory gene expressions obtained from the microarray are unreflective of the enriched macrophage content.

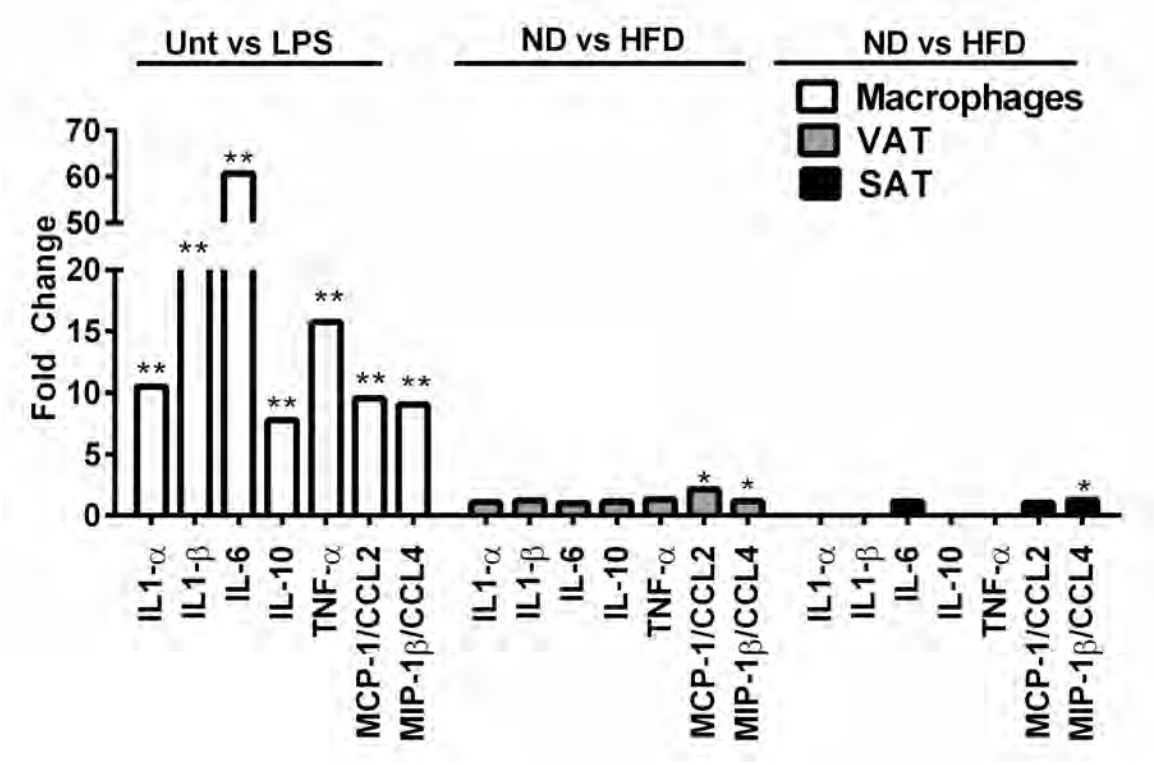

Figure 2.4. Genomic profiling of inflammatory markers in obese AT reveals minimal or no change in expression compared to M1-activated macrophages. Thioglycollate elicited PECs were isolated from 10-week old WT mice and stimulated *ex vivo* with LPS for 6 hours. VAT and SAT was harvested from 13-week HFD-challenged WT mice. RNA was extracted from PECs and whole AT of ND and HFD fed mice and microarray analysis was performed. The data are representative of 12 DIO, 12 lean mice and 3 experimental replicates *ex vivo*. The data represents the average fold change of classical inflammatory gene mRNAs. LPS-treatment in PECs (white bars) significantly upregulates inflammatory gene expression indicating M1 polarization and activation of classical inflammatory signaling. These genes demonstrate little or no significance in VAT (grey bars) or SAT (black bars) of DIO mice compared with lean control mice. The values represent the mean ± SEM. An unpaired student's t-test was used for comparisons between groups. * $p \leq 0.05$, *** $p \leq 0.005$.

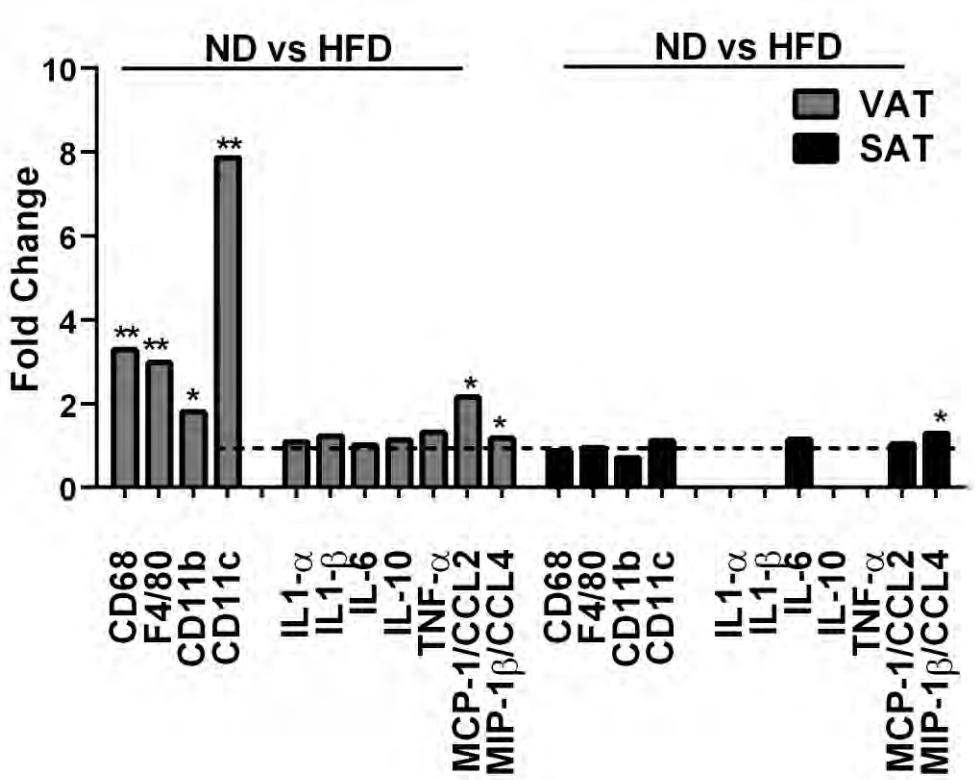

Figure 2.5. Genomic profiling of inflammatory markers show minimal or no increase in obese VAT despite macrophage-specific gene enrichment. VAT and SAT was isolated from 13-week HFD-challenged mice. RNA was extracted from the whole AT of ND and HFD fed mice and microarray analysis was performed. The data are representative of 12 DIO and 12 lean mice. Macrophage-specific marker genes (CD68, F4/80, CD11b, and CD11c) are compared with mRNAs of inflammatory genes in VAT (grey bars) and SAT (black bars) to illustrate the blunted immune response in AT albeit macrophage-specific genes are enriched in VAT. The values represent the mean ± SEM. An unpaired student's t-test was used for comparisons between groups. ***** $p \leq 0.05$.

DIO mouse VAT inflammatory gene expression is proportional to the increase in macrophage-specific markers.

We used a quantitative approach to clarify genomics data revealing a blunted immune response in the AT, particularly in the DIO mouse VAT. Classical RT-PCR analysis is dependent upon the normalization of each gene of interest to a ubiquitously expressed, invariant endogenous control or housekeeping gene, which is unaffected by the stimulus utilized in the experiment. Standard normalization of qRT-PCR analysis uses the same reference gene for each experimental analysis including, but not limited to: β-actin, cyclophilin-B, and ribosomal 36B4. As expected, inflammatory gene expression relative to ribosomal 36B4 or cyclophilin-B, we observed robust increases in TNF-α, IL-1β, IL-6, interferon-γ (IFN-γ), IL-10 and MCP-1/CCL2 expression in DIO mice compared with lean control mice **(Figure 2.6 A-F; * $p \leq 0.05$, ** $p \leq 0.01$, *** $p \leq 0.001$)**. However, relative to macrophage-specific markers (CD68, F4/80 and CD11c), that were a measure of the macrophage content within the VAT, this increase in TNF-α, IFN-γ, IL-10 and MCP-1/CCL2 was ameliorated, and in this case a significant decrease in their expression was observed when DIO mice were compared with lean control mice (**Figure 2.6 A, D-F; * $p \leq 0.01$,*** $p \leq 0.001$**), which was not observed relative to macrophage marker CD11b (**Figure 2.6, A, D-F**). In the case of IL-1β, we observed no expression change relative to general macrophage markers, but a significant decrease when normalized to M1 activation marker CD11c in DIO mice compared with lean control mice (**Figure 2.6 B, ***$p \leq 0.001$**). Lastly, a slight decrease in IL-6 expression was observed relative macrophage-specific genes in the VAT of DIO mice compared

with lean controls: however, it does not return to baseline values (**Figure 2.6 C**). Together, these data indicate that the classical markers of M1 activation and AT inflammation increase proportionally to the increase in general macrophage markers. Thus, the obesity-induced rise in AT inflammation may be because of increased macrophage number and proportions within obese VAT, and that the expanding VATM population may not be M1 polarized in DIO mice.

.

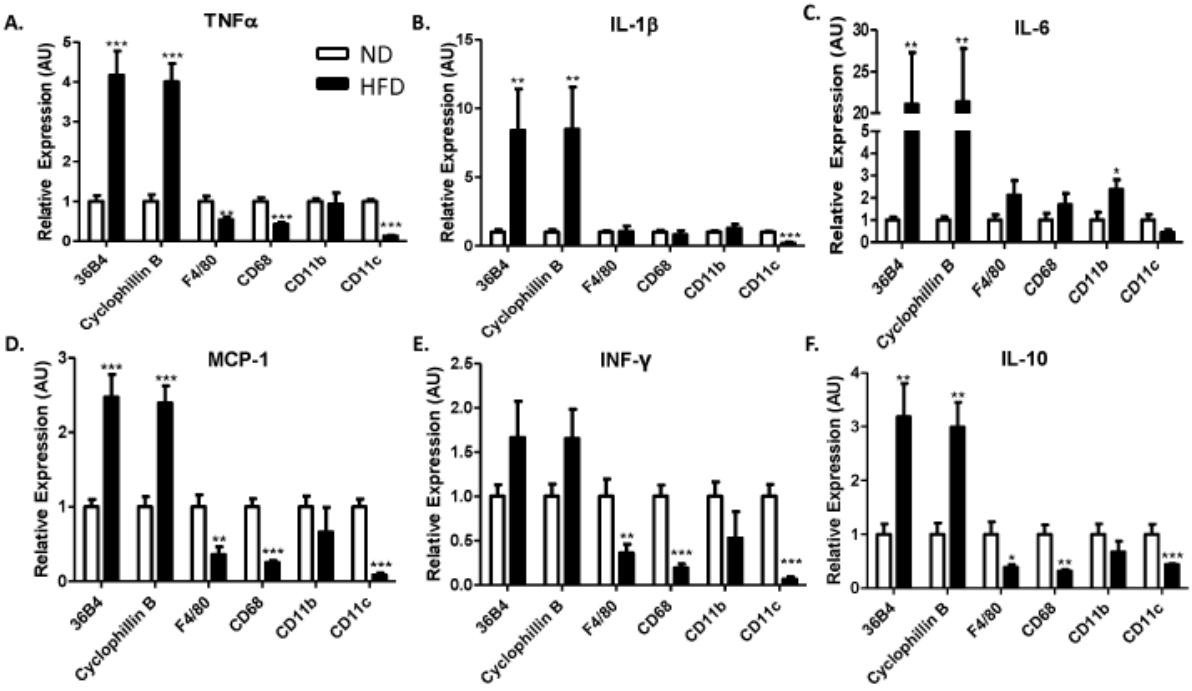

Figure 2.6. Classical inflammatory gene expression is proportional to macrophage-specific marker genes in obese VAT. VAT was isolated from 13-week HFD-challenged. RNA was extracted from whole VAT of ND and HFD fed mice and subjected to qRT-PCR analysis. The data is representative of 12 DIO and 12 lean mice. Both standard reference housekeeping genes and macrophage-specific marker genes (CD68, F4/80, CD11b, and CD11c) were used to normalize the expression of inflammatory genes: **A.** TNF-α, **B.** IL-1β, **C.** IL-6, **D.** MCP-1/CCL2, **E.** IFN-γ, and **F.** IL-10. The values represent the mean ± SEM. An unpaired student's t-test was used for comparisons between groups. ***** $p \leq 0.05$, ****** $p \leq 0.01$, ******* $p \leq 0.001$.

2.5. Discussion

Over the last decade, the concepts adapted by metabolic research and immunology have converged as many studies have reported significant elevations in the number of ATMs in VAT and SAT of obese humans and mice that are tightly associated with chronic inflammation and IR (56, 252, 261). We combined gene expression profiling with computational analysis of two anatomically distinct AT depots, VAT and SAT, to determine whether obese AT inflammation is because of ATM expansion or activation. Consistent with the current model of obesity-induced ATM enrichment, we observed significant increases in standard macrophage-specific gene expression (F4/80, CD68, CD11b, and CD11c) in DIO mouse VAT compared with lean control mice, without changes in the SAT ATM content (**Figure 2.2 and Figure 2.3**). As expected, classical markers of M1 activation and AT inflammation are increased in DIO mouse VAT (but not SAT), however, this increase is proportional to the increase in general macrophage markers (**Figures 2.4-2.6**). This contrasts with the *ex vivo* M1 polarization model in which inflammatory marker expression is massively increased while general macrophage markers are unaffected by macrophage activation. To this end, the data herein suggest that the changes in the overall inflammatory profile of DIO mouse VAT is mainly because of quantitative increases of the ATM population and not because of qualitative changes in macrophage activation states.

In human obesity, it is understood that body type and specific differences in fat distribution affect whole-body metabolism, as the AT location is tightly associated with inflammation; VAT being associated with a more adverse risk profile than SAT for the

metabolic syndrome and T2DM (61). The anatomical location of VAT versus SAT is essential to their involvement in metabolic disease progression and IR, as expansion of VAT in humans contributes to increased hepatic delivery of FFAs because of increased AT lipolysis, thus driving hepatic IR (161). In contrast, the FFAs released from SAT are delivered into peripheral circulation, reducing their affect on hepatic IR (161). TZD treatment to improve insulin sensitivity increases total fat mass mostly in SAT fat stores, and this increased SAT, especially in the lower extremities, is associated with a decreased risk of disturbed glucose metabolism and dyslipidemia, independent of VAT expansion (209, 218). This indicates that SAT plays a protective role in the context of metabolic disease. Thus, it is not surprising that in our study the inflammatory signature of the SAT was unchanged with limited macrophage infiltration when compared with the VAT from the same DIO mice (**Figure 2.2 and Figure 2.3**). This suggests that not only is the SAT resistant to HFD-induced inflammation, but that VAT and SAT are anatomically distinct AT depots that respond differently to DIO. Thus, it is possible that the contrasting affects of SAT and VAT on systemic insulin sensitivity may be due to dissimilar tissue microenvironments between the two depots, indicating a correlation between VAT inflammation and disturbed glucose tolerance in DIO mice (**Figure 2.1 and Figure 2.2 A and C**).

These data encouraged the endeavor to expand upon the standard model of AT inflammation and determine whether the inflammatory profile of the DIO mouse VAT is because of obesity-induced macrophage enrichment or activation. We predicted that our data would coincide with the initial paradigm of obesity-induced macrophage activation

in VAT and we hypothesized that DIO causes robust increases in VAT inflammatory gene expression (86, 252, 261). We used LPS-stimulated macrophages as an *ex vivo* model of macrophage activation, because the literature indicates that VATMs display the characteristic phenotype of M1 macrophages (**Figure 2.4**) (134-136, 142). We report significant elevations in pro-inflammatory gene expression in LPS-stimulated macrophages compared with unstimulated cells, without changes in macrophage-specific marker genes, like F4/80; thus permitting their use as a measure of macrophage content within obese AT (**Figure 2.2 A and Figure 2.4**). Although we observed a significant enrichment of these macrophage marker genes in DIO mouse VAT compared with lean control mice, the genomic analysis revealed little or no changes in the classical inflammatory markers of M1 activation and AT inflammation (**Figure 2.4 and Figure 2.5**). Increased M1 polarization of VATMs should result in disproportionately higher expression of inflammatory markers (TNF-α, IL-6, IL-1β) in DIO mouse VAT compared to common M1/M2 markers. Unexpectedly, the genomics analysis revealed that these inflammatory cytokines were unchanged despite significant increases in macrophage marker gene expression suggesting that the expanded ATM population may not be M1 polarized (**Figure 2.5**).

Although our genomics analysis indicates an inconsistency with published data regarding the inflammatory profile of VAT, it is important to note that the time-course of high fat feeding is in accordance with the recent literature. The mice used in this study were challenged with a HFD for 13-weeks and demonstrated decreased glucose tolerance and hyperinsulinemia (**Figure 2.1 B-C**). Lee et al. assessed the temporal events

underlying IR development during high fat feeding and found that lipotoxicity was causal for short-term diet-induced IR, while chronic inflammation emerged as a more dominant mechanism once obesity is established by long-term HFD challenge (128). Even though lipotoxicity may not be the driving force for diet-induced IR in the long-term, *in vitro* treatment of macrophages with saturated FAs or conditioned medium from adipocyte cell lines increased M1 gene expression providing evidence that lipids released from adipocytes drives M1 polarization in obese AT (211, 225, 262). It is also well established that macrophages infiltrate obese AT to internalize cell debris from necrotic adipocytes and studies comparing the histology of lean and obese VAT illustrates the formation of CLS around these dying adipocytes (137, 252). These CLS are not solely infiltrating macrophages, as a recent study from our laboratory discovered that proliferation *in situ* is an important process by which macrophages accumulate in inflamed AT of both genetic and DIO mouse models of obesity (1). In agreement with this, the histology from DIO mouse VAT illustrated significant enrichment of an F4/80^{+} macrophage population with the appearance of CLS when compared with lean control mice (**Figure 2.3 C and D**). It was also recently discovered that macrophages aid in sequestering FAs released from dying adipocytes, giving rise to foam cell formation within obese AT (118, 188, 252). The accumulation of lipid species and LDs in ATMs are observed in classically activated M1 macrophages, introducing an alternative role of M1 ATMs in obesity (188). This discovery coincides with our proposed idea that expanded population of ATMs may act in a non-inflammatory role, as our genomics analysis reveal minimal or no changes in inflammatory gene expression, despite macrophage gene enrichment.

We further explored this idea by assessing the changes of inflammatory gene expressions relative to macrophage specific markers to distinguish between increased macrophage activation or increased macrophage content in DIO mouse VAT by qRT-PCR analysis (**Figure 2.6**). Classical analysis of qRT-PCR data is dependent upon the normalization of each gene of interest to an invariant endogenous control; thus, the quality of the normalized data cannot be better than the quality of this reference gene. Importantly, these reference genes are unaffected by experimental stimuli and in this case being DIO and LPS-driven macrophage activation (238). In our laboratory, 36B4 and cyclophilin-B have proven to be reliable references genes in multiple cell types and tissues including AT. Thus, we used these genes to confirm published data, but also used standard macrophage-specific genes that signify the macrophage content within the AT to determine proportional changes in inflammatory gene expression. As expected, relative to 36B4 or cyclophilin-B, we observed robust increases in the expression of TNF-α, IL-1β, IFN-γ, IL-10 and MCP-1/CCL2 when DIO mice are compared with lean control mice (**Figure 2.6**). However, relative to macrophage marker genes F4/80, CD68, and CD11c, a dramatic overall decrease in expression was observed (**Figure 2.6**). Furthermore, a more robust decrease was evident when DIO mouse VAT expressions were compared with lean control mice (**Figure 2.6**). Interestingly, inflammatory gene expressions were decreased when normalized to CD11b compared with 36B4 or cyclophilin-B; however, no decrease was evident when compared with lean control mice (**Figure 2.6**). This observation may be because CD11b is not solely an ATM marker; it is also expressed by many leukocytes including monocytes, neutrophils, granulocytes, dendritic cells, NK

cells and a subset of $CD8^+$ T cells (29). Recent literature suggest that many subtypes of immune cells are responsible for AT inflammation and are required to control both the macrophage content and the polarization state within obese AT (115, 162-163, 259). Thus, CD11b may not be an appropriate gene for normalization of macrophage infiltration into the VAT of DIO mice. Conversely, CD11c is a classic marker used to characterize M1-polarized ATMs in the AT of obese mice. Our data illustrates dramatic decreases in inflammatory gene expression when normalized to this M1 macrophage specific gene (63, 136). Consistent with these findings, a recent publication by Xu et al., determined that the expression of most inflammatory genes was unchanged between purified $CD11c^-$ and $CD11c^+$ ATM populations in an unbiased analysis of lean, diet-induced and genetically obese mice (262). This parallels our study because although some M1 genes were increased, most of the M1 genes (TNF-α, IL-1β, IL-6) were reduced when normalized to macrophage-specific genes, indicating a lack of ATM activation in DIO mouse AT (262). Therefore, our data suggest that the increased inflammatory gene expressions in AT is due to an increase in overall macrophage cell number within the VAT and not indicative of ATM polarization toward a classical M1 phenotype.

Lastly, we explored the possibility of macrophage plasticity and that these macrophages may be in an alternative state of activation. Alternatively activated M2 macrophages predominate in the AT of lean mice and function to maintain tissue integrity by their involvement in tissue repair and extracellular matrix/remodeling (135-136, 188). ATMs from 5-week old *ob/ob* mice express high levels of genes involved in extracellular matrix/remodeling and anti-inflammatory macrophage markers (Arg1 and

CD209e) indicating M2-macrophage involvement in mild obesity as expression levels are reduced in 16-week old severely obese *ob/ob* mice (188). Our data regarding M2 macrophage activation within the obese AT was inconclusive and requires further analysis (data not shown). More recently, however, it was discovered that the AT microenvironment does not activate or drive inflammatory polarization of ATMs per se, but induces a differentiation program in which lipid uptake and lysosome biogenesis are coordinately regulated (262). In conjunction with these results, liposomal-mediated ATM depletion increased circulating FFA concentrations (**Table 3.1**), confirming their role in lipid uptake and suggesting that AT lipid metabolism may not be confined to the adipocyte, but that ATMs also play a role (118).

The data provided herein demonstrate the complexities of ATM function in DIO mouse VAT and encourage the on-going studies to understand these complex roles of ATMs in obesity and inflammation. Our data suggest that relative changes in the overall inflammatory signature of VAT is induced by quantitative increases in the number of macrophages enriched in obese AT rather than qualitative changes in ATM polarization to a classical inflammatory M1-like state (**Figure 2.7**). These data also do not disqualify the current model in which factors secreted from the AT can recruit and activate both resident and infiltrating macrophages or that inflammatory factors secreted from ATMs are largely responsible for the metabolic consequences that accompany obesity. This study, however, does indicate that although DIO mouse VATMs are enriched in number, this expanding macrophage population of ATMs may not be present with the purpose to exacerbate AT inflammation; VATM populations may include cells with alternative,

possibly beneficial functions in obese AT to serve alternative and trophic functions, even in the obese state in mice.

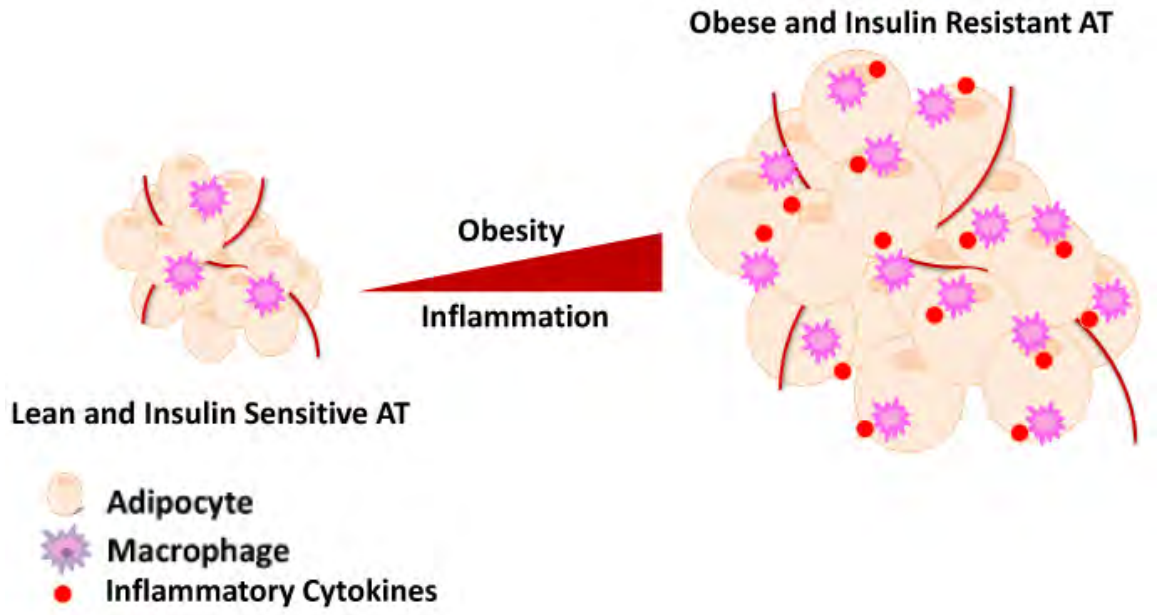

Figure 2.7. VAT inflammation is increased relative to the increased macrophage content in obese AT. Lean and insulin sensitive AT maintains normal metabolic function and contains resident tissue macrophages with a characteristic phenotype of alternative activation. As obesity develops, adipocytes undergo hypertrophy owing to increased TG storage. As the expansion limit of AT is reached, triglyceride storage and metabolic dysfunction occur as well as insulin resistance. Obese IR VAT has increased levels of immune cells and expansion of ATM populations that contribute to the increased inflammatory signature of obese IR VAT. However, the VAT inflammation is increased proportionally to the changes in increased ATM content indicating that the quantitative changes in macrophage cell number and not qualitative changes in the activation state of the expanding ATM populations promote the transition to an inflammatory tissue environment in obese mouse VAT.

2.6. Experimental Procedures

Animals, Diets and Treatments

Wild type male C57Bl6/J mice were obtained from the Jackson Laboratory (Bar Harbor, ME). Animals used for HFD studies were fed standard chow diet (LabDiet PicoLab 5053, Purina Mills, St. Louis, MO) until 8 weeks of age and then divided into two groups; one was fed chow diet and the other group was fed HFD (45 kcal% fat, D12451, Research Diets, New Brunswick, NJ) for 13 weeks. Animals were housed in the University of Massachusetts (UMass) Medical School Animal Medicine facility with a 12-hour light/dark cycle and given *ad libitum* access to food and water. Animals were weighed weekly for the duration of the diet study. IPGTT was performed as previously described (187). The AUC for the IPGTT was calculated using the trapezoidal method (187). At the completion of the HFD, mice were fasted for 6 hours and then euthanized with CO2 inhalation and bilateral pneumothorax. All of the experiments were performed in accordance with protocols approved by the Institutional Animal Care and Use Committees (IACUC) at UMass Medical School.

Sample Storage

SAT and VAT were harvested and snap frozen in liquid nitrogen for RNA or paraffin embedded for immunohistochemical analysis. Blood was drawn via the retro-orbital sinus into EDTA tubes; plasma was centrifuged at 10,000 rpm for 10 min and aliquotted. All of the samples were stored at -80C.

Primary cell isolations and culture

10-week old C57BL6/J male mice were i.p. injected with 4% thioglycollate broth (Sigma–Aldrich). At 5 days following the injection, mice were euthanized by CO_2 inhalation, and the peritoneal cavity was washed with 5 ml ice-cold PBS to isolate PECs. Peritoneal fluid was filtered through a 70 μm diameter pore nylon mesh and centrifuged at 270 x *g* for 10 min. The pellet was first treated with red blood cell lysis buffer (8.3 g of NH_4Cl, 1.0 g of $KHCO_3$ and 1.8 ml of 5% EDTA) and then plated in DMEM (Dulbecco's modified Eagle's medium) supplemented with 10% (v/v) FBS (fetal bovine serum), 50 μg/ml streptomycin and 50 units/ml penicillin. At 24 hours after isolation, PECs were either untreated or treated with LPS for 6 hours.

RNA isolation and quantitative RT-PCR

Whole VAT and SAT were isolated, snap frozen in liquid nitrogen, and stored at −80°C. Tissues were homogenized using the gentleMACs Dissociator (Miltenyi Biotec) and RNA was isolated following the manufacturer's protocol (TriPure, Roche). RNA was isolated from cultured PECs according to the manufacture's protocol. Precipitated RNA was treated with DNAse (DNA-free, Life Technologies) prior to reverse transcription (iScript Reverse transcriptase, BioRad). SYBR green quantitative PCR (iQ SYBR green supermix, BioRad) was performed on the BioRad CFX97. Expression was normalized to the ribosomal gene *36B4* or standard macrophage marker genes (F4/80, CD68, CD11b, CD11c) and expressed relative to the expression of ND mice or untreated PECs. The

internal loading controls 36B4 or cyclophilin-B did not change with diet or LPS treatment. Melt curve analysis was performed to determine PCR reaction product specificity. Primer sequences were designed with Primer Bank. Primer sequences are as follows: 36B4: 5'- TCCAGGCTTTGGGCATCA-3', 3'- CTTTATCAGCTGCACATCACTCAGA-5'; CD11b: 5'- CCATGACCTTCCAAGAGAATGC-3', 3'-ACCGGCTTGTGCTGTAGTC-5'; CD11c: 5'- CTGGATAGCCTTTCTTCTGCTG-3', 3'- GCACACTGTGTCCGAACTCA-5'; F4/80: 5'- CCCCAGTGTCCTTACAGAGTG-3', 3'- GTGCCCAGAGTGGATGTCT-5'; CD68: 5'-GGACCCACAACTGTCACTCA-3', 3'-AAGCCCCACTTTAGCTTTACC-5'; IL1-β: 5'- GCAACTGTTCCTGAACTCAACT-3', 3'- ATCTTTTGGGGTCCGTCAACT-5'; TNF-α: 5'-CAGGCGGTGCCTATGTCTC-3'; IL-6: 5'- TAGTCCTTCCTACCCCAATTTCC-3', 3'- TTGGTCCTTAGCCACTCCTTC-5'; IFN-γ: 5'-AATGAACGCTACACACTGCATC-3', 3'-CCATCCTTTTGCCAGTTCCTC-5'; MCP-1/CCL2: 5'- TTAAAAACCTGGATCGGAACCAA-3', 3'- GCATTAGCTTCAGATTTACGGGT-5'

Histology and Immunohistochemistry

AT samples (n = 3 per group) from lean and DIO mice were fixed in 4% formalin for immunohistochemistry. Briefly, samples were embedded in paraffin, sectioned, and stained with rat anti-mouse F4/80 antibodies (ABd Serotec, Raleigh, NC) (1:40 dilution). Staining was visualized with HRP-linked rabbit anti-rat secondary antibodies. Staining

with the secondary antibodies alone was performed as a negative control. Images were taken with a Zeiss Microscope and PixeLINK SE Software

Microarray Analysis

RNA was isolated from SAT, VAT and PECs as previously described. RNA concentrations were determined using a Nanodrop 2000 Spectrophotometer (Thermo Fisher, Willmington, DE). The RNA quality was assessed using an Agilent 2100 Bioanalyzer (Agilent Technologies, Santa Clara, CA). Only samples with a RNA Integrity Number > 7.5 and normal 18 and 28s fractions on microfluidic electrophoresis were used. In total, 250 ng total RNA was used as template for cDNA synthesis and *in vitro* transcription using the Ambion WT Expression kit (Ambion, Carlsbad, CA). Second strand cDNA was then labeled with the Affymetrix WT Terminal Labeling kit and samples were hybridized to Affymetrix Mouse Gene 1.0 ST arrays (Affymetrix, Santa Clara, CA). Gene chip expression array analysis for individual genes was performed as previously described (230), filtering for $p < 0.05$ and a fold change > 2. Four biological replicate hybridizations per genotype and diet and 3 biological replicates per *in vitro* condition were performed for a total of 18 hybridizations. Robust multi-array average (RMA) was adopted in the UMASS Microarray Computational Environment (MACE) to preprocess raw oligonucleotide microarray data. The preprocessed data are stored as base 2 log transformed real signal numbers and are used for fold change calculations and statistical tests and to determine summary statistics. Mean signal values and standard deviations are computed for each gene across triplicate experiments and

stored in the database. The fold change of expression of a gene in two experiments is the ratio of mean signal values from these experiments and is always a number greater than one. If the ratio is less than one, the negative value of the inverse ratio is stored as fold change. All down regulated genes therefore have a negative fold change value and up regulated genes have a positive fold change. In both cases this value is greater or equal than one. To determine differential gene expression in two hybridization experiments, MACE internally conducts a student's t-test with the expression signal values of the two hybridizations for all genes in the set. The t-test value and test p-value are stored in MACE and can be queried through the MACE user interface.

Statistical Analysis

All of the values are demonstrated as the mean ± SEM. For experiments other than the microarray analyses, a student's t-test for two-tailed distributions with equal variances was used for comparison between 2 groups. Differences less than $p < 0.05$ were considered to be significant. The AUC for the IPGTT was calculated using a student's t-test after performing a baseline correction for the basal glucose values for each individual mouse. All of the data were entered into Microsoft Excel, and statistical analyses were performed with Graph Pad Prism 5.0.

Chapter III: IL-1 Signaling in Obesity-induced Hepatic Lipogenesis and Steatosis

This chapter is submitted in the published format: Kimberly A. Negrin, Rachel J. Roth Flach, Marina T. DiStefano, Anouch Matevossian, Randall H. Friedline, DaeYoung Jung, Jason K. Kim, Michael P. Czech. IL-1 Signaling in Obesity-induced Hepatic Lipogenesis and Steatosis. PLoS One (submitted 2014)

3.1. Abstract

Non-alcoholic fatty liver disease is prevalent in human obesity and T2DM, and is characterized by increases in both hepatic TG accumulation (denoted as steatosis) and expression of pro-inflammatory cytokines such as IL-1β. We report here that the development of hepatic steatosis requires IL-1 signaling, which upregulates Fas to promote hepatic lipogenesis. Using clodronate liposomes to selectively deplete liver KCs in *ob/ob* mice, we observed remarkable amelioration of obesity-induced hepatic steatosis and reductions in liver weight, TG content and lipogenic enzyme expressions. Similar results were obtained with DIO mice, although VATM depletion also occurred in response to clodronate liposomes in this model. There were no differences in the food intake, whole body metabolic parameters, serum β-hydroxybutyrate levels or lipid profiles due to clodronate-treatment, but hepatic cytokine gene expressions including IL-1β were decreased. Conversely, primary mouse hepatocyte treatment with IL-1β significantly increased TG accumulation and Fas expression. Furthermore, the administration of IL-1Ra to DIO mice markedly reduced obesity-induced steatosis and hepatic lipogenic gene expression. Collectively, our findings suggest that IL-1β signaling upregulates hepatic lipogenesis in obesity, and is essential for the induction of pathogenic hepatic steatosis in obese mice.

3.2. Introduction

The prevalence of obesity represents a fully fledged epidemic as greater than 300 million adults are clinically obese worldwide (91). Obesity is a prominent risk factor for IR, T2DM, NAFLD and other metabolic disorders because it impairs systemic metabolic homeostasis. A major hallmark of obesity is AT dysfunction, which is characterized by a chronic state of low-grade inflammation, and by a decreased ability of adipocytes to efficiently store excess nutrients and lipids as TGs (77, 91, 267). This in turn is thought to increase circulating FFAs and ectopic lipid deposition within insulin sensitive tissues, such as muscle and liver, causing IR. The intracellular hepatic lipid accumulation and subsequent formation of LDs within hepatocytes can activate resident tissue macrophages, otherwise denoted as KCs, which release pro-inflammatory cytokines, including TNF-α, IL-6 and IL-1β (2, 229, 232). This inflammation enhances NAFLD progression to fibrosis, cirrhosis, chronic liver disease, and exacerbates IR (2, 165, 229, 232, 252)

Recently, macrophage depletion techniques have been used to determine the effects of macrophage function on insulin sensitivity. Conditional macrophage ablation in combination with transgenic and gene deletion mouse models have demonstrated that $CD11c^{+}$ macrophages, Nlrp3-inflammasome components and pro-inflammatory cytokines promote glucose intolerance and IR in both DIO and genetic mouse models of obesity (9, 54, 144, 179, 237, 251, 254). Drug-encapsulated liposome administration has been utilized to selectively deplete KCs and VATMs to improve glucose and insulin sensitivity and reduce hepatic steatosis in DIO mouse models (18, 54, 239). Lastly, anti-cytokine

therapy or pharmacological blockade of pro-inflammatory cytokines has also been successful in improving systemic glucose and insulin tolerance as well as β-cell function in obese mice and human subjects (45, 174, 237). One such drug is Anakinra (Kineret), which is recombinant IL-1Ra that blocks IL-1 signaling via the IL-1 receptor (45, 125, 205). However, previous work utilizing clodronate liposomes to deplete KCs in DIO mice have reported contradictory conclusions regarding the involvement of KCs in obesity-driven steatosis, clouding the roles of these cells in this syndrome (31, 54, 124, 223).

The present studies were designed to clarify this issue and elucidate the mechanism by which KC-derived pro-inflammatory cytokines regulate whole body and hepatic lipid metabolism in obesity. We targeted KCs *in vivo* by i.p. clodronate liposome administration in two animal models of obesity: DIO and *ob/ob* mice. The results herein demonstrate that clodronate liposome-mediated KC depletion, regardless of VATM content in both DIO and *ob/ob* mice, abrogated hepatic steatosis by reducing hepatic *de novo* lipogenic gene expression. Additionally, we observed significant decreases in hepatic inflammation and hypothesized that IL-1β may be responsible for the increased TG accumulation in obese mouse livers. In agreement with this hypothesis, IL-1β treatment increased hepatic lipid deposition and Fas expression in primary mouse hepatocytes. Furthermore, the pharmacological inhibition of IL-1 signaling by administration of recombinant human IL-1Ra to DIO mice attenuated obesity-induced hepatic steatosis and reduced hepatic lipogenic gene expression. These data illustrate the

importance of IL-1β in obesity-driven hepatic steatosis, and suggest that liver inflammation controls hepatic lipogenesis in obesity.

3.3. Results

Clodronate liposome-mediated KC depletion ameliorates hepatic steatosis in DIO and *ob/ob* mice.

Resident tissue macrophages aid in tissue homeostasis, but obesity can promote low-grade inflammation in insulin sensitive tissues. Conflicting literature has complicated our understanding of the role of KCs and hepatic inflammation in lipid homeostasis in obese mouse livers (19, 31, 54, 124). Thus, we sought to investigate the mechanism whereby KCs and KC-derived cytokines regulate whole body and hepatic lipid metabolism in two mouse models of obesity after clodronate liposome-mediated KC depletion. We employed a 2-dose injection scheme of clodronate liposomes (250 mg/kg) or an equivalent volume of control PBS liposomes to deplete KCs *in vivo* (**Figure 3.1**). Liposomes were injected i.p. into DIO or *ob/ob* mice every 3-days over the course of 6 days during the final week of a 13-week HFD challenge. It has been established that short-term diet-induced IR is caused by lipotoxicity, which occurs after only 3 days of high fat feeding (128). Chronic inflammation emerges as a more dominant mechanism once obesity is established by a long-term, 10-week high fat feeding (128). Therefore, late phase injections were utilized in this study. We observed no changes in the total animal body weight of PBS or clodronate liposome-treated mice upon completion of the experiments (**Figure 3.2 and 3.6 Legends**).

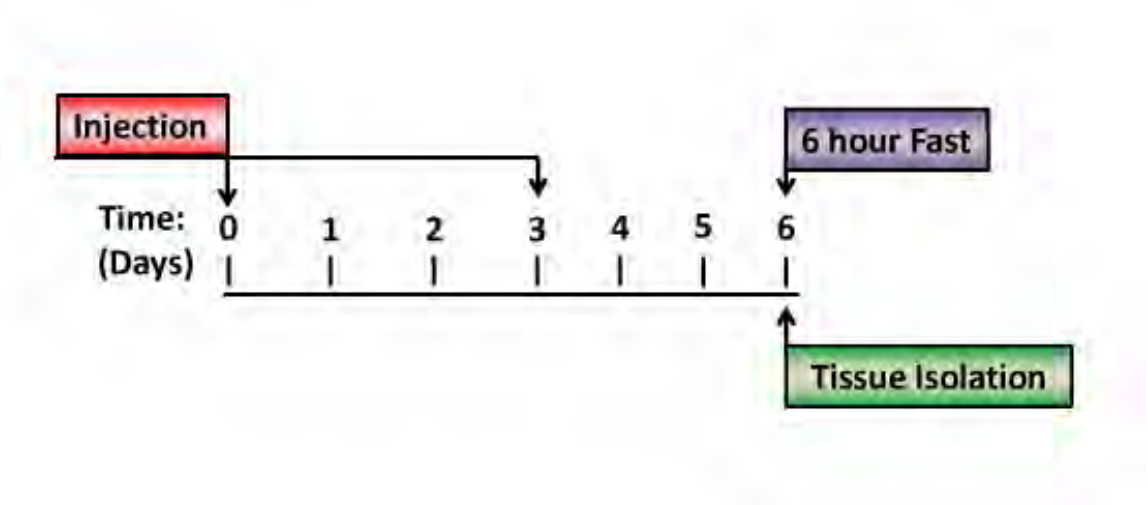

Figure 3.1. Injection scheme for intraperitoneal administration of clodronate liposomes into obese mice. 13-week HFD-challenged WT mice or 8-week old *ob/ob* mice were injected with 2 doses of 250 mg/kg clodronate-encapsulated liposomes or PBS-liposomes i.p. for 6 days in a 3-day interval. WT mice were injected during the final week of HFD challenge. Mice were fasted on day 6 for 6 hours at the start of the light cycle and blood was collected via retro-orbital sinus after isoflurane anesthesia. The tissues were collected immediately after sacrifice by CO2 asphyxia and cervical dislocation.

Previous studies employing i.p. clodronate liposome administration in DIO mice report inconsistencies in the ability to deplete both KCs and VATMs from the liver and VAT, respectively (19, 31, 54). To first confirm the efficiency of macrophage depletion within the clodronate-treated DIO mouse VAT, we isolated the SVF from the VAT on day 6 from animals that had been injected with clodronate or an equivalent volume of PBS liposomes. Cells were characterized by FACS analysis and macrophages were identified as cells that were positive for CD11b and F4/80 antigen and negative for the eosinophil marker Siglec F (227, 260)**.** In PBS liposome-treated DIO animals, approximately 27% of Siglec F-negative SVF cells were positive for both CD11b and F4/80 (**Figure 3.2 A-B**). However, in clodronate-treated DIO animals, this percentage decreased to 14%, which was a 45% decrease compared with PBS liposome-treated mice. Moreover, the percentage of the M1-type inflammatory macrophage marker, CD11c, of the total SVF cells was reduced 68% in clodronate-treated mice compared with PBS liposome-treated mice (**Figure 3.2 A-B; $p < 0.05$**). As assessed by qRT-PCR, we observed an 82% and 65% decrease in F4/80 and CD11c gene expression, respectively, in clodronate-treated DIO mouse livers compared with control animals (**Figure 3.2 D; $p \leq 0.01, 0.05$**). We also isolated SAT, lung and spleen to determine if clodronate-liposomes are capable of depleting resident tissue macrophages within other tissues. We observed a reduction in splenic macrophage content without affecting macrophages present within the lungs or SAT of clodronate-treated mice compared with PBS liposome-treated control mice (data not shown). We also isolated primary hepatocytes from clodronate-treated DIO mice via perfusion and observe no changes in pro-apoptotic

gene expression, indicating that the hepatocellular apoptosis pathway is unaffected by clodronate liposome treatment **(Figure 3.3 A-B).** Taken together, these results indicate that both macrophages in VAT and KCs in the liver of DIO mice were greatly reduced by the clodronate treatments.

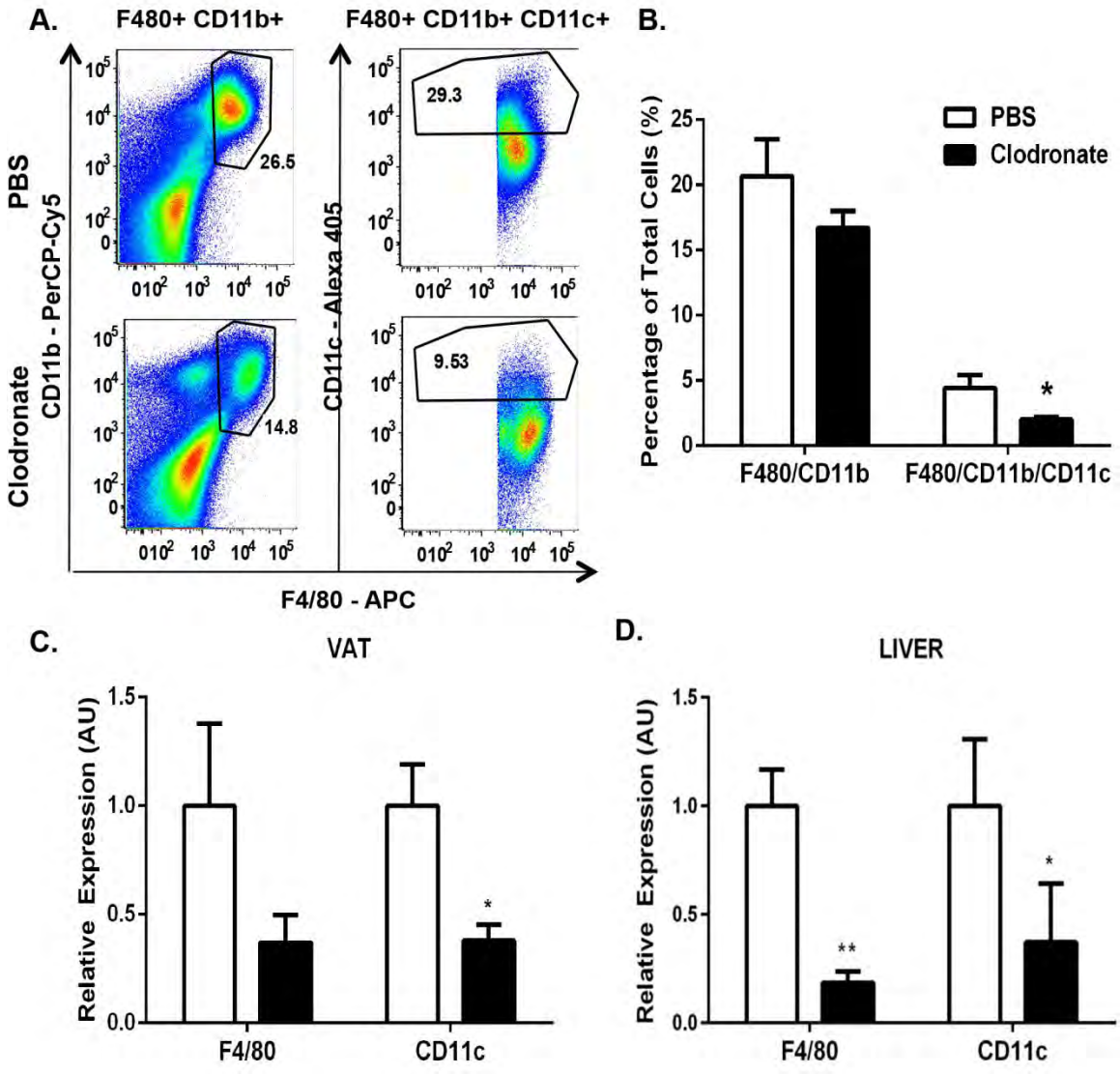

Figure 3.2. Clodronate liposomes effectively deplete KCs and VATMs of DIO mice.

Figure 3.2. Clodronate liposomes effectively deplete KCs and VATMs of DIO mice. 13-week HFD-challenged WT mice were injected with 2 doses of clodronate liposomes (250 mg/kg) or PBS liposomes i.p. over 6 days with a 3-day interval during the last week of high fat feeding. We observed no changes in the total animal body weight of PBS liposome-treated mice (42.4 ± 1.8 to 41.6 ± 1.9) or clodronate-treated mice (44.01 ± 2.2 to 41.5 ± 2.6). VAT SVF was isolated and FACS analysis was performed. **A.**) Upper panels, PBS liposome-treated mice. Lower panels, clodronate-treated mice. Left panels, SiglecF-negative, CD11b- and F4/80-positive cells. Right panels, CD11c-positive cells. Panels are representative of 6 animals per group. **B.**) The percentage of the total number of cells counted for both CD11b- and F4/80-positive cells and CD11c-positive cells in the VAT of DIO mice. RNA was extracted and qRT-PCR was performed for standard macrophage markers (F480, CD11c) in **C.**) VAT and **D.**) liver of DIO mice. The values represent the mean ± SEM. An unpaired student's t-test was used for comparisons between groups. * $p \leq 0.05$, ** $p \leq 0.01$.

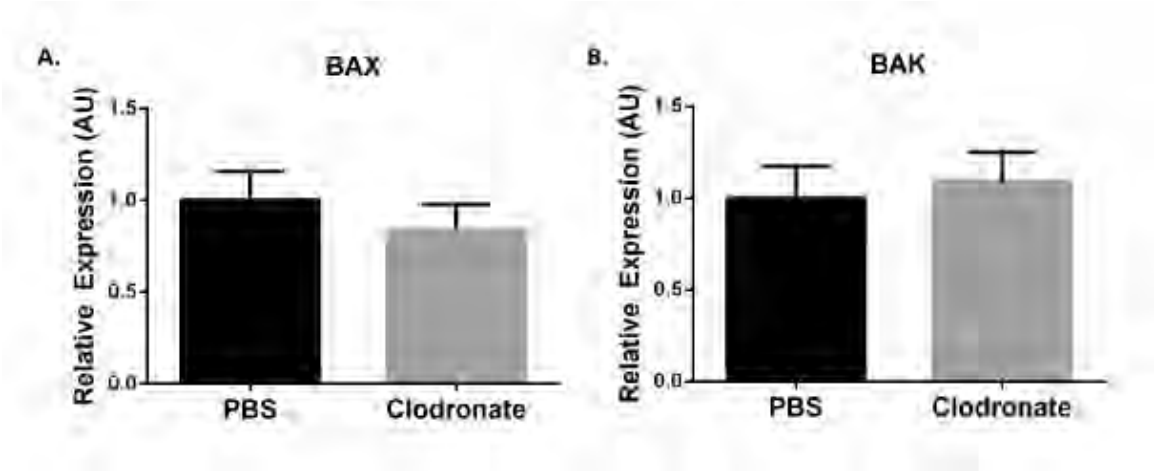

Figure 3.3. Pro-apoptotic genes that regulate intrinsic cell-death are unchanged in primary hepatocytes isolated from clodronate-treated DIO mice. 16-week HFD-challenged WT mice were injected with 2 doses of clodronate liposomes (250 mg/kg) or PBS liposomes i.p. over 6 days with a 3-day interval during the last week of high fat feeding. Hepatocytes were isolated via perfusion and RNA was extracted for qRT-PCR analysis of pro-apoptosis gene expression **A.**) Bax and **B.**) Bak. The values represent the mean ± SEM. An unpaired student's t-test was used for comparisons between groups (n.s.).

Upon dissection of the mice, we noted a macroscopic reduction in the steatotic appearance of the livers of clodronate-treated DIO animals compared with PBS liposome-treated control mice. In agreement with this observation, DIO mouse liver weights as a percentage of total animal body weight were decreased by 19% in clodronate-treated mice compared with PBS liposome-treated mice (**Figure 3.4 B; $p \leq 0.01$**). Clodronate-treated DIO mice displayed a significant reduction of liver TGs when compared with PBS liposome-treated mice, as observed microscopically by H&E and Oil-Red-O staining (**Figure 3.4 A**). Quantitative analysis revealed that KC depletion resulted in a 62% decrease in hepatic TG content in clodronate-treated DIO mice compared with the PBS liposome-treated controls (**Figure 3.4 C; $p \leq 0.05$**). Clodronate-treated mice displayed no fibrotic changes or indications of necrosis compared with PBS liposomes-treated mice, as observed microscopically by masson's trichrome and TUNEL staining (**Figure 3.5 A-D)**. These data demonstrate that clodronate-mediated KC and VATM depletion results in a remarkable reduction in hepatic TG content and amelioration of obesity-induced steatosis in DIO mice

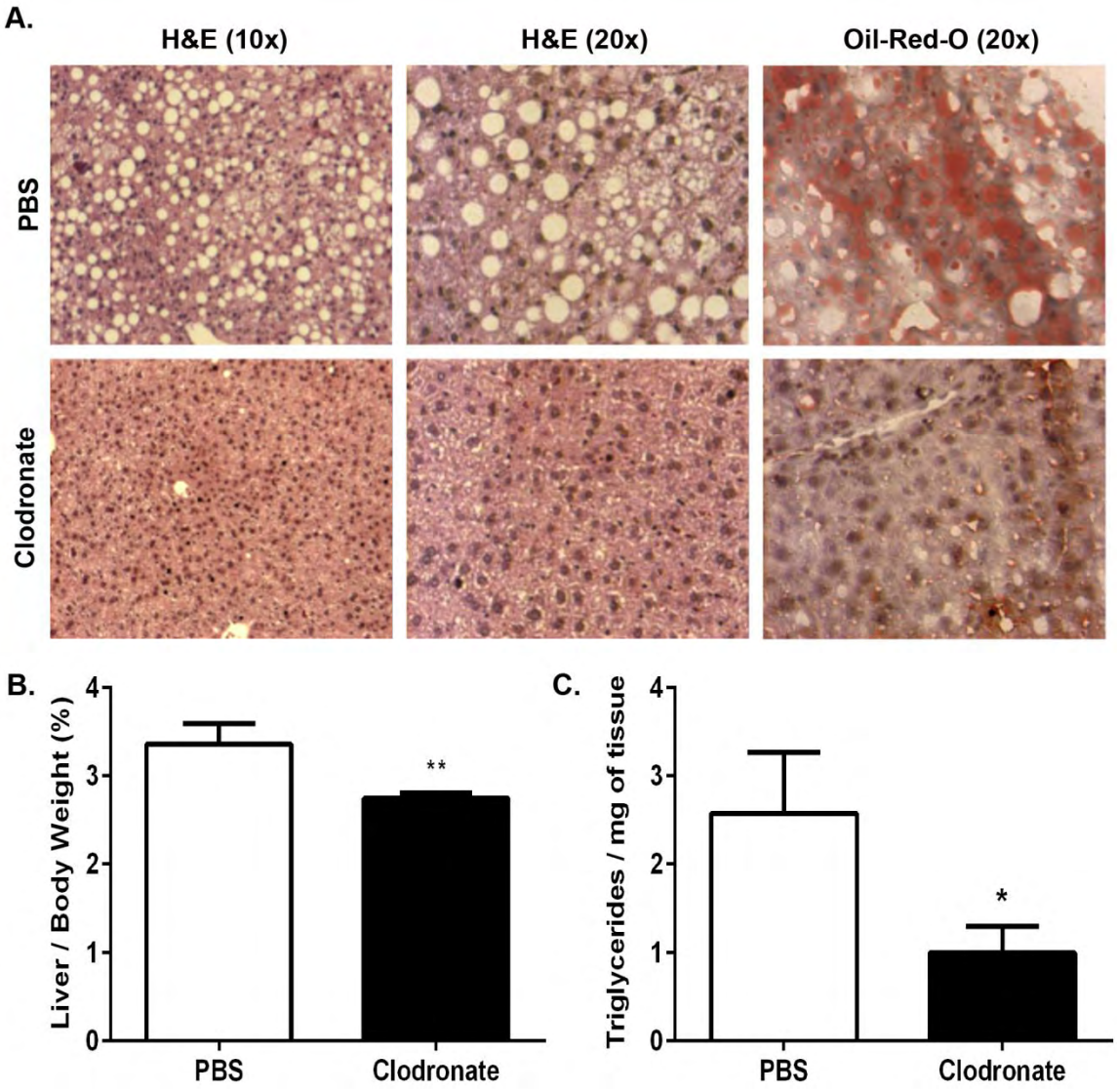

Figure 3.4. Clodronate liposome-mediated KC and VATM depletion ameliorates hepatic steatosis in DIO mice. 13-week HFD-challenged WT mice were injected with 2 doses of clodronate liposomes (250 mg/kg) or PBS liposomes i.p. over 6 days with a 3-day interval during the last week of high fat feeding. **A.**) DIO mouse livers were isolated, fixed in 10% formalin, embedded in paraffin, and stained with H&E or frozen in OCT and stained with Oil-Red-O to assess steatosis. Images are representative of 12-16 animals at 10x and 20x magnification. **B.**) DIO mouse livers were weighed and the data is represented as a percentage of the total body weight. **C.**) The total TGs were extracted and normalized to tissue weight. The values represent the mean ± SEM. An unpaired student's t-test was used for comparisons between groups. * $p \leq 0.05$, ** $p \leq 0.01$.

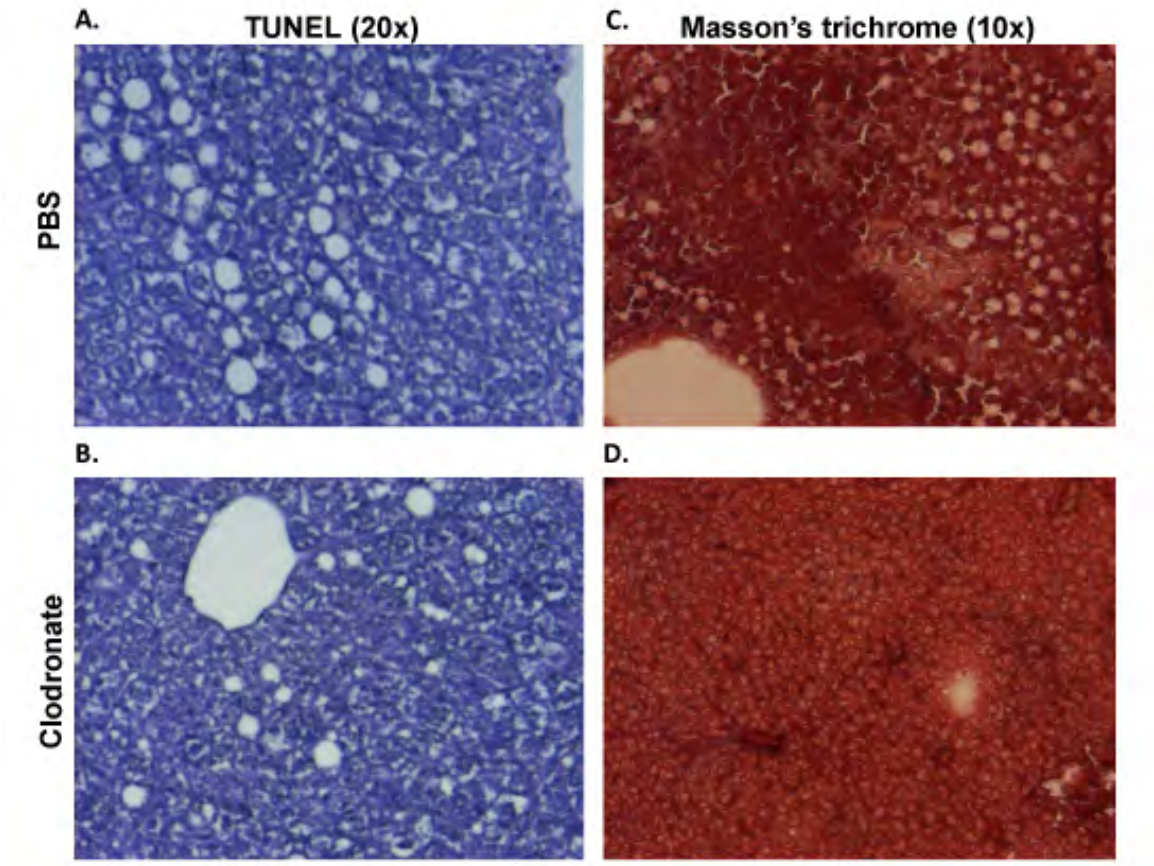

Figure 3.5. **Livers isolated from clodronate-treated DIO mice display no evidence of necrosis or fibrosis.** 13-week HFD-challenged WT mice were injected with 2 doses of clodronate liposomes (250 mg/kg) or PBS liposomes i.p. over 6 days with a 3-day interval during the last week of high fat feeding. DIO mouse livers were isolated, fixed in 10% formalin, embedded in paraffin, and stained with **A-B.**) TUNEL to assess necrosis or **C-D.**) masson's trichrome to assess fibrotic changes and overall hepatic health. Images are representative of 4 animals per group at 10x and 20x magnification.

In order to determine whether these results would also apply to a genetic model of obesity, we used the leptin-deficient *ob/ob* mouse in a subsequent set of experiments. Unexpectedly, no reduction in *ob/ob* mouse VATM content was observed after clodronate treatment as assessed by either FACS analysis or qRT-PCR (**Figure 3.6 A-C**). Thus, clodronate treatment depleted VATMs in the DIO mouse model of obesity, but not in *ob/ob* mice when compared with their respective PBS liposome-treated controls. However, we observed a 94% and 60% decrease in F4/80 and CD11c gene expression, respectively, in *ob/ob* mouse livers after clodronate treatment compared with PBS liposome-treated mice (**Figure 3.6 D; $p \leq 0.001, 0.05$**). These data illustrate that clodronate administration can effectively and efficiently deplete KCs from the livers of both DIO and *ob/ob* mice, whereas VATM depletion only occurs in the DIO mouse model. This finding is particularly insightful because ability to deplete KCs in the absence of VATM depletion in *ob/ob* mice provides a novel model for determining the KC-mediated affects on obesity-induced hepatic steatosis.

In spite of the fact that cell depletion due to clodronate was restricted to KCs and not VATMs in the *ob/ob* mouse model, a similar reduction in the steatotic appearance of the livers of clodronate-treated *ob/ob* animals compared with PBS liposome-treated animals was apparent (**Figure 3.7**). In agreement with this observation, *ob/ob* mouse liver weights as a percentage of total body weight were decreased 30% in the clodronate-treated animals compared with PBS liposome-treated animals (**Figure 3.7 B; $p \leq 0.01$**). Microscopic analysis of livers stained with H&E and Oil-Red-O revealed a significant reduction of liver TGs in clodronate-treated *ob/ob* mice compared with the PBS

liposome-treated mice (**Figure 3.7 A**). Quantification of hepatic TG content revealed that KC depletion resulted in a 45% decrease in hepatic TGs in clodronate-treated *ob/ob* mice compared with the PBS liposome-treated controls (**Figure 3.7 C; $p \leq 0.05$**). Collectively, these data illustrate that clodronate liposome-mediated KC depletion, in two mouse models of obesity, results in a marked reduction of hepatic TG content and amelioration of obesity-induced hepatic steatosis. Notably, this reduction of hepatic TGs occurs independently of VATM depletion in the *ob/ob* mouse model, demonstrating the importance of KCs in the regulation of hepatic lipid metabolism.

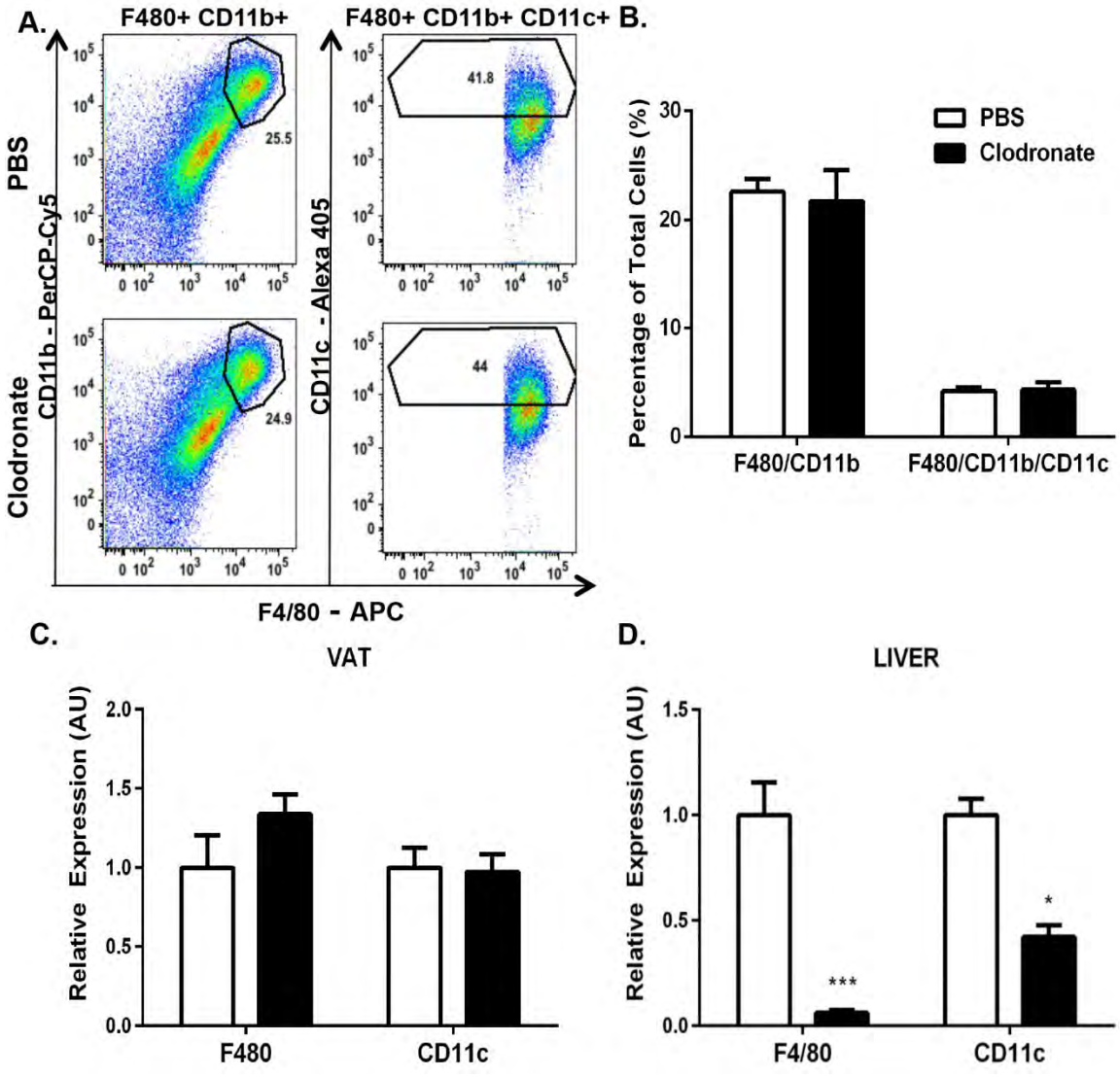

Figure 3.6. Clodronate liposomes deplete KCs but not VATMs in *ob/ob* mice.

Figure 3.6. Clodronate-encapsulated liposomes deplete KCs but not VATMs in *ob/ob* mice. 8-week *ob/ob* mice were injected with 2 doses of clodronate liposomes (250 mg/kg) or PBS liposomes by i.p. for 6 days with a 3-day interval. We observed no changes in the total animal body weight of PBS liposome-treated mice (44.2 ± 0.7 to 45.2 ± 0.6) or clodronate -treated mice (41.9 ± 1.4 to 41.1 ± 1.7). VAT SVF was isolated and FACS analysis was performed. **A.**) Upper panels, PBS liposome-treated mice. Lower panels, clodronate-treated animals. Left panels, SiglecF-negative, CD11b- and F4/80-positive cells. Right panels, CD11c-positive cells. Panels are representative of 4-6 animals per group. **B.**) The percentage of the total number of cells counted for both CD11b- and F4/80-positive cells and CD11c-positive cells in the VAT of *ob/ob* mice. RNA was extracted and qRT-PCR was performed for standard macrophage markers (F480, CD11c) in **C.**) VAT and **D.**) liver of *ob/ob* mice. The values represent the mean ± SEM. An unpaired student's t-test was used for comparisons between groups. * $p \leq 0.05$, *** $p \leq 0.001$.

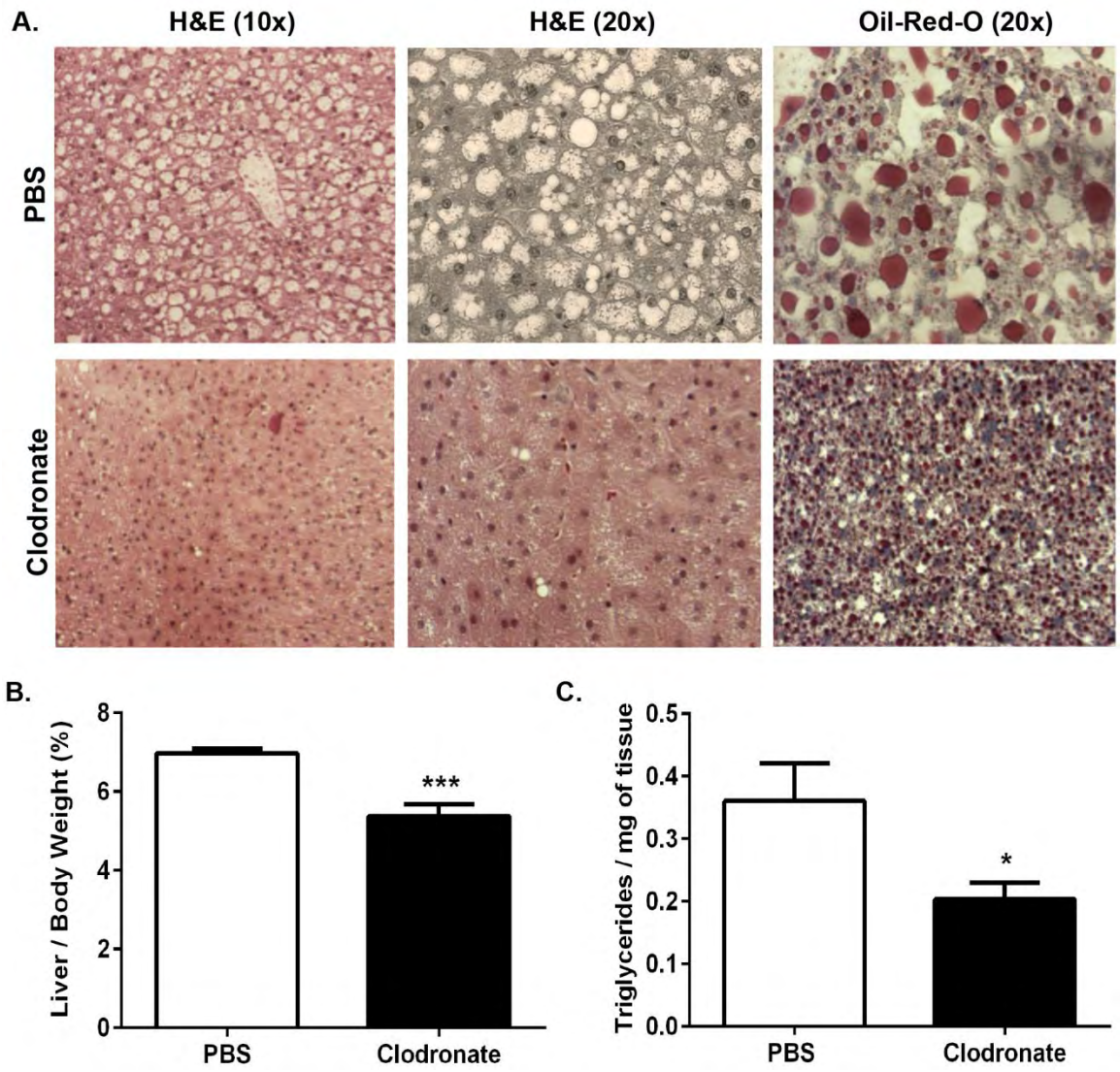

Figure 3.7. Clodronate liposome-mediated KC depletion ameliorates hepatic steatosis in *ob/ob* mice. 8-week old male ob/ob mice were injected with 2 doses of clodronate liposomes (250 mg/kg) or PBS liposomes by i.p. over 6 days with a 3-day interval. **A.**) The *ob/ob* mouse livers were isolated, fixed in 10% formalin, embedded in paraffin, and stained with H&E or frozen in OCT and stained with Oil-Red-O to assess steatosis. The images are representative of 7-10 animals at 10x and 20x magnification. **B.)** The *ob/ob* mouse livers were weighed and the data is represented as a percentage of the total body weight. **C.**) The total TGs were extracted and normalized to tissue weight. The values represent the mean ± SEM. An unpaired student's t-test was used for comparisons between groups. * $p \leq 0.05$, *** $p \leq 0.001$.

Clodronate liposome-mediated KC depletion decreases hepatic lipogenic gene expression in DIO and *ob/ob* mice.

The striking reduction of hepatic TGs in the clodronate-treated mice could be mediated by different pathways, including increased fatty acid oxidation, increased VLDL secretion, reduced influx of non-esterified FFAs from AT, and/or reduced hepatic DNL (46). To assess whether clodronate liposome treatment affected basal whole-body metabolic parameters, mice challenged with a HFD for 13-weeks and subjected to metabolic cage analysis throughout the duration of clodronate or PBS liposome treatment. We determined that there were no differences in the food consumption, water intake or physical activity between groups throughout the course of liposome treatment (**Table 3.1**). There were also no differences in the EE, respiratory exchange ratio (RER), or serum β-hydroxybutyrate levels in clodronate-treated DIO mice compared with PBS liposome-treated control mice (**Table 3.1**). Moreover, there were no changes in serum lipoprotein concentrations (**Table 3.1**) or the expression of genes promoting fatty acid oxidation, including PPARα or carnitine palmitoyltransferase-1a (Cpt1a) in clodronate-treated DIO or *ob/ob* mouse livers compared with PBS liposome-treated mice (**Figure 3.8**). These data suggest that whole body fatty acid oxidation is not affected by clodronate-treatment in DIO mice, and therefore we explored whether hepatic lipogenesis contributed to the reduced hepatic TG content in the clodronate-treated mice. Evaluation of liver samples by qRT-PCR analysis revealed reduced PPARγ expression and downstream genes that encode lipogenic enzymes including scd1, dgat, fasn, and acc2 as well as cell death-inducing DFFA-like effector A (cidea), which contributes to LD

formation in both DIO and *ob/ob* clodronate-treated mice (**Figure 3.9 A-B; $p \leq 0.05$**). Consistent with these data, a 40% decrease in Fas protein expression was observed in the livers of the clodronate-treated DIO mice compared with PBS-liposome treated mice (**Figure 3.9 C-D; $p \leq 0.05$**). Collectively, these data suggest that depleting KCs DIO and *ob/ob* mouse livers is associated with decreased hepatic steatosis, which is mediated at least, in part, by down-regulating hepatic lipogenesis.

Metabolic Parameter	PBS (DIO)	Clodronate (DIO)	PBS (ob/ob)	Clodronate (ob/ob)
FBG (mg/dL)	235 ± 11.9	**171 ± 11.1	404 ± 29.6	**256 ± 20.0
Fasting Insulin (ng/mL)	2.0 ± 0.3	*0.7 ± 0.1	6.6 ± 0.5	*3.9 ± 1.0
FFAs (mmol/L)	0.30 ± 0.02	*0.40 ± 0.08	0.52 ± 0.03	0.41 ± 0.09
TGs (mg/dL)	56.6 ± 17.8	61.5 ± 13.9	32.2 ± 5.1	**67.5 ± 9.8
Cholesterol (mg/dL)	131 ± 18.5	151 ± 28.8	N.A.	N.A.
HDL (mg/dL)	121 ± 11.3	138 ± 19.1	N.A.	N.A.
LDL (mg/dL)	12 ± 2.4	21 ± 8.6	N.A.	N.A.
B-hydroxybutyrate (uM)	0.3 ± 0.02	0.27 ± 0.04	N.A.	N.A.
Food Intake (g/day)	2.67 ± 0.17	2.51 ± 0.21	N.A.	N.A.
Water Intake (g/day)	1.78 ± 0.07	1.68 ± 0.11	N.A.	N.A.
Total Activity (counts/day: 24hr)	3290 ± 381	3165 ± 95	N.A.	N.A.
VO2 (ml/hr/kg: 24hr)	4838 ± 120	4759 ± 78	N.A.	N.A.
VCO2 (ml/hr/kg: 24hr)	3723 ± 114	3650 ± 61	N.A.	N.A.
EE (ml/hr/kg: 24hr)	23.18 ± 0.60	23.05 ± 0.33	N.A.	N.A.
RER (ml/hr/kg:24 hr)	0.771 ± 0.01	0.759 ± .00	N.A.	N.A.

Table 3.1. Macrophage depletion by clodronate liposomes improves fasting glycemia and insulin levels in DIO and *ob/ob* mice with no changes in the metabolic profile.

Table 3.1. Macrophage depletion by clodronate liposomes improves fasting glycemia and insulin levels in DIO and *ob/ob* mice with no changes in the metabolic profile. 13-week HFD-challenged WT mice or 8-week *ob/ob* mice were injected with 2 doses of clodronate liposomes (250 mg/kg) or PBS liposomes i.p. over 6 days with a 3-day interval. The data is representative of 12-16 DIO and 7-10 *ob/ob* animals. DIO mice were housed in metabolic cages prior to treatment for baseline analysis. The animals were housed in metabolic cages until completion of the experiment. EDTA plasma was drawn from the retro orbital sinus for serum analysis. Metabolic cage data is representative of 4-6 animals. The values represent the mean ± SEM. An unpaired student's t-test was used for comparisons between groups. * $p \leq 0.05$, ** $p \leq 0.01$.

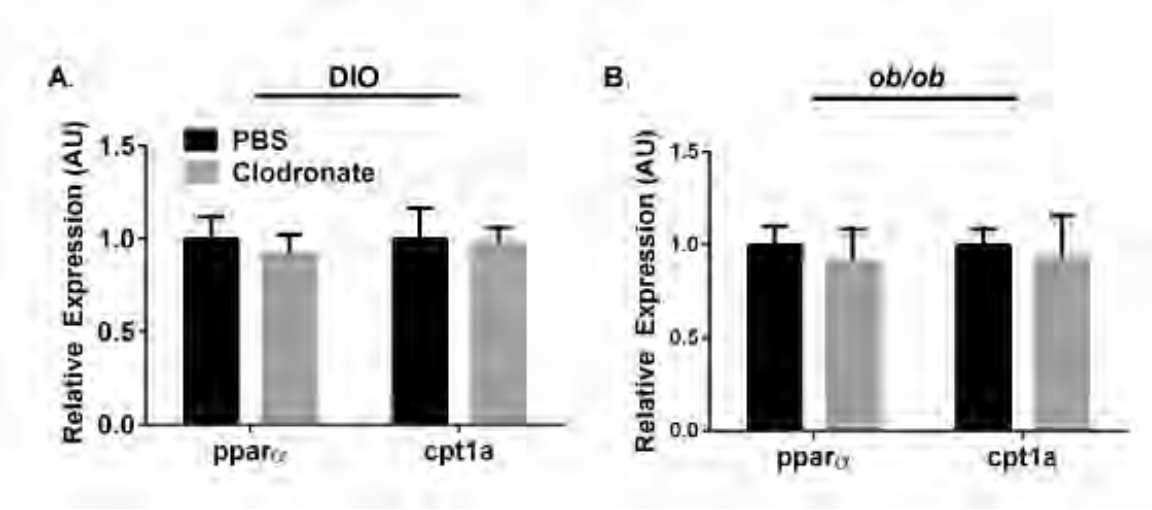

Figure 3.8. Clodronate liposome-mediated KC depletion in DIO and *ob/ob* mice has no affect on the hepatic expression of genes involved in fatty acid oxidation. 13-week HFD-challenged WT mice or 8-week *ob/ob* mice were injected with 2 doses of clodronate liposomes (250 mg/kg) or PBS liposomes by i.p. over 6 days with a 3-day interval. The data are representative of 12-16 DIO and 7-10 *ob/ob* animals. Livers were isolated, RNA was extracted and subjected to qRT-PCR analysis for fatty acid oxidation gene expression (pparα and cpt1a) in **A.**) DIO and **B.**) *ob/ob* mice. The values represent the mean ± SEM. An unpaired student's t-test was used for comparisons between groups (n.s.).

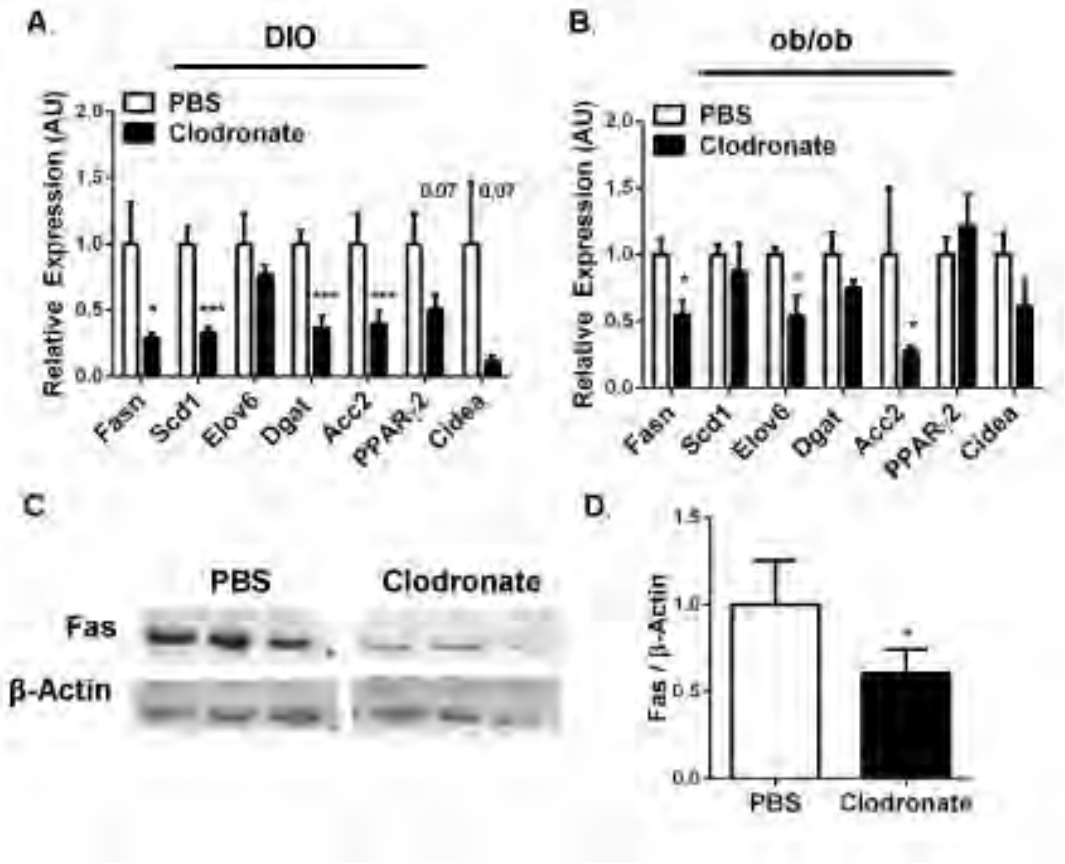

Figure 3.9. Clodronate liposome-mediated KC depletion in DIO and *ob/ob* mice significantly reduces hepatic expression of genes involved in lipogenesis. 13-week HFD-challenged WT mice or 8-week *ob/ob* mice were injected with 2 doses of clodronate liposomes (250 mg/kg) or PBS liposomes by i.p. over 6 days with a 3-day interval. The data are representative of 12-16 DIO and 7-10 *ob/ob* animals. Livers were isolated, RNA was extracted and subjected to qRT-PCR analysis for lipogenic gene expression (Fasn, Acc2, Dgat, Scd1, Elov6, PPARγ, Cidea) in **A.**) DIO and **B.**) *ob/ob* mice. **C**.) Protein was extracted from the DIO mouse livers and Western blot analysis was performed to detect Fas expression. PBS and Clodronate samples are from the same film, cut due to sample separation. **D**.) Relative densitometry from C. The values represent the mean ± SEM. An unpaired student's t-test was used for comparisons between groups. * $p \leq 0.05$, *** $p \leq 0.001$.

Clodronate liposome-mediated KC depletion reduces hepatic inflammation in DIO and *ob/ob* mice.

Inflammasome activation and the subsequent increase of IL-1β in obesity have received much attention because mouse models deficient in inflammasome components including NLR family pyrin domain containing 3 (Nlrp3), apoptosis-associated speck-like protein containing CARD (ASC), and caspase-1 implicate their involvement in obesity-induced hepatic steatosis progression (44, 76, 229, 254). To explore the underlying mechanism by which macrophage depletion ameliorated hepatic steatosis, we analyzed inflammatory gene expression in the livers of clodronate liposome versus PBS liposome-treated DIO and *ob/ob* mice by qRT-PCR. Consistent with macrophage depletion, we observed a 40%-75% reduction in the mRNA expression of pro-inflammatory cytokines TNF-α, IL-1β, IL-1α and the Nlrp3 in the livers of clodronate-treated DIO mice (**Figure 3.10 A; $p \leq 0.001$**). We observed an even more robust 65%-72% reduction in the expression of these genes in the livers of clodronate liposome-treated *ob/ob* mice compared with PBS liposome-treated *ob/ob* mice (**Figure 3.10 B; $p \leq 0.05$**). However, no changes in the mRNA expression of IL-1α were observed in clodronate-treated *ob/ob* mouse livers (**Figure 3.10 B**). Taken together, these data demonstrate that clodronate-liposome mediated KC depletion decreases the inflammatory program in steatotic livers of obese mice.

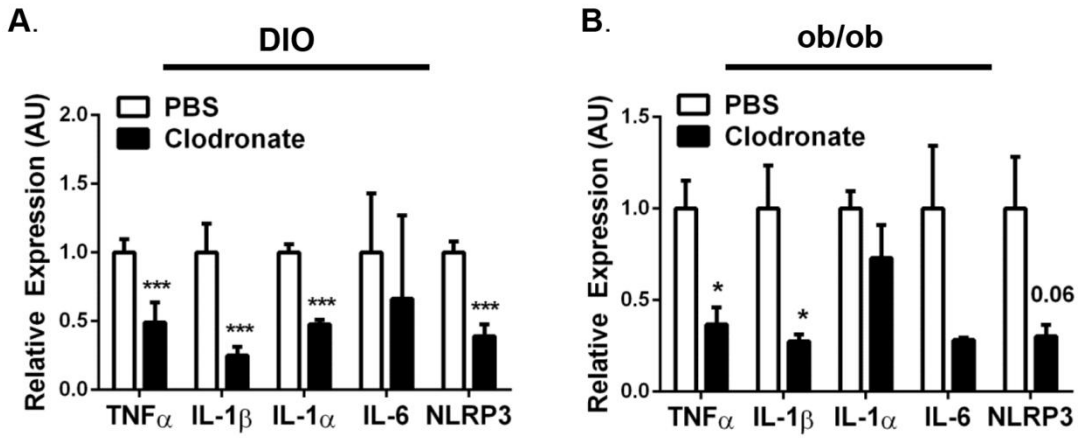

Figure 3.10. Clodronate liposome-mediated KC depletion in DIO and *ob/ob* mice significantly reduces hepatic expression of genes involved in inflammation. 13-week HFD-challenged mice or 8-week *ob/ob* mice were injected with 2 doses of clodronate liposomes (250 mg/kg) or PBS liposomes by i.p. over 6 days with a 3-day interval. The data are representative of 12-16 DIO and 7-10 *ob/ob* animals. Livers were isolated, RNA was extracted and subjected to qRT-PCR for inflammatory gene expression (TNF-α, IL-1β, IL-1α, IL-6, Nlrp3) in **A**.) DIO and **B**.) *ob/ob* mice. The values represent the mean ± SEM. An unpaired student's t-test was used for comparisons between groups. * $p \leq 0.05$, *** $p \leq 0.001$.

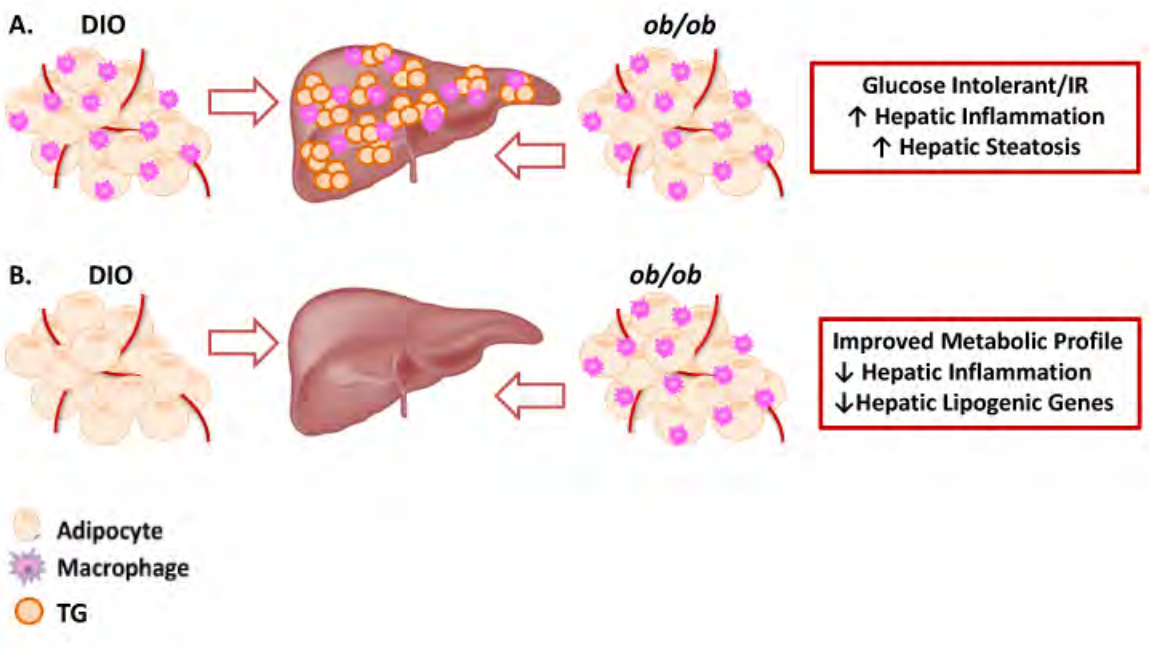

Figure 3.11. Clodronate liposome-mediated KC depletion ameliorates hepatic steatosis in obese mice independently of VATM content. A.) DIO and *ob/ob* mice present with glucose intolerance, IR, hepatic steatosis and VATM enrichment with associated inflammation in both the liver and AT. Steatosis is caused, in part, by an increased lipogenic program in obesity. **B.)** i.p. administration of clodronate-encapsulated liposomes depletes VATMs and KCs, improves the metabolic profile and ameliorates diet-induced steatosis by reducing hepatic inflammation, TG accumulation and lipogenic gene expression in DIO mice. Clodronate liposome-mediated KC depletion in *ob/ob* mice improves the metabolic profile and markedly reduces hepatic inflammation, steatosis and lipogenic gene expression without affecting VATM content.

Physiological concentrations of recombinant IL-1β stimulate TG accumulation in isolated primary mouse hepatocytes.

Recent reports have implicated the involvement of the Nlrp3 inflammasome in the development of hepatic steatosis (44, 181, 229). Based upon the reduced Nlrp3 and IL-1β mRNA expression in the livers of both the DIO and *ob/ob* clodronate-treated mice, we hypothesized that IL-1β might play a key role in steatosis development in hepatocytes. We isolated primary hepatocytes and assessed TG accumulation after 24-hour treatment with recombinant IL-1β or PBS (**Figure 3.12**). Microscopic evaluation revealed a dose-dependent increase in TG accumulation with increasing physiological doses of IL-1β as measured by Oil-Red-O staining (**Figure 3.12 A**) (181). To quantify the increased TG accumulation we measured total hepatocyte TGs and found a 50% increase in the recombinant IL-1β (10 ng/ml) treated hepatocytes compared with untreated cells (**Figure 3.12 D; $p \leq 0.001$**). Western blotting revealed a 30% increase in Fas protein expression in the recombinant IL-1β (10 ng/ml) treated hepatocytes compared with untreated cells (**Figure 3.12 B-C; $p \leq 0.05$**). . Taken together, these data support the hypothesis that IL-1β promotes TG accumulation by upregulating *de novo* lipogenesis in primary hepatocytes and is important for the pathogenesis of obesity-induced steatosis.

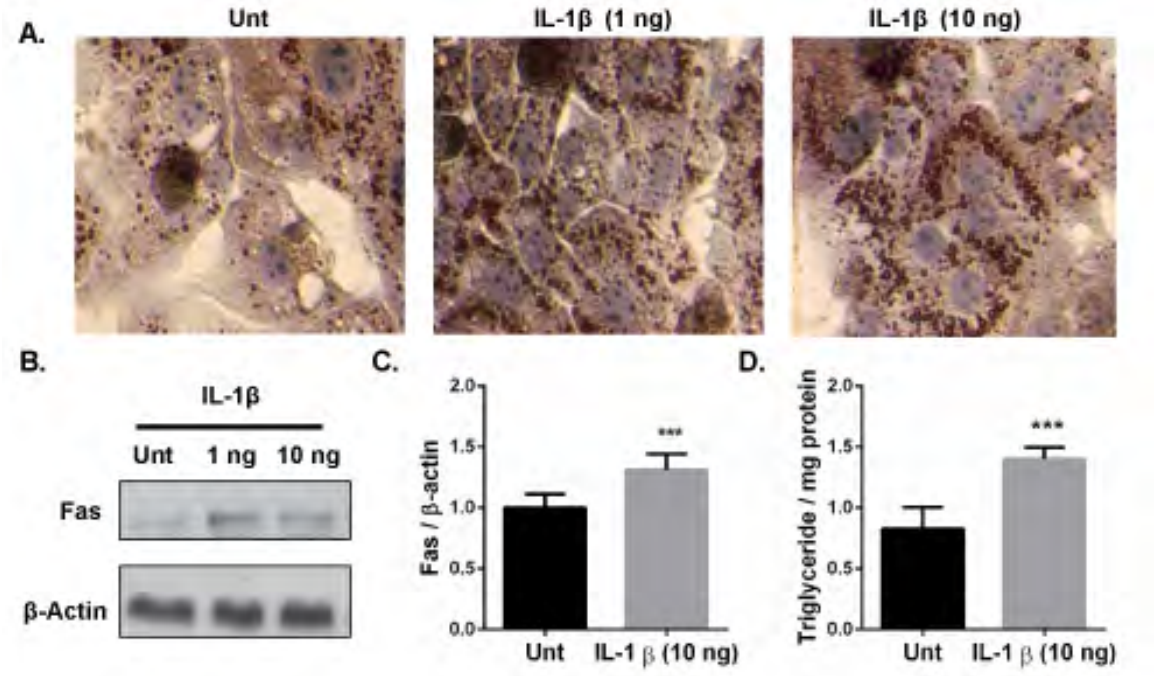

Figure 3.12. Physiological concentrations of IL-1β elicit a biological response in primary mouse hepatocytes to increase TG accumulation and Fas expression. WT primary hepatocytes were isolated via perfusion, stimulated with the indicated doses of recombinant mouse IL-1β and evaluated after 24-hours. **A.**) Cells were fixed in 10% formalin and stained with Oil-Red-O to assess TG accumulation. **B.**) Fas expression was analyzed in primary hepatocyte cell lysates after a 24-hour stimulation with the indicated doses of recombinant IL-1β and normalized to β-actin. **C**.) Relative densitometry from B. **D**.) The total TGs were extracted and measured after a 24-hour stimulation with recombinant IL-1β (10 ng/mL) and normalized to the amount of total protein. The data are representative of 4 experiments. All stimulations were performed in duplicate. Values represent the mean ± SEM. A paired student's t-test was used for comparisons between groups * $p \leq 0.05$, *** $p \leq 0.001$.

Pharmacological blockade of the IL-1 signaling pathway ameliorates diet-induced steatosis in mice.

The activity and signaling cascades downstream of IL-1α and IL-1β are tightly regulated by IL-1Ra, an endogenous antagonist of the IL-1 receptor (37, 40, 123). IL-1Ra negatively regulates IL-1 signaling by binding and blocking its receptor without activation, and mice lacking IL-1Ra has amplified steatosis compared with WT animals (101). To directly determine whether pharmacological inhibition of IL-1 signaling has a protective effect against NAFLD in DIO mice, we treated mice with recombinant human IL-1Ra (Anakinra). We fed mice a HFD for 9-weeks to establish IR and steatosis and then i.p. administered IL-1Ra (32.5 mg/kg) or an equal volume of saline daily for the final 32 days of a 13-week HFD challenge. To confirm that IL-1Ra was biologically active in these mice, we performed intraperitoneal glucose tolerance tests (GTTs) 28 days after the start of injections (**Figure 3.13 C-D**). Consistent with previous studies (125, 205), IL-1Ra treatment improved glucose tolerance without affecting the total animal body weight in DIO mice (**Figure 3.13; $p \leq 0.05$**). Serum recombinant human IL-1Ra levels were increased in IL-1Ra-treated mice compared with saline-treated mice, confirming that a physiological excess of IL-1Ra was present in circulation (**Figure 3.14; $p \leq 0.01$**).

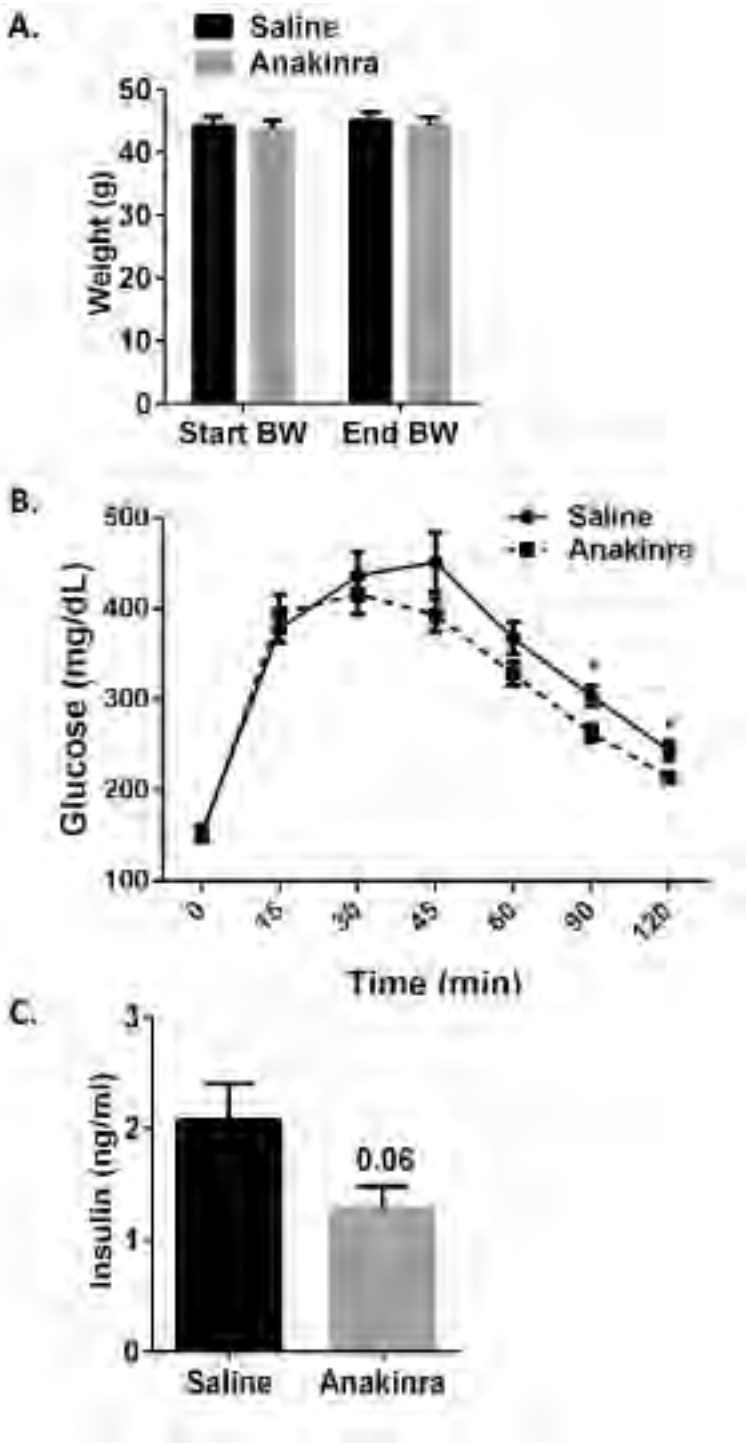

Figure 3.13. Pharmacological intervention via inhibition of IL-1 signaling improves glucose tolerance in DIO mice.

Figure 3.13. Pharmacological intervention via inhibition of IL-1 signaling improves glucose tolerance in DIO mice. 13-week HFD-challenged WT mice were started on daily injections of IL-1Ra (Anakinra; 32 mg/kg) or saline by i.p. administration at 32 days prior to sacrifice. The data are representative of 10 mice per group. At the end of 13 weeks, Anakinra-treated mice displayed no changes in the **A.**) total animal body weight and were more glucose tolerant as demonstrated by the **B.**) IPGTT of saline (circles) and HFD (squares) at 13 weeks of HFD (injection day 28) with a reduced AUC that was calculated with a baseline correction (22731 ± 1593 vs. 19777 ± 1284 (min*mg/dL) n.s.). **C.**) The fasting insulin levels for the IPGTT. The values represent the mean ± SEM. An unpaired student's t-test was used for comparisons between groups. * $p \leq 0.05$, ** $p \leq 0.01$.

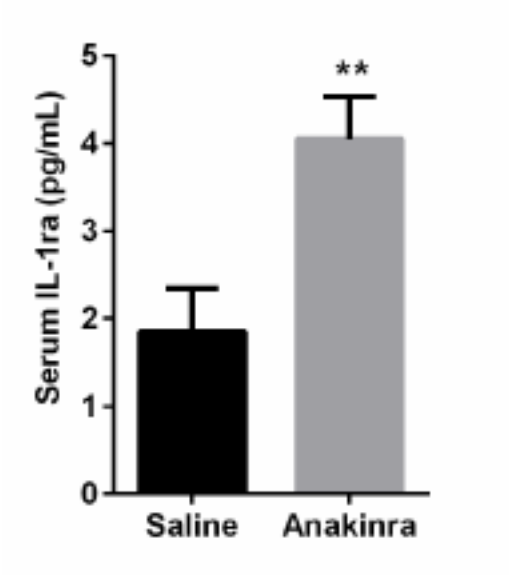

Figure 3.14. Recombinant human IL-Ra treatment results in increased serum IL-1Ra concentrations in DIO mice. 13-week HFD-challenged WT mice were started on daily injections of IL-1Ra (Anakinra; 32 mg/kg) or saline by i.p administration at 32 days prior to sacrifice. The data are representative of 10 mice per group. EDTA plasma was drawn via the retro orbital sinus and serum was analyzed for IL-1Ra by ELISA. The values represent the mean ± SEM. An unpaired student's t-test was used for comparisons between groups ** $p \leq 0.01$.

Upon dissection of the mice, a macroscopic reduction in the steatotic appearance of the IL-1Ra-treated mouse livers was observed compared with saline-treated mice (**Figure 3.15 A-C**). In agreement with this observation, liver weights as a percentage of body weight were reduced by approximately 20% in IL-1Ra-treated mice compared with saline-treated mice (**Figure 3.15 B**). Microscopic analysis of steatosis, as assessed by H&E and Oil-Red-O staining, revealed a significant improvement in the liver steatosis in the IL-1Ra-treated animals compared with saline-treated controls (**Figure 3.15 A**). To quantify this improvement, we measured total hepatic TGs and found a 30% reduction in IL-1Ra-treated mice compared with saline-treated mice (**Figure 3.15 C; $p \leq 0.05$**). Importantly, these data demonstrate that inhibition of IL-1 signaling by IL-1Ra administration in obese mice is sufficient to reduce hepatic TG content and improve obesity-induced hepatic steatosis.

To further confirm the activity of IL-1Ra in these mice, RNA was extracted from the livers of the IL-1Ra or saline-treated DIO mice to evaluate the mRNA expression of pro-inflammatory cytokines, including IL-1β and TNF-α. There was a reduction in hepatic TNF-α and IL-1β, however, we observed no changes in IL-1α, IL-6 or Nlrp3 expression in the IL-1Ra-treated mice compared with saline-treated control mice (**Figure 3.16 A; $p \leq 0.05$**). To assess whether the improved steatosis in the IL-1Ra-treated mice was due to altered lipid metabolism, genes involved in fatty acid synthesis and fatty acid oxidation were analyzed. Consistent with our previous findings in the clodronate-treated mice, reduced expression of genes involved in fatty acid synthesis and lipogenesis (elov6,

dgat, fasn, acc2) was observed in the IL-1Ra-treated mice compared with saline-treated control animals (**Figure 3.16 B; $p \leq 0.05$**). We observed no changes in the expression of genes related to fatty acid oxidation, such as pparα or cpt1a (**Figure 3.16 C**). Taken together, these data demonstrate that IL-1Ra administration protects against hepatic steatosis to a similar extent as clodronate liposome-mediated KC depletion in obese mice. Importantly, these findings also suggest that IL-1 signaling plays a significant role in the progression of obesity-induced steatosis by activating the lipogenic pathway in hepatocytes.

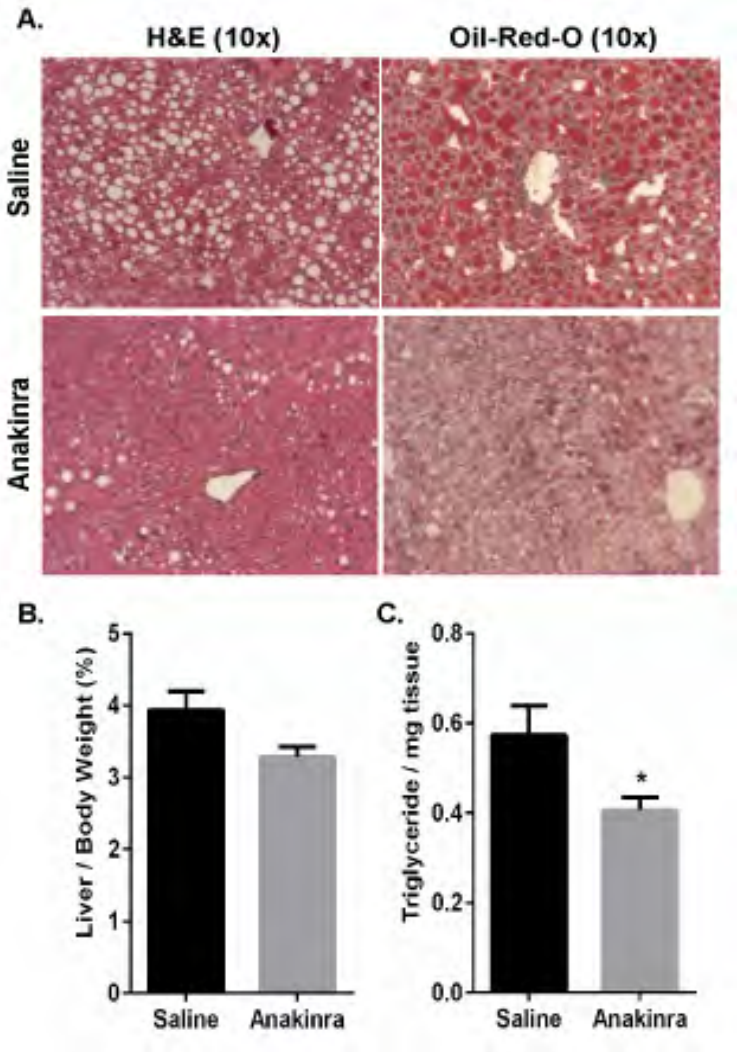

Figure 3.15. Pharmacological intervention via inhibition of IL-1 signaling ameliorates diet-induced steatosis in DIO mice. . 13-week HFD-challenged mice were started on daily injections of IL-1Ra (Anakinra; 32 mg/kg) or saline by i.p administration at 32 days prior to sacrifice. The data are representative of 10 mice per group. **A**.) The livers were isolated, fixed in 10% formalin, embedded in paraffin, and stained with H&E or frozen in OCT and stained with Oil-Red-O to assess steatosis. **B.**) The livers were isolated, weighed and represented as a percentage of the total animal body weight. **C**.) The total TGs were extracted and normalized to tissue weight. The values represent the mean ± SEM. An unpaired student's t-test was used for comparisons between groups * $p \leq 0.05$, ** $p \leq 0.01$.

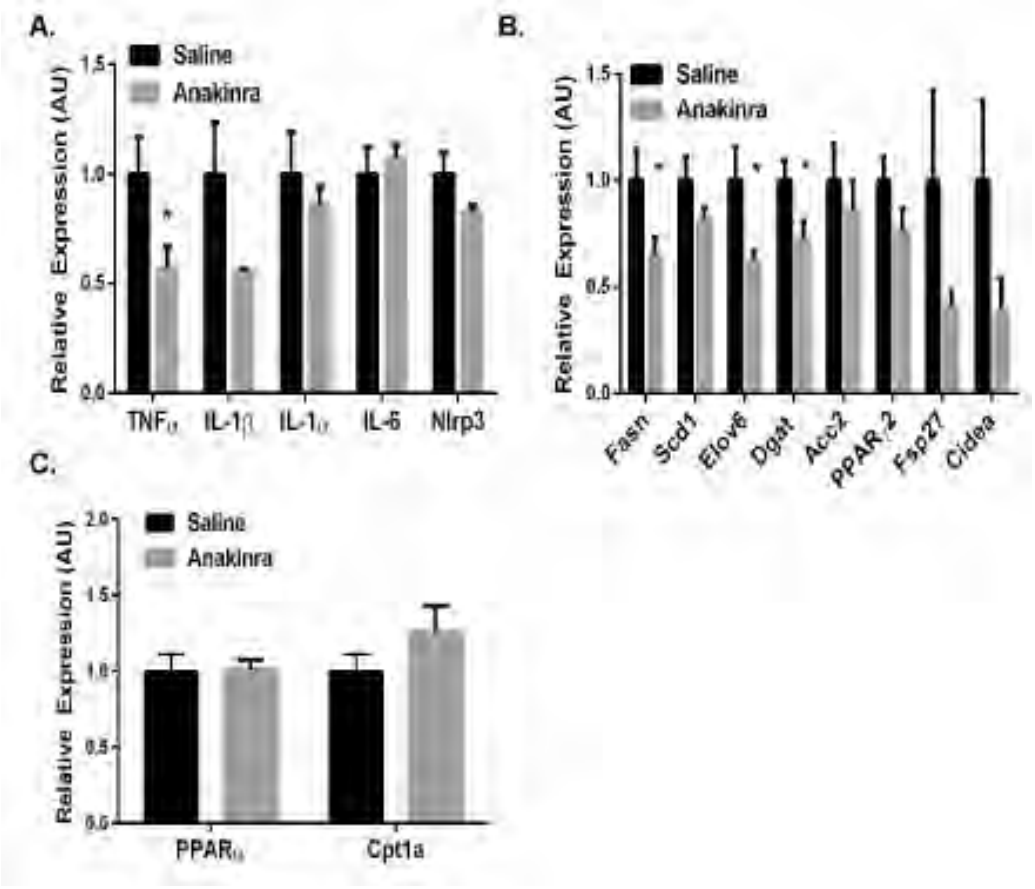

Figure 3.16. Pharmacological intervention via inhibition of IL-1 signaling reduces hepatic expression of genes involved in inflammation and lipogenesis in DIO mice. 13-week HFD-challenged mice were started on daily injections of IL-1Ra (Anakinra; 32 mg/kg) or saline by i.p administration at 32 days prior to sacrifice. The data are representative of 10 mice per group. The livers were isolated, RNA was extracted and subjected to qRT-PCR for expression of genes involved in **A**.) inflammation (TNF-α, IL-1β, IL-1α, IL-6, Nlrp3), **B**.) lipogenesis (Fasn, Acc2, Dgat, Scd1, Elov6, PPARγ, Cidea) and **C**.) fatty acid oxidation (PPARα, Cpt1a). The values represent the mean ± SEM. An unpaired student's t-test was used for comparisons between groups * $p \leq 0.05$, ** $p \leq 0.01$.

3.4. Discussion

The key results presented herein demonstrate that the macrophage-derived inflammatory mediator IL-1β potentiates the hepatic manifestation of the metabolic syndrome by stimulating lipogenesis and hepatic steatosis in obese mice (**Figures. 3.9, 3.11, 3.15, 3.16**). Utilizing clodronate liposomes to selectively deplete liver KCs in genetically obese *ob/ob* mice, we report remarkable amelioration of hepatic steatosis and significant reductions in hepatic inflammation and lipogenic gene expression (**Figures 3.7, 3.9-3.11**). Similar results were obtained in the DIO model treated with clodronate liposomes (**Figures 3.4, 3.9-3.11**). We also show that pharmacological blockade of IL-1 signaling by IL-1Ra dramatically improves hepatic steatosis by significantly decreasing inflammation and lipogenic gene expression in DIO mouse livers (**Figures 3.15 and 3.16**). Taken together, these data indicate that inflammation not only drives liver disease progression, but also facilitates the increased lipogenic program and increased TG content in obese mouse livers.

Inflammation in both VAT and liver appear to play important roles in mediating disrupted metabolism in obesity. Immune activation and macrophage recruitment to obese AT is correlated with systemic IR and may contribute to adipocyte dysfunction with limited ability to sequester triglyceride and ectopic lipid deposition (7). Lipid-laden KCs in the liver, resulting from increased influx of excess FFAs in circulation and increased hepatic DNL, are primed to recruit immune cells and exhibit a pro-inflammatory phenotype that exacerbates hepatic inflammation and TG accumulation, thus promoting obesity-induced steatosis and NAFLD (129). However, the specific role

of KCs in obesity-induced hepatic steatosis remains unclear because the authors of numerous studies on this point have come to contradictory conclusions (18, 31, 54, 124). For example, Bu et al, administered clodronate liposomes by i.p. as a preventative treatment against DIO and reported protection against diet-induced steatosis; however, the data show robust decreases in VATM content, but only modest reductions in KC content in the livers of clodronate-treated DIO mice (18). The use of CD11c-diptheria toxin transgenic mice to deplete macrophages in AT revealed normalization of insulin sensitivity in obese mice; however, this method also did not alter KCs in the liver (179). Feng and colleagues reported significant improvements in obesity-induced steatosis with marked reductions in VATM and KC content in clodronate liposome-treated DIO mice (54). On the contrary, Clemente, et al reported significant increases in both hepatic TG and VATM content in DIO mice treated with clodronate liposomes by i.p., and Lanthier, et al reported significant reductions in KCs without changes to the hepatic TG or VATM contents after intravenous clodronate liposome administration in DIO mice (31, 124). Thus, the differences in methods used amongst these studies, including dissimilar administration routes, inconsistent injection timelines, varied diets and feeding schedules, and inconsistent clodronate concentrations have confounded our understanding of the role of KCs in hepatic lipid metabolism.

We approached this problem by studying both a DIO mouse model and a genetic mouse model of obesity. Our studies presented here on the *ob/ob* mouse, which responded to the clodronate treatment with selective KC depletion without macrophage cell depletion in VAT or SAT, was particularly insightful (**Figure 3.6**). This selectivity

of macrophage depletion of KCs but not VATMs in the *ob/ob* mouse may relate to an impaired ability of AT macrophages from *ob/ob* mice to take up liposomes. Li et al demonstrated that lipid-laden macrophages from the peritoneum and atherosclerotic lesions of *ob/ob* mice have an impaired ability to clear apoptotic cells, suggesting a generalized defect in the phagocytic ability of *ob/ob* macrophages (130). Additionally, clodronate preferentially depletes F4/80^{high} CD11b^{low} macrophages, consistent with the expression profile of KCs, whereas clodronate does not effectively deplete F4/80^{low} CD11b^{high} macrophages from other tissues or in systemic circulation (99, 114). For these reasons, by utilizing the *ob/ob* mouse, we were able to characterize the metabolic consequences of selective KC depletion in the absence of generalized macrophage depletion in other tissues, providing us with a novel KC depletion system. Thus, the striking improvement of obesity-induced hepatic steatosis in the clodronate-treated *ob/ob* mice reveals a profound regulation by KCs on hepatic lipid metabolism.

Our data also revealed remarkable improvements in obesity-induced hepatic steatosis with reductions in liver weight and hepatic TG content in the clodronate-treated DIO mice when compared with PBS liposome-treated control animals (**Figure 3.4**). A recent report by Bu et al suggests that this clodronate liposome-induced reduction of hepatic TGs in DIO mice is dependent upon VATM depletion (19). In our study, cell depletion due to clodronate liposomes was observed for both KC and VATMs in the DIO mouse model (**Figures 3.3 and 3.6**), precluding a specific interpretation regarding which pool of cells may be responsible for the metabolic effects observed in this mouse model. However, our results in the *ob/ob* mouse showing a selective KC effect on hepatic lipids

suggests that KCs may also drive liver TG accumulation in the DIO model, and that both KCs and VATMs are important in modulating obesity-induced hepatic steatosis (**Figure 3.11**).

The hallmark of NAFLD is the excessive accumulation of TG in hepatocytes caused by alterations in hepatic lipid metabolism. Mechanisms contributing to excessive hepatic TG accumulation in obesity are disruptions in lipid disposal via β-oxidation or VLDL secretion, but primarily due to enhanced hepatic DNL and increased FFA delivery to the liver (186). Increased lipolysis of expanded AT and the consequent rise in circulating FFAs account for 60% of the hepatic TGs in obese patients presenting with NAFLD (57). Clodronate liposome-treatment reduced VATM content in DIO mice, and these mice present with increased circulating FFAs (**Figure 3.3 A-C, Table 3.1**). These data are consistent with Kosteli, et al. demonstrating that macrophage cell depletion in VAT leads to increased expression of the TG lipase ATGL and increased lipolysis in mice (118). We report no changes in circulating FFAs in clodronate-treated *ob/ob* mice, and deem this to be due to the inability to deplete VATMs in this model; however, these mice exhibit increased circulating TGs (**Figure 3.6 A-C, Table 3.1**). Importantly, the rise in circulating FFAs in clodronate-treated DIO mice is accompanied by remarkable hepatic TG clearance without changes in the cholesterol profile, circulating ketones, or EE when the mice are subjected to metabolic cage analysis (**Figure 3.4, Table 3.1**). Using a multiple-stable-isotope approach, Donnelly et al. estimated *de novo* lipid synthesis accounts for 30% of the hepatic TG content in NAFLD patients (46). We report reduced expression of genes related to *de novo* hepatic lipogenesis (Fasn, Acc2,

Dgat, Scd1) in both DIO and *ob/ob* clodronate-treated mice (**Figure 3.9 A-D**). Consistent with our data, the liver-specific Scd1 KO mice are protected from obesity-induced hepatic steatosis, while exhibiting reduced rates of hepatic fatty acid synthesis and decreased expression of key lipogenic enzymes (Fasn and Acc1/2) (148). Mao, et al generated liver-specific Acc1 KO mice with decreased rates of DNL; however, a compensatory up regulation of Acc2 occurred in other studies utilizing these mice (81, 141). Inhibition of Acc1/Acc2 by antisense oligonucleotides reversed diet-induced hepatic steatosis in mice (81, 141, 206). Collectively, our data suggests that the clearance of hepatic TGs after clodronate liposome-mediated KC depletion in the livers of obese mice is associated with decreased hepatic steatosis which is mediated, at least in part, by down regulating hepatic DNL.

Obese humans that present with NAFLD have increased circulating and hepatic levels of TNF-α, IL-1β, IL-6 and other acute phase proteins when compared with lean control subjects (45, 153, 252). KC depletion significantly reduced hepatic gene expression of these pro-inflammatory cytokines in both clodronate-treated DIO and *ob/ob* mice (**Figure 3.10 A-B**). We also report decreased Nlrp3 expression, an essential inflammasome component that is necessary for caspase-1 activation and IL-1β release, in both clodronate-treated DIO and *ob/ob* mice compared with PBS liposome-treated controls (**Figure 3.10 A-B**). Our data also demonstrated no change in the inflammasome-independent cytokine IL-1α gene expression in clodronate-treated *ob/ob* mouse livers (**Figure 3.10 B**). Even though clodronate-mediated KC depletion improves hepatic steatosis in both models, we only observe a decrease in IL-1α expression in the

clodronate-treated DIO mouse livers compared with control mice (**Figure 3.10 A**). Adoptive transfer experiments reveal that IL-1α is a hepatocyte-derived cytokine, rather than from KCs or recruited bone marrow-derived cells in obese mice (105-106). Furthermore, IL-1α and IL-1β are expressed at different phases of the inflammatory response and are derived from different cell types, suggesting that they may have distinct biological roles (194). Additionally, IL-1β KO mice are protected from diet-induced steatosis, whereas IL-1α KO mice develop steatosis (105). Although in our studies we cannot discount IL-1α involvement, we hypothesize that it does not play a role in obesity-induced hepatic steatosis development. Thus, the decreases in hepatic inflammation after clodronate liposome-mediated KC depletion suggest that inflammasome activation required to increase IL-1β production from KCs is important for obesity-induced hepatic inflammation.

IL-1β rapidly increases hepatic lipid accumulation *in vivo* by acutely increasing the rates of hepatic fatty acid synthesis (76). To further address the steatogenic potential of IL-1β, we assessed whether IL-1β would increase hepatic TG accumulation in a cell autonomous manner. IL-1β treatment increased TG accumulation and expression of the key lipogenic enzyme, Fas, in primary hepatocytes (**Figure 3.12**). In agreement with the decreased hepatic inflammation observed in clodronate-treated mice, caspase-1-deficient mice (that lack IL-1β expression) exhibit attenuated diet-induced hepatic steatosis and significant decreases in hepatic lipogenic gene expression compared with WT control mice (44). These data suggest that IL-1β influences hepatocyte lipid metabolism in obese mice by stimulating the DNL pathway to drive hepatic TG accumulation. However,

Stienstra and colleagues suggested that IL-1β-mediated suppression of hepatic PPARα and fatty acid oxidation was responsible for hepatic lipid accumulation in obesity (224). We report no changes in either PPARα or Cpt1a gene expression, RER, oxygen consumption or circulating β-hydroxybutyrate levels in clodronate-treated DIO mice compared with PBS liposome-treated mice, suggesting functional hepatic fatty acid oxidation in our clodronate-treated DIO mice (**Figure 3.8 and Table 3.1**).

The inflammatory response associated with obesity arises from an activation of the innate immune system, concurrently increasing anti-inflammatory cytokines to neutralize these pro-inflammatory changes. IL-1Ra, a naturally occurring antagonist of IL-1 signaling, is released as an acute phase protein and is produced by hepatocytes, macrophages/monocytes, and even adipocytes to balance the inflammatory affects of IL-1α/β (65, 101, 103). Circulating IL-1Ra positively correlates with obesity, and IL-1Ra KO mice exhibit a dramatic exacerbation of hepatic steatosis (101, 145). Pioglitazone, an oral anti-diabetic drug, decreases hepatic steatosis and attenuates the subclinical inflammation in NAFLD patients; however prominent side effects include increased adiposity and weight gain (13, 189). Anakinra, also used as a therapeutic in obese, diabetic patients, improves pancreatic islet function and glucose tolerance, but has not been studied in the context of NAFLD (45). We demonstrated here that pharmacological blockade of IL-1 signaling by IL-1Ra administration is sufficient to improve hepatic steatosis and the metabolic profile in DIO mice (**Figures 3.13-3.16**). Daily IL-1Ra administration to DIO mice significantly improved glucose tolerance as detected by IPGTT without changes to the total animal body weight (**Figure 3.13 A-C**).

Collectively, we report a significant improvement in obesity-induced steatosis as assessed by hepatic Oil-Red-O staining, decreased liver weight and reductions in the hepatic TG content of IL-1Ra-treated mice compared with saline-treated control mice (**Figure 3.15**). The expression of pro-inflammatory cytokines and genes involved in fatty acid synthesis (Fasn, Dgat, Scd1) are reduced significantly in the livers of IL-1Ra-treated mice, thus confirming our findings in the clodronate-treated DIO and *ob/ob* mouse models (**Figure 3.9 and Figure 3.10**). Importantly, inhibition of IL-1 signaling did not affect fatty acid oxidation gene expression (**Figure 3.16 C**). These data suggest that inhibition of IL-1 signaling by IL-1Ra administration is sufficient to improve obesity-induced hepatic steatosis by decreasing hepatic lipogenic gene expression and TG accumulation in DIO mouse livers.

In summary, our findings demonstrate that KC depletion in two mouse models of obesity markedly reduces hepatic inflammation and obesity-induced steatosis. With selective depletion of KCs in the *ob/ob* mouse, our data suggests that this improvement in hepatic steatosis is independent of VATM depletion (**Figure 3.11**), and that KCs and KC-derived cytokines, including IL-1β are important for hepatic metabolism regulation. Our data also suggests that the significant reduction in hepatic TGs observed in both clodronate-treated DIO and *ob/ob* mice is mediated, in part, by down regulating hepatic inflammation and DNL. Additionally, we report that inhibition of IL-1 signaling by administration of IL-1Ra markedly improves hepatic steatosis in DIO mice by significantly reducing hepatic inflammation and lipogenic gene expression (**Figure 3.17**).

Therefore, the results herein suggest that IL-1β signaling mediates hepatocyte TG accumulation by driving the *de novo* lipogenic signaling pathway in obese mouse livers and that IL-1β represents a promising therapeutic target in the treatment of obesity-induced NAFLD.

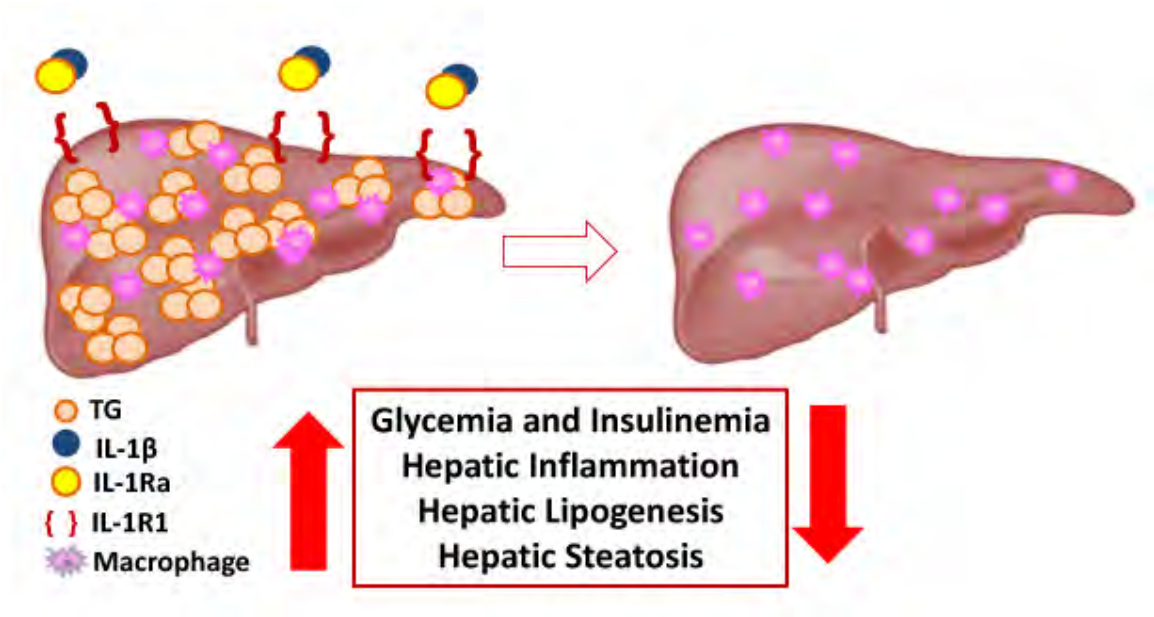

Figure 3.17. Pharmacological blockade of IL-1 signaling by IL-1Ra administration ameliorates hepatic steatosis in DIO mice. IL-1β elicits a biological response to increase hepatocellular TG accumulation and Fas protein expression in a cell autonomous manner *ex vivo*. This was confirmed *in vivo* by daily i.p. IL-1Ra administration to glucose intolerant DIO mice for 32 days. Mice have marked reductions in hepatic TG accumulation, lipogenic gene expression and inflammation accompanied by significant metabolic improvements determined by GTT.

3.5. Experimental Procedures

Animals, Diets and Treatments

Wild type male C57Bl/6J and *ob/ob* mice were purchased from Jackson laboratories (Bar Harbor, ME). Animals were fed ad libitum with free access to water and housed in the University of Massachusetts Medical School (UMASS) Animal Medicine facility with a 12:12-h light-dark cycle. Animals were weighed weekly for the duration of the diet study. Animals utilized for the clodronate-encapsulated liposome and IL-1Ra studies were fed a HFD (45 kcal% fat; D12451; Research Diets) starting at 4 wks of age for 13-14 weeks. 8-week-old *ob/ob* mice were fed a standard chow diet (LabDiet PicoLab 5053). Liposome-encapsulated clodronate (250 mg/kg) or an equivalent volume of PBS-liposomes was administered twice intraperitoneally (i.p.) with a three day interval over the course of 6 days the final week of the HFD-challenge. Mice were started on daily i.p. injections of recombinant human IL-1Ra (32 mg/kg) or saline (Anakinra; Amgen) starting after 9 weeks of HFD and 32 days prior to sacrifice. IPGTTs were performed as previously described after 28 daily IL-Ra injections (265). Measurements of EE, RER, indirect calorimetry, and physical activity using metabolic cages (TSE Systems, Bad Homburg, Germany) were performed by the UMass Mouse Metabolic Phenotyping Center. At experimental completions, mice were fasted for 6 hours at the start of the light cycle and then euthanized with CO_2 inhalation and cervical dislocation. All of the

experiments were performed in accordance with protocols approved by the Institutional Animal Care and Use Committees (IACUC) at UMass Medical School.

Sample Storage

Liver and VAT were harvested and snap frozen in liquid nitrogen for RNA and protein or OCT for Oil-Red-O analysis. Blood was drawn via the retro-orbital sinus into EDTA tubes; plasma was centrifuged at 10,000 rpm for 10 min and aliquotted. All of the samples were stored at -80C.

Primary cell isolation and culture

Anesthetized 8-week old WT mice were perfused via the inferior vena cava as previously described (15). Briefly, mice were perfused with a 0.5 mM EGTA solution followed by enzymatic collagenase digestion (Sigma) in 1mM CaCl2. Hepatocytes were washed with 1mM CaCl2 (3x) and separated by centrifugation. Primary hepatocytes were seeded in 6-well plates. Before starting stimulation experiments, hepatocytes were rested for 3 hours in M199 media containing 1% Penicillin/Streptomycin, 10% FA-free BSA, 2% FBS, Dexamethasone (100uM), and Insulin (100nM) at 37 °C and 5% CO2. Subsequently, culture media was replaced and cells were maintained in M199 media containing Penicillin/Streptomycin, Dexamethasone and Insulin. Insulin was present in all experimental media to maintain the health of the primary cultures. Cells were left untreated or treated with 10 ng/ml recombinant IL-1β (Millipore) for 24 hours.

RNA isolation and quantitative RT-PCR

Liver and VAT were isolated, snap frozen in liquid nitrogen, and stored at −80°C. Tissues were homogenized using the gentleMACs Dissociator (Miltenyi Biotec) and isolated following the manufacturers protocol (TriPure, Roche). Precipitated RNA was treated with DNAse (DNA-free, Life Technologies) prior to reverse transcription (iScript Reverse transcriptase, BioRad). SYBR green quantitative PCR (iQ SYBR green supermix, BioRad) was performed on the BioRad CFX97. Gene expression was normalized to the ribosomal gene 36B4 and expressed relative to the expression of PBS liposome- or saline-treated mice. The internal loading control, 36B4, did not change with liposome or IL-1Ra treatment. Melt curve analysis was performed to determine the PCR reaction product specificity. Primer sequences were designed with Primer Bank. Primer sequences are as follows: 36B4: 5'- TCCAGGCTTTGGGCATCA-3', 3'-CTTTATCAGCTGCACATCACTCAGA-5', CD11c: 5'-CTGGATAGCCTTTCTTCTGCTG-3',3'- GCACACTGTGTCCGAACTCA-5'; F4/80: 5'- CCCCAGTGTCCTTACAGAGTG-3', 3'- GTGCCCAGAGTGGATGTCT-5'; IL1β: 5'- GCAACTGTTCCTGAACTCAACT-3', 3'- ATCTTTTGGGGTCCGTCAACT-5'; TNFα: 5'-CAGGCGGTGCCTATGTCTC-3', 3'-CGATCACCCCGAAGTTCAGTAG-5'; IL-6: 5'- TAGTCCTTCCTACCCCAATTTCC-3', 3'-TTGGTCCTTAGCCACTCCTTC-5'; IL-1α: 5'- GCACCTTACACCTACCAGAGT-3', 3'- TGCAGGTCATTTAACCAAGTGG-5'; NLRP3: 5'-

ATTACCCGCCCGAGAAAGG-3', 5'-TCGCAGCAAAGATCCACACAG-3', FASn: 5'-GGAGGTGGTGATAGCCGGTAT-3', 5'-TGGGTAATCCATAGAGCCCAG-3', DGAT: 5'- TCCGTCCAGGGTGGTAGT-3', 5'-TGAACAAAGAATCTTGCAGACGA-3', ELOV6: 5'-GAAAAGCAGTTCAACGAGAACG-3', 5'- AGATGCCGACCACCAAAGATA-3', ACC2: 5'- GGAGGCTGCATTGAACACAAGT-3', 5'-TGCCTCCAAAGCGAGTGACAAA-3', PPARG2: 5'-ATGGGTGAAACTCTGGGAG-3', 5'- GTGGTCTTCCATCACGGAGA-3', SCD1: 5'-TTCTTGCGATACACTCTGGTGC-3', 5'-CGGGATTGAATGTTCTTGTCGT-3', PPARα: 5'-AGAGCCCCATCTGTCCTCTC-3', 5'-ACTGGTAGTCTGCAAAACCAAA-3', CPT1A: 5'-GCTGCTTCCCCTCACAAGTTCC-3', 5'-GCTTTGGCTGCCTGTGTCAGTATGC-3', BAX: 5'-AGACAGGGGCCTTTTTGCTAC-3', 5'-AATTCGCCGGAGACACTCG-3', BAK: 5'-CAGCTTGCTCTCATCGGAGAT-3', 5'-GGTGAAGAGTTCGTAGGCATTC-3'

Protein Analysis

Tissue pieces were homogenized in a Dounce homogenizer in RIPA protein lysis buffer [50 mM Tris (pH 7.4), 0.1% SDS, 400 mM NaCl, 0.5% deoxycholate, 1% NP40,1 mM EDTA, 25 mM sodium fluoride, 1 mM sodium orthovanadate, 1 mM benzamidine, 1 mM phenylmethylsulfonyl fluoride, and 10 μg/ml of aprotinin and leupeptin. Primary

hepatocytes were homogenized in lysis buffer (150 mM NaCl, 2% SDS, and 2mM EDTA, 25 mM sodium fluoride, 1 mM sodium orthovanadate, 1 mM benzamidine, 1 mM phenylmethylsulfonyl fluoride, and 10 μg/ml of aprotinin and leupeptin. Samples were sonicated using a microtip and protein content was quantified using a BCA protein assay kit (Thermo Scientific). Proteins were resolved on a 10% SDS-PAGE gel, transferred to a nitrocellulose membrane, blocked with 5% non-fat milk in TBST (0.05% Tween 20 in Tris-buffered saline), washed with TBST, and incubated with primary antibodies overnight. The blots were washed with TBST, and a horseradish peroxidase secondary antibody was applied. Proteins were visualized using Western Lightening Plus ECL (PerkinElmer). Primary antibodies used were Fas and β-Actin (Cell Signaling; 1:1000 and 1:10,000).

Histology

Livers were isolated and fixed in 10% formalin, paraffin embedded, and stained with hematoxylin and eosin (H&E) or frozen in OCT and stained with Oil-Red-O. Images were taken with an Axiovert 35 Zeiss microscope (Zeiss, Germany) equipped with an Axiocam CCl camera at 10x or 20x magnification.

Non-Esterified Fatty Acid (NEFA) measurements

EDTA plasma was collected from the retro-orbital sinus after isoflurane anesthesia. NEFA were measured with a colorimetric assay (WAKO) using the manual procedure according to manufacturer's instructions.

Triglyceride measurements

Total hepatic TG content measurement was performed as previously described (60). Briefly, total lipids were extracted from liver samples (100 mg) or primary hepatocyte cultures using a 2:1 mixture of chloroform and methanol. The organic layer was dried overnight and reconstituted in a solution containing 60% butanol and 40% of a 2:1 mixture of Triton-X114 and methanol. Total TGs were measured with a colorimetric assay (Sigma) using the manual procedure according to manufacturer's instructions.

ELISA Assay

EDTA plasma was collected from the retro-orbital sinus after isoflurane anesthesia. The exogenously administered IL-1Ra was measured using specific ELISA recognizing human IL-1Ra (R&D systems Inc.) and fasting insulin levels using a rat/mouse insulin ELISA (Millipore). Both assays were measured in duplicate and according to the manufacturers′ instructions.

Flow cytometry

The VAT SVF was isolated by digestion in HBSS, 2.5% BSA and 2 mg/mL collagenase for 45 minutes and strained through a 70 μm filter followed by red blood cell lysis. Cells were blocked with mouse IgG in FACS buffer (1% BSA/PBS). Cells were stained with antibodies directed towards F4/80 (APC, ABD serotec), CD11b (Percp 5.5, BD), Siglec F (PE, BD) and CD11c (V450, BD). The data were collected on an LSRII (BD) and were analyzed with FlowJo software. Samples were gated for scatter and single cells. Gates were drawn based on fluorescence minus one (FMO) controls. A total of 100,000 events were recorded.

Liposome Preparation

Cholesterol (16mg) and phosphatidylcholine (172 mg) (Sigma-Aldrich) were dissolved in chloroform in a round-bottom flask. The chloroform was evaporated at 37°C in a rotary evaporator under vacuum until a thin lipid film formed. 2 g of dichloromethylenediphosphonic acid disodium salt (clodronate) (Sigma-Aldrich) were dissolved in 10 ml of PBS. The clodronate-PBS solution or the control-PBS solution was added to the lipid film and shaken at 4 *g* for 30 minutes. The solution was sonicated for 2 minutes at room temperature in a water bath sonicator (150 watts). The liposomes were washed and centrifuged at 20,000 *g* for 2 hours, and resuspended in 8 ml of PBS. An aliquot of each liposome preparation was subjected to 1:2 phenol:chloroform extraction to determine the incorporated clodronate concentration within the liposomes and

analyzed via liquid chromatography mass spectroscopy on a Waters Acquity UPLC with a Phenomenex 2.1 x 100mm Synergi 4u Polar-RP 80A column. A standard curve was created using QuanLynx and samples were then quantified against this calibration curve.

Statistical Analysis

All of the values are presented as the mean ± SEM. For all experiments a student's t-test for two-tailed distributions with equal variances was used for comparison between 2 groups. Differences less than $p < 0.05$ were considered to be significant. The AUC for the IPGTT was calculated using a student's t-test after performing a baseline correction for the basal glucose values for each individual mouse. All of the data were entered into Microsoft Excel, and statistical analyses were performed with Graph Pad Prism 5.0.

IV: CONCLUSIONS AND FUTURE DIRECTIONS

4.1. Summary of Aims

One of the major underlying mechanisms leading to obesity-induced IR is adipocyte and macrophage dysfunctions. As previously mentioned, AT is the physiological site for lipid storage and essential in maintaining systemic glucose homeostasis, which is reinforced by the fact that lipodystrophic humans and mice are also IR (77, 88, 150). Thus, impairments in AT function including the dysregulation of the lipogenesis-lipolysis balance and the synthesis and secretion of insulin sensitizing endocrine hormones reflects changes not only in AT, but systemic insulin sensitivity. Furthermore, hepatic IR occurs as a consequence of adipocyte dysfunction as the liver becomes a reservoir for AT-derived FAs, leading to NAFLD and exacerbating the MS. In combination with alterations in lipid metabolism, macrophage-derived inflammation has been linked to the progression of obesity-induced IR in obese humans and mice (55, 82, 252). As a result, the perception and understanding of metabolism and immunology have evolved largely in parallel and have led to the discoveries described herein. Thus, the goals outlined for this thesis were to not only to better understand the roles of macrophages within AT and liver, but how they affect the essential processes necessary to maintain metabolic homeostasis, specifically lipid metabolism.

4.2. The Complex Roles of Adipose Tissue Macrophages

In Chapter II of this thesis, we established that VAT responds differently to DIO than SAT, because our data demonstrates that SAT is resistant to both HFD-induced inflammation and macrophage infiltration by genomic and qRT-PCR analysis. This is consistent with studies reporting that obese patients with increased SAT stores in the lower extremities remain IS, whereas VAT expansion and measures of waist circumference are correlated with increased risk for IR and T2DM (218). We also demonstrated that although DIO mouse VAT is enriched for macrophage-specific gene expression, the VAT inflammatory profile was surprisingly proportional to macrophage-specific genes (F4/80, CD68, CD11b, and CD11c) indicating that the obesity-induced expansion of the ATM population occurs without activation to an M1 state. The genomics analysis determined that DIO mouse VAT inflammatory gene expression was unchanged even though the macrophage-specific marker genes were significantly elevated, which was particularly insightful because we discovered a discrepancy in our biased way of thinking and encouraged our endeavor to confirm previous reports attributing obese AT inflammation to M1 polarized VATMs. We used macrophage marker genes like F4/80 and CD11c as reference genes in qRT-PCR analysis of VAT as a strategy to distinguish between two possible outcomes: increased activation or recruitment of M1 polarized macrophages or recruitment or expansion of the macrophage population occurs without activation. Increased activation of VATMs should demonstrate disproportionately higher expression of inflammatory markers (TNF-α, IL-6, IL-1β) compared to these macrophage marker genes, like F4/80. On the other hand, if

recruitment or expansion of the macrophage population occurs without activation, we would expect proportionate increases in both categories of markers. Relative to 36B4 or cyclophilin B expression, our data coincided with the vast literature reporting significant increases in DIO mouse VAT inflammatory gene expression. Surprisingly, when expressed relative to macrophage marker genes and not standard housekeeping genes, this increased inflammatory profile was abrogated and proportional to the expression of macrophage markers indicating that VATMs are not activated.

Although our study was not designed to characterize ATM polarization, we sought to confirm previous ATM expression profiles that suggest that obesity polarizes ATMs toward a M1 activation state (135, 137). Because macrophage populations present in lean AT display characteristics of those involved in tissue repair and remodeling, we hypothesized that macrophages recruited to obese AT are not driving inflammation, but serve an alternative function to maintain AT homeostasis and integrity under conditions of metabolic stress (26, 63). Thus, we hypothesized that the relative inflammatory changes observed in VAT may be due to quantitative increases in macrophage content rather than qualitative changes in M1 polarization in DIO mouse VATMs. For example, if macrophage content increases 10-fold, then the order of magnitude change in cytokine expression should also increase 10-fold. Thus, when inflammatory genes are expressed relative to ubiquitously expressed housekeeping genes, the increased inflammatory signature of obese VAT will be significant and when expressed relative to macrophage genes, the inflammatory changes will be proportional to these genes. A recent publication by Xu et al. confirmed our hypothesis by the meticulous analysis and

characterization of purified ATMs in multiple obese mouse models. This study used expression microarrays to generate transcription profiles of VATMs from lean WT and *ob/ob* mice comparing $CD11c^+$ and $CD11c^-$ VATM transcriptomes (262). The authors did not observe immune or inflammatory pathway enrichment in either population, and TNF-α, IL-1β and other classical inflammatory genes had reduced rather than increased expression of $CD11c^+$ VATMs (262). Interestingly, they discovered an obesity-induced program of lysosome biogenesis and their data suggest that secreted factors, including AT-derived lipids, induce a program in which lipid uptake and lysosomal biogenesis are coordinately regulated (262). In our clodronate liposome experiments, we observed significantly increased serum FFA levels in VATM-depleted DIO mice, which is consistent with the idea that ATMs facilitate lipid sequestration from the circulation. Taken together, these findings enhance the current paradigm depicting ATMs solely as inflammatory cells, to a colony of ATMs that consist of many subpopulations that mediate many functions within obese AT aside from inflammation. These data provide insight to focus our studies on trophic macrophage functions including macrophage population involvement in tissue remodeling, angiogenesis regulation, lipid sequestration, and other non-inflammatory roles in the context of obesity and IR (22, 118, 177, 188, 227).

The data herein provide insight that although ATMs have been labeled as mediators of IR, it is likely that macrophages exert a multitude of effects on adipocyte physiology that are dependent upon the tissue microenvironment. To address the complex roles of ATMs, our laboratory has developed GeRPs, an *in vivo* siRNA delivery

system that targets VATMs in obese mice (7-8). Recently, our laboratory has demonstrated that GeRP-mediated selective silencing of VATM LPL decreases ATM foam cell formation and exacerbates glucose intolerance in genetically obese mice (Aouadi, M. et al; submitted). These data demonstrate that the lipid buffering ability of ATMs has a profound impact on systemic glucose tolerance by their ability to sequester excess lipids in obese mouse VAT. Via GeRP-mediated silencing technology, our studies can assess the direct roles of lipid uptake, fatty acid esterification and synthesis, lysosome biogenesis, and other functions that may illustrate the ATM-mediated impact on systemic glucose tolerance and adipocyte biology in obese mouse models. A recently developed novel assay to image tumor-associated collagen turnover has discovered M2-macrophage mannose-receptor (CD206)-dependent collagen internalization (139). One approach to studying the multi-functional roles of ATMS may include collagen turnover imaging in combination with GeRP-mediated silencing of CD206 or extracellular matrix remodeling proteins in DIO mouse VATMs to determine their involvement in obese AT remodeling and collagen degradation.

4.3. KCs Regulate Hepatic Lipid Metabolism

In Chapter III of this thesis we used clodronate liposome-mediated macrophage depletion to confirm published data and determine the mechanism of ATM-mediated lipid metabolism dysregulation in obesity. Surprisingly, our project took an exciting turn and we discovered that the *ob/ob* mouse provides the ability to study the effects of macrophage depletion on KCs without affecting VATM content. We established *in vivo* that clodronate liposome-mediated KC depletion, regardless of VATM content in both DIO and *ob/ob* mice, abrogated hepatic steatosis by reducing hepatic *de novo* lipogenic gene expression. The observed reductions in hepatic inflammation in macrophage depleted obese mice led to the hypothesis that IL-1β may be responsible for obesity-induced increased hepatic TG accumulation. We determined that IL-1β treatment increases FAS protein expression and TG accumulation in primary mouse hepatocytes. IL-1Ra administration recapitulated these results by reducing hepatic TG accumulation and lipogenic gene expression in DIO mice. Thus, these data highlight the importance of the inflammatory cytokine IL-1β in obesity-driven hepatic steatosis and suggests that liver inflammation controls hepatic lipogenesis in obesity.

In parallel to the studies described herein, several studies have also investigated the role of KCs in hepatic inflammation and steatosis in obese mice. These studies used anti-inflammatory drug administration, macrophage depletion strategies and bone-marrow transplantation in combination with mice deficient in inflammatory genes (9, 31, 54, 105, 179, 181, 224). Taken together, it is understood that both KCs and hepatic inflammation regulate hepatocyte lipid metabolism but the inconsistencies in published

data confound our understanding of the KC-mediated regulation of diet-induced hepatic steatosis. As described in the discussion section of Chapter III, the abundant usage of macrophage depletion strategies in the literature provides a pandemonium of conclusions, partially because each study addressed the KC-induced modulations of hepatic lipid metabolism under different conditions. The administration route of the liposomes is pertinent to draw conclusions because this affects particle biodistribution and determines the liposome-mediated impact on macrophage populations in all tissues, including the liver and AT. Additionally, the distinct kinetics and temporal patterns of hepatic TG accumulation in HFD-challenged mice are dependent upon the fat content and feeding duration (6, 67). Thus, with variations of these parameters taken into account, it is difficult to draw conclusions regarding the role of KCs in hepatic lipid metabolism. On the contrary, immune cells also infiltrate the liver, which upregulates hepatic inflammation and progression of obesity-induced NALFD to NASH (2). By targeting KCs using a novel system in *ob/ob* mice we demonstrated that KCs are mediators of hepatic inflammation and steatosis, which are both causal to obesity-induced hepatic IR.

To this end, future endeavors to extend the current studies described herein will utilize a novel method to target KCs *in vivo* and address the specific role of IL-1β in hepatic lipid metabolism in the context of obesity-induced hepatic steatosis. Our laboratory has recently developed a method to directly target KCs *in vivo* via intravenous GeRP-mediated siRNA delivery (Tencerova, M. et al; submitted). Using this system, IL-1β siRNA could be administered to both DIO and *ob/ob* mice to confirm our findings in macrophage depleted and IL-1Ra-treated DIO mice, and provide a novel system to study

the mechanism whereby IL-1β regulates hepatic Fas expression. Preliminary data suggest that hepatic inflammation may affect intrahepatocellular citrate concentrations, thus providing a substrate for DNL. Furthermore, the specific silencing of KC-derived IL-1β will allow us to address functional questions and quantitatively measure hepatic lipogenic capacity in the absence of IL-1β *in vivo*. Lastly, IL-1Ra can ameliorate alcohol-induced fatty liver, which provided a foundation for our study to expand upon these findings. Our study reveals therapeutic implications for pharmacological inhibition of IL-1 signaling by providing a platform for IL-1Ra in obesity-induced NAFLD treatment. The broader therapeutic implications of IL-1Ra may be in hepatitis C virus (HCV) prevention by attenuating viral replication via IL-1Ra-induced reductions in hepatic FA biosynthesis (27, 87). In theory, decreased hepatic FA biosynthesis would reduce the enzyme activity and substrate availability that are necessary to construct viral particle bilayers, thus attenuating HCV replication and progression.

4.4. Future Work and Therapeutic Implications

The projects described herein study the complex roles of ATMs and KCs in modulating lipid metabolism in metabolic disease. The studies described above complement each other because VAT and liver are both anatomically linked and are essential in IR and metabolic disease progression. Expansion of VAT in humans contributes to the increased hepatic FFA delivery derived from increased AT lipolysis, thus driving hepatic steatosis and IR (161). Furthermore, exposure of KCs to dietary and adipocyte-derived FAs stimulates canonical inflammatory signaling cascades and cytokine upregulation, and negatively effects insulin signaling and hepatic glucose metabolism, thus providing a substantial link connecting both adipocyte lipid metabolism dysregulation with alterations in hepatic insulin sensitivity.

Macrophages are present in all tissues of the body and display tremendous heterogeneity with diverse phenotypes and functions that are reflective of their local metabolic and immune microenvironment (140, 142). The correlation between AT inflammation and IR and T2DM progression in obese mice and humans demonstrates a pathogenic role of ATMs, but there is no direct and concrete evidence proving that ATMs or other tissue macrophages act as pathogenic mediators in IR and T2DM (56, 196, 252, 261). Although our studies don't address this issue *per se*, the above findings have led to many new questions and directions for further research studying the complex roles of macrophages in obesity and metabolic disease. The discoveries made herein provide new insight and appreciation for the multi-functional nature of macrophages and support the conclusion that the roles of macrophages in obesity are not are not a simple distinction

between alternative and classical activation: the complex roles of macrophages in obesity-induced IR are not black and white.

Our data and recent publications provide evidence that ATMs serve a multitude of functions within obese AT not only as drivers of IR, but also as responders to aid and protect adipose tissue function in obesity as we and others report an immune response that is reflective of the increased ATM content in DIO mouse VAT. Many attempts have been made to block the macrophage infiltration into obese AT, but recent literature provides evidence that local macrophage proliferation and macrophage retention mechanisms may also be responsible for the increased ATM content that occurs in obesity (1, 191). Thus, instead of blocking macrophage enrichment it may be better suited to study the purpose of these macrophages to enhance our understanding of their presence and function within the obese VAT. To this end, our findings do not conflict with the abundant literature supporting the current model that inflammatory gene expression in obese AT modulates metabolic function, but bring awareness to the study of immunometabolism. Immune and metabolic studies combined have successfully reversed glucose intolerance in the context of obesity by the vast use of systemic and cell-type specific gene depletion methods, systemic cell-type ablation, and transgenic overexpression in combination with dietary manipulation and drug administration in thousands of animal models of immune and metabolic disease. On the other hand, our understanding of T2DM as an inflammatory disease remains unclear and is unable to fully transcend into clinical therapeutics.

Much clinical success has been achieved with TZD administration to promote insulin sensitivity in obese T2DM patients by increasing adipocyte lipid storage capacity (149, 209). TZD treatments also reduce ATM content with a corresponding decrease in inflammatory gene expressions in obese human and mouse AT (36, 261). Surprisingly, the established connection between adipocyte dysfunction, immune cell-derived inflammation and IR has been confounded by the less than spectacular success observed with anti-inflammatory drug trials in humans. Several trials attempted to neutralize TNF-α and failed to reduce hyperglycemia in T2DM patients or improve insulin sensitivity in obese IR patients (169, 178). It is important to note the limitations of these studies because they used single injections, small sample sizes and failed to demonstrate attenuated TNFα action, thus impacting the ability to draw proper conclusions. Converesly, human trials involving IL-1Ra or salsalate administration have demonstrated promising results by reducing systemic markers of inflammation and improving insulin sensitivity and glucose control in obese individuals, thus supporting the roles of inflammation in obesity-induced IR (59, 71, 125, 196). IL-1Ra is currently being administered to over-weight T1DM patients who lack residual β-cell function. This study will address the direct effects of anti-inflammatory treatment on systemic insulin sensitivity without affects on β-cell properties (Trial #NCT01285245). Taken together, these data raise many clinically critical questions that will require carefully designed longitudinal clinical studies to further our understanding of T2DM as an inflammatory disease.

To this end, the studies described herein provide clinical implications for anti-inflammatory therapy as we demonstrate the complexities of macrophage-mediated functions in insulin sensitive tissues and the role of inflammatory cytokine IL-1β in hepatic lipid metabolism modulation and systemic glucose tolerance in DIO mice, which is reversed via IL-1Ra intervention. The use of anti-inflammatory therapy to ameliorate obesity-associated NAFLD was perhaps the most important contribution to this body of work and is full of promise for future clinical application. It is likely that the future of therapeutics will be multi-faceted and combine therapeutic approaches to enhance glucose tolerance and overall health in obese, IR and T2DM patients.

References

1. **Amano SU, Cohen JL, Vangala P, Tencerova M, Nicoloro SM, Yawe JC, Shen Y, Czech MP, and Aouadi M.** Local proliferation of macrophages contributes to obesity-associated adipose tissue inflammation. *Cell Metab* 19: 162-171, 2014.
2. **Anderson N and Borlak J.** Molecular mechanisms and therapeutic targets in steatosis and steatohepatitis. *Pharmacol Rev* 60: 311-357, 2008.
3. **Angulo P.** Current best treatment for non-alcoholic fatty liver disease. *Expert Opin Pharmacother* 4: 611-623, 2003.
4. **Angulo P.** Obesity and nonalcoholic fatty liver disease. *Nutr Rev* 65: S57-63, 2007.
5. **Angulo P, Hui JM, Marchesini G, Bugianesi E, George J, Farrell GC, Enders F, Saksena S, Burt AD, Bida JP, Lindor K, Sanderson SO, Lenzi M, Adams LA, Kench J, Therneau TM, and Day CP.** The NAFLD fibrosis score: a noninvasive system that identifies liver fibrosis in patients with NAFLD. *Hepatology* 45: 846-854, 2007.
6. **Anstee QM and Goldin RD.** Mouse models in non-alcoholic fatty liver disease and steatohepatitis research. *Int J Exp Pathol* 87: 1-16, 2006.
7. **Aouadi M, Tencerova M, Vangala P, Yawe JC, Nicoloro SM, Amano SU, Cohen JL, and Czech MP.** Gene silencing in adipose tissue macrophages regulates whole-body metabolism in obese mice. *Proc Natl Acad Sci U S A* 110: 8278-8283, 2013.
8. **Aouadi M, Tesz GJ, Nicoloro SM, Wang M, Chouinard M, Soto E, Ostroff GR, and Czech MP.** Orally delivered siRNA targeting macrophage Map4k4 suppresses systemic inflammation. *Nature* 458: 1180-1184, 2009.
9. **Arkan MC, Hevener AL, Greten FR, Maeda S, Li ZW, Long JM, Wynshaw-Boris A, Poli G, Olefsky J, and Karin M.** IKK-beta links inflammation to obesity-induced insulin resistance. *Nat Med* 11: 191-198, 2005.
10. **Avruch J.** Insulin signal transduction through protein kinase cascades. *Mol Cell Biochem* 182: 31-48, 1998.
11. **Baron SH.** Salicylates as hypoglycemic agents. *Diabetes Care* 5: 64-71, 1982.
12. **Bechmann LP, Hannivoort RA, Gerken G, Hotamisligil GS, Trauner M, and Canbay A.** The interaction of hepatic lipid and glucose metabolism in liver diseases. *J Hepatol* 56: 952-964, 2012.
13. **Belfort R, Harrison SA, Brown K, Darland C, Finch J, Hardies J, Balas B, Gastaldelli A, Tio F, Pulcini J, Berria R, Ma JZ, Dwivedi S, Havranek R, Fincke C, DeFronzo R, Bannayan GA, Schenker S, and Cusi K.** A placebo-controlled trial of pioglitazone in subjects with nonalcoholic steatohepatitis. *N Engl J Med* 355: 2297-2307, 2006.
14. **Belfort R, Mandarino L, Kashyap S, Wirfel K, Pratipanawatr T, Berria R, Defronzo RA, and Cusi K.** Dose-response effect of elevated plasma free fatty acid on insulin signaling. *Diabetes* 54: 1640-1648, 2005.
15. **Berry MN and Friend DS.** High-yield preparation of isolated rat liver parenchymal cells: a biochemical and fine structural study. *J Cell Biol* 43: 506-520, 1969.
16. **Bruun JM, Helge JW, Richelsen B, and Stallknecht B.** Diet and exercise reduce low-grade inflammation and macrophage infiltration in adipose tissue but not in skeletal muscle in severely obese subjects. *Am J Physiol Endocrinol Metab* 290: E961-967, 2006.

17. **Bryant NJ, Govers R, and James DE.** Regulated transport of the glucose transporter GLUT4. *Nat Rev Mol Cell Biol* 3: 267-277, 2002.
18. **Bu L, Gao M, Qu S, and Liu D.** Intraperitoneal Injection of Clodronate Liposomes Eliminates Visceral Adipose Macrophages and Blocks High-fat Diet-induced Weight Gain and Development of Insulin Resistance. *AAPS J*, 2013.
19. **Bu L, Gao M, Qu S, and Liu D.** Intraperitoneal Injection of Clodronate Liposomes Eliminates Visceral Adipose Macrophages and Blocks High-fat Diet-induced Weight Gain and Development of Insulin Resistance. *AAPS J* 15: 1001-1011, 2013.
20. **Bugianesi E, Gentilcore E, Manini R, Natale S, Vanni E, Villanova N, David E, Rizzetto M, and Marchesini G.** A randomized controlled trial of metformin versus vitamin E or prescriptive diet in nonalcoholic fatty liver disease. *Am J Gastroenterol* 100: 1082-1090, 2005.
21. **Cancello R, Henegar C, Viguerie N, Taleb S, Poitou C, Rouault C, Coupaye M, Pelloux V, Hugol D, Bouillot JL, Bouloumie A, Barbatelli G, Cinti S, Svensson PA, Barsh GS, Zucker JD, Basdevant A, Langin D, and Clement K.** Reduction of macrophage infiltration and chemoattractant gene expression changes in white adipose tissue of morbidly obese subjects after surgery-induced weight loss. *Diabetes* 54: 2277-2286, 2005.
22. **Cao Y.** Angiogenesis modulates adipogenesis and obesity. *J Clin Invest* 117: 2362-2368, 2007.
23. **Caspar-Bauguil S, Cousin B, Galinier A, Segafredo C, Nibbelink M, Andre M, Casteilla L, and Penicaud L.** Adipose tissues as an ancestral immune organ: site-specific change in obesity. *FEBS Lett* 579: 3487-3492, 2005.
24. **Cawthorn WP and Sethi JK.** TNF-alpha and adipocyte biology. *FEBS Lett* 582: 117-131, 2008.
25. **Chajek-Shaul T, Friedman G, Stein O, Shiloni E, Etienne J, and Stein Y.** Mechanism of the hypertriglyceridemia induced by tumor necrosis factor administration to rats. *Biochim Biophys Acta* 1001: 316-324, 1989.
26. **Chawla A, Nguyen KD, and Goh YP.** Macrophage-mediated inflammation in metabolic disease. *Nat Rev Immunol* 11: 738-749, 2011.
27. **Cherry S, Kunte A, Wang H, Coyne C, Rawson RB, and Perrimon N.** COPI activity coupled with fatty acid biosynthesis is required for viral replication. *PLoS Pathog* 2: e102, 2006.
28. **Choi JJ, Park MY, Lee HJ, Yoon DY, Lim Y, Hyun JW, Zouboulis CC, and Jin M.** TNF-alpha increases lipogenesis via JNK and PI3K/Akt pathways in SZ95 human sebocytes. *J Dermatol Sci* 65: 179-188, 2012.
29. **Christensen JE, Andreasen SO, Christensen JP, and Thomsen AR.** CD11b expression as a marker to distinguish between recently activated effector CD8(+) T cells and memory cells. *Int Immunol* 13: 593-600, 2001.
30. **Cinti S, Mitchell G, Barbatelli G, Murano I, Ceresi E, Faloia E, Wang S, Fortier M, Greenberg AS, and Obin MS.** Adipocyte death defines macrophage localization and function in adipose tissue of obese mice and humans. *J Lipid Res* 46: 2347-2355, 2005.
31. **Clementi AH, Gaudy AM, van Rooijen N, Pierce RH, and Mooney RA.** Loss of Kupffer cells in diet-induced obesity is associated with increased hepatic steatosis, STAT3 signaling, and further decreases in insulin signaling. *Biochim Biophys Acta* 1792: 1062-1072, 2009.
32. **Cohen P.** The twentieth century struggle to decipher insulin signalling. *Nat Rev Mol Cell Biol* 7: 867-873, 2006.

33. **Czech MP, Tencerova M, Pedersen DJ, and Aouadi M.** Insulin signalling mechanisms for triacylglycerol storage. *Diabetologia* 56: 949-964, 2013.
34. **Davis JE, Gabler NK, Walker-Daniels J, and Spurlock ME.** Tlr-4 deficiency selectively protects against obesity induced by diets high in saturated fat. *Obesity (Silver Spring)* 16: 1248-1255, 2008.
35. **Dentin R, Girard J, and Postic C.** Carbohydrate responsive element binding protein (ChREBP) and sterol regulatory element binding protein-1c (SREBP-1c): two key regulators of glucose metabolism and lipid synthesis in liver. *Biochimie* 87: 81-86, 2005.
36. **Di Gregorio GB, Yao-Borengasser A, Rasouli N, Varma V, Lu T, Miles LM, Ranganathan G, Peterson CA, McGehee RE, and Kern PA.** Expression of CD68 and macrophage chemoattractant protein-1 genes in human adipose and muscle tissues: association with cytokine expression, insulin resistance, and reduction by pioglitazone. *Diabetes* 54: 2305-2313, 2005.
37. **Dinarello CA.** Anti-inflammatory Agents: Present and Future. *Cell* 140: 935-950, 2010.
38. **Dinarello CA.** Immunological and inflammatory functions of the interleukin-1 family. *Annu Rev Immunol* 27: 519-550, 2009.
39. **Dinarello CA.** Interleukin-1, interleukin-1 receptors and interleukin-1 receptor antagonist. *Int Rev Immunol* 16: 457-499, 1998.
40. **Dinarello CA.** Interleukin-1beta and the autoinflammatory diseases. *N Engl J Med* 360: 2467-2470, 2009.
41. **Dinarello CA, Donath MY, and Mandrup-Poulsen T.** Role of IL-1beta in type 2 diabetes. *Curr Opin Endocrinol Diabetes Obes* 17: 314-321, 2010.
42. **Diraison F, Moulin P, and Beylot M.** Contribution of hepatic de novo lipogenesis and reesterification of plasma non esterified fatty acids to plasma triglyceride synthesis during non-alcoholic fatty liver disease. *Diabetes Metab* 29: 478-485, 2003.
43. **Dixon JB, Bhathal PS, Hughes NR, and O'Brien PE.** Nonalcoholic fatty liver disease: Improvement in liver histological analysis with weight loss. *Hepatology* 39: 1647-1654, 2004.
44. **Dixon LJ, Flask CA, Papouchado BG, Feldstein AE, and Nagy LE.** Caspase-1 as a central regulator of high fat diet-induced non-alcoholic steatohepatitis. *PLoS One* 8: e56100, 2013.
45. **Donath MY, Boni-Schnetzler M, Ellingsgaard H, Halban PA, and Ehses JA.** Cytokine production by islets in health and diabetes: cellular origin, regulation and function. *Trends Endocrinol Metab* 21: 261-267, 2010.
46. **Donnelly KL, Smith CI, Schwarzenberg SJ, Jessurun J, Boldt MD, and Parks EJ.** Sources of fatty acids stored in liver and secreted via lipoproteins in patients with nonalcoholic fatty liver disease. *J Clin Invest* 115: 1343-1351, 2005.
47. **Elgazar-Carmon V, Rudich A, Hadad N, and Levy R.** Neutrophils transiently infiltrate intra-abdominal fat early in the course of high-fat feeding. *J Lipid Res* 49: 1894-1903, 2008.
48. **Elias I, Franckhauser S, Ferre T, Vila L, Tafuro S, Munoz S, Roca C, Ramos D, Pujol A, Riu E, Ruberte J, and Bosch F.** Adipose tissue overexpression of vascular endothelial growth factor protects against diet-induced obesity and insulin resistance. *Diabetes* 61: 1801-1813, 2012.
49. **Esposito K, Giugliano G, and Giugliano D.** Metabolic effects of liposuction--yes or no? *N Engl J Med* 351: 1354-1357; author reply 1354-1357, 2004.
50. **Feingold KR and Grunfeld C.** Tumor necrosis factor-alpha stimulates hepatic lipogenesis in the rat in vivo. *J Clin Invest* 80: 184-190, 1987.

51. **Feingold KR, Serio MK, Adi S, Moser AH, and Grunfeld C.** Tumor necrosis factor stimulates hepatic lipid synthesis and secretion. *Endocrinology* 124: 2336-2342, 1989.
52. **Feingold KR, Soued M, Adi S, Staprans I, Neese R, Shigenaga J, Doerrler W, Moser A, Dinarello CA, and Grunfeld C.** Effect of interleukin-1 on lipid metabolism in the rat. Similarities to and differences from tumor necrosis factor. *Arterioscler Thromb* 11: 495-500, 1991.
53. **Feingold KR, Soued M, Serio MK, Adi S, Moser AH, and Grunfeld C.** The effect of diet on tumor necrosis factor stimulation of hepatic lipogenesis. *Metabolism* 39: 623-632, 1990.
54. **Feng B, Jiao P, Nie Y, Kim T, Jun D, van Rooijen N, Yang Z, and Xu H.** Clodronate liposomes improve metabolic profile and reduce visceral adipose macrophage content in diet-induced obese mice. *PLoS One* 6: e24358, 2011.
55. **Ferrante AW, Jr.** The immune cells in adipose tissue. *Diabetes Obes Metab* 15 Suppl 3: 34-38, 2013.
56. **Ferrante AW, Jr.** Macrophages, fat, and the emergence of immunometabolism. *J Clin Invest* 123: 4992-4993, 2013.
57. **Ferre P and Foufelle F.** Hepatic steatosis: a role for de novo lipogenesis and the transcription factor SREBP-1c. *Diabetes Obes Metab* 12 Suppl 2: 83-92, 2010.
58. **Feuerer M, Herrero L, Cipolletta D, Naaz A, Wong J, Nayer A, Lee J, Goldfine AB, Benoist C, Shoelson S, and Mathis D.** Lean, but not obese, fat is enriched for a unique population of regulatory T cells that affect metabolic parameters. *Nat Med* 15: 930-939, 2009.
59. **Fleischman A, Shoelson SE, Bernier R, and Goldfine AB.** Salsalate improves glycemia and inflammatory parameters in obese young adults. *Diabetes Care* 31: 289-294, 2008.
60. **Folch J, Lees M, and Sloane Stanley GH.** A simple method for the isolation and purification of total lipides from animal tissues. *J Biol Chem* 226: 497-509, 1957.
61. **Fox CS, Massaro JM, Hoffmann U, Pou KM, Maurovich-Horvat P, Liu CY, Vasan RS, Murabito JM, Meigs JB, Cupples LA, D'Agostino RB, Sr., and O'Donnell CJ.** Abdominal visceral and subcutaneous adipose tissue compartments: association with metabolic risk factors in the Framingham Heart Study. *Circulation* 116: 39-48, 2007.
62. **Fried SK, Bunkin DA, and Greenberg AS.** Omental and subcutaneous adipose tissues of obese subjects release interleukin-6: depot difference and regulation by glucocorticoid. *J Clin Endocrinol Metab* 83: 847-850, 1998.
63. **Fujisaka S, Usui I, Bukhari A, Ikutani M, Oya T, Kanatani Y, Tsuneyama K, Nagai Y, Takatsu K, Urakaze M, Kobayashi M, and Tobe K.** Regulatory mechanisms for adipose tissue M1 and M2 macrophages in diet-induced obese mice. *Diabetes* 58: 2574-2582, 2009.
64. **Furukawa S, Fujita T, Shimabukuro M, Iwaki M, Yamada Y, Nakajima Y, Nakayama O, Makishima M, Matsuda M, and Shimomura I.** Increased oxidative stress in obesity and its impact on metabolic syndrome. *J Clin Invest* 114: 1752-1761, 2004.
65. **Gabay C, Gigley J, Sipe J, Arend WP, and Fantuzzi G.** Production of IL-1 receptor antagonist by hepatocytes is regulated as an acute-phase protein in vivo. *Eur J Immunol* 31: 490-499, 2001.
66. **Gabay C, Smith MF, Eidlen D, and Arend WP.** Interleukin 1 receptor antagonist (IL-1Ra) is an acute-phase protein. *J Clin Invest* 99: 2930-2940, 1997.
67. **Garbow JR, Doherty JM, Schugar RC, Travers S, Weber ML, Wentz AE, Ezenwajiaku N, Cotter DG, Brunt EM, and Crawford PA.** Hepatic steatosis, inflammation, and ER stress in mice maintained long term on a very low-carbohydrate ketogenic diet. *Am J Physiol Gastrointest Liver Physiol* 300: G956-967, 2011.

68. **Garvey WT, Maianu L, Huecksteadt TP, Birnbaum MJ, Molina JM, and Ciaraldi TP.** Pretranslational suppression of a glucose transporter protein causes insulin resistance in adipocytes from patients with non-insulin-dependent diabetes mellitus and obesity. *J Clin Invest* 87: 1072-1081, 1991.
69. **Girard J, Ferre P, and Foufelle F.** Mechanisms by which carbohydrates regulate expression of genes for glycolytic and lipogenic enzymes. *Annu Rev Nutr* 17: 325-352, 1997.
70. **Giugliano G, Nicoletti G, Grella E, Giugliano F, Esposito K, Scuderi N, and D'Andrea F.** Effect of liposuction on insulin resistance and vascular inflammatory markers in obese women. *Br J Plast Surg* 57: 190-194, 2004.
71. **Goldfine AB, Conlin PR, Halperin F, Koska J, Permana P, Schwenke D, Shoelson SE, and Reaven PD.** A randomised trial of salsalate for insulin resistance and cardiovascular risk factors in persons with abnormal glucose tolerance. *Diabetologia* 56: 714-723, 2013.
72. **Golozoubova V, Cannon B, and Nedergaard J.** UCP1 is essential for adaptive adrenergic nonshivering thermogenesis. *Am J Physiol Endocrinol Metab* 291: E350-357, 2006.
73. **Golozoubova V, Hohtola E, Matthias A, Jacobsson A, Cannon B, and Nedergaard J.** Only UCP1 can mediate adaptive nonshivering thermogenesis in the cold. *FASEB J* 15: 2048-2050, 2001.
74. **Greenberg AS, Coleman RA, Kraemer FB, McManaman JL, Obin MS, Puri V, Yan QW, Miyoshi H, and Mashek DG.** The role of lipid droplets in metabolic disease in rodents and humans. *J Clin Invest* 121: 2102-2110, 2011.
75. **Griffin ME, Marcucci MJ, Cline GW, Bell K, Barucci N, Lee D, Goodyear LJ, Kraegen EW, White MF, and Shulman GI.** Free fatty acid-induced insulin resistance is associated with activation of protein kinase C theta and alterations in the insulin signaling cascade. *Diabetes* 48: 1270-1274, 1999.
76. **Grunfeld C, Soued M, Adi S, Moser AH, Dinarello CA, and Feingold KR.** Evidence for two classes of cytokines that stimulate hepatic lipogenesis: relationships among tumor necrosis factor, interleukin-1 and interferon-alpha. *Endocrinology* 127: 46-54, 1990.
77. **Guilherme A, Virbasius JV, Puri V, and Czech MP.** Adipocyte dysfunctions linking obesity to insulin resistance and type 2 diabetes. *Nat Rev Mol Cell Biol* 9: 367-377, 2008.
78. **Haemmerle G, Lass A, Zimmermann R, Gorkiewicz G, Meyer C, Rozman J, Heldmaier G, Maier R, Theussl C, Eder S, Kratky D, Wagner EF, Klingenspor M, Hoefler G, and Zechner R.** Defective lipolysis and altered energy metabolism in mice lacking adipose triglyceride lipase. *Science* 312: 734-737, 2006.
79. **Haemmerle G, Zimmermann R, Strauss JG, Kratky D, Riederer M, Knipping G, and Zechner R.** Hormone-sensitive lipase deficiency in mice changes the plasma lipid profile by affecting the tissue-specific expression pattern of lipoprotein lipase in adipose tissue and muscle. *J Biol Chem* 277: 12946-12952, 2002.
80. **Han MS, Jung DY, Morel C, Lakhani SA, Kim JK, Flavell RA, and Davis RJ.** JNK expression by macrophages promotes obesity-induced insulin resistance and inflammation. *Science* 339: 218-222, 2013.
81. **Harada N, Oda Z, Hara Y, Fujinami K, Okawa M, Ohbuchi K, Yonemoto M, Ikeda Y, Ohwaki K, Aragane K, Tamai Y, and Kusunoki J.** Hepatic de novo lipogenesis is present in liver-specific ACC1-deficient mice. *Mol Cell Biol* 27: 1881-1888, 2007.

82. **Hardy OT, Perugini RA, Nicoloro SM, Gallagher-Dorval K, Puri V, Straubhaar J, and Czech MP.** Body mass index-independent inflammation in omental adipose tissue associated with insulin resistance in morbid obesity. *Surg Obes Relat Dis* 7: 60-67, 2011.
83. **Harman-Boehm I, Bluher M, Redel H, Sion-Vardy N, Ovadia S, Avinoach E, Shai I, Kloting N, Stumvoll M, Bashan N, and Rudich A.** Macrophage infiltration into omental versus subcutaneous fat across different populations: effect of regional adiposity and the comorbidities of obesity. *J Clin Endocrinol Metab* 92: 2240-2247, 2007.
84. **Hegarty BD, Bobard A, Hainault I, Ferre P, Bossard P, and Foufelle F.** Distinct roles of insulin and liver X receptor in the induction and cleavage of sterol regulatory element-binding protein-1c. *Proc Natl Acad Sci U S A* 102: 791-796, 2005.
85. **Hehlgans T and Pfeffer K.** The intriguing biology of the tumour necrosis factor/tumour necrosis factor receptor superfamily: players, rules and the games. *Immunology* 115: 1-20, 2005.
86. **Heilbronn LK and Campbell LV.** Adipose tissue macrophages, low grade inflammation and insulin resistance in human obesity. *Curr Pharm Des* 14: 1225-1230, 2008.
87. **Herker E, Harris C, Hernandez C, Carpentier A, Kaehlcke K, Rosenberg AR, Farese RV, Jr., and Ott M.** Efficient hepatitis C virus particle formation requires diacylglycerol acyltransferase-1. *Nat Med* 16: 1295-1298, 2010.
88. **Herrero L, Shapiro H, Nayer A, Lee J, and Shoelson SE.** Inflammation and adipose tissue macrophages in lipodystrophic mice. *Proc Natl Acad Sci U S A* 107: 240-245, 2010.
89. **Hirosumi J, Tuncman G, Chang L, Gorgun CZ, Uysal KT, Maeda K, Karin M, and Hotamisligil GS.** A central role for JNK in obesity and insulin resistance. *Nature* 420: 333-336, 2002.
90. **Hosogai N, Fukuhara A, Oshima K, Miyata Y, Tanaka S, Segawa K, Furukawa S, Tochino Y, Komuro R, Matsuda M, and Shimomura I.** Adipose tissue hypoxia in obesity and its impact on adipocytokine dysregulation. *Diabetes* 56: 901-911, 2007.
91. **Hotamisligil GS.** Inflammation and metabolic disorders. *Nature* 444: 860-867, 2006.
92. **Hotamisligil GS, Budavari A, Murray D, and Spiegelman BM.** Reduced tyrosine kinase activity of the insulin receptor in obesity-diabetes. Central role of tumor necrosis factor-alpha. *J Clin Invest* 94: 1543-1549, 1994.
93. **Hotamisligil GS, Peraldi P, Budavari A, Ellis R, White MF, and Spiegelman BM.** IRS-1-mediated inhibition of insulin receptor tyrosine kinase activity in TNF-alpha- and obesity-induced insulin resistance. *Science* 271: 665-668, 1996.
94. **Hotamisligil GS, Shargill NS, and Spiegelman BM.** Adipose expression of tumor necrosis factor-alpha: direct role in obesity-linked insulin resistance. *Science* 259: 87-91, 1993.
95. **Hotta K, Funahashi T, Bodkin NL, Ortmeyer HK, Arita Y, Hansen BC, and Matsuzawa Y.** Circulating concentrations of the adipocyte protein adiponectin are decreased in parallel with reduced insulin sensitivity during the progression to type 2 diabetes in rhesus monkeys. *Diabetes* 50: 1126-1133, 2001.
96. **Hu E, Liang P, and Spiegelman BM.** AdipoQ is a novel adipose-specific gene dysregulated in obesity. *J Biol Chem* 271: 10697-10703, 1996.
97. **Huang S and Czech MP.** The GLUT4 glucose transporter. *Cell Metab* 5: 237-252, 2007.
98. **Hundal RS, Petersen KF, Mayerson AB, Randhawa PS, Inzucchi S, Shoelson SE, and Shulman GI.** Mechanism by which high-dose aspirin improves glucose metabolism in type 2 diabetes. *J Clin Invest* 109: 1321-1326, 2002.

99. **Ikarashi M, Nakashima H, Kinoshita M, Sato A, Nakashima M, Miyazaki H, Nishiyama K, Yamamoto J, and Seki S.** Distinct development and functions of resident and recruited liver Kupffer cells/macrophages. *J Leukoc Biol* 94: 1325-1336, 2013.
100. **Inouye KE, Shi H, Howard JK, Daly CH, Lord GM, Rollins BJ, and Flier JS.** Absence of CC chemokine ligand 2 does not limit obesity-associated infiltration of macrophages into adipose tissue. *Diabetes* 56: 2242-2250, 2007.
101. **Isoda K, Sawada S, Ayaori M, Matsuki T, Horai R, Kagata Y, Miyazaki K, Kusuhara M, Okazaki M, Matsubara O, Iwakura Y, and Ohsuzu F.** Deficiency of interleukin-1 receptor antagonist deteriorates fatty liver and cholesterol metabolism in hypercholesterolemic mice. *J Biol Chem* 280: 7002-7009, 2005.
102. **Jager J, Gremeaux T, Cormont M, Le Marchand-Brustel Y, and Tanti JF.** Interleukin-1beta-induced insulin resistance in adipocytes through down-regulation of insulin receptor substrate-1 expression. *Endocrinology* 148: 241-251, 2007.
103. **Juge-Aubry CE, Somm E, Chicheportiche R, Burger D, Pernin A, Cuenod-Pittet B, Quinodoz P, Giusti V, Dayer JM, and Meier CA.** Regulatory effects of interleukin (IL)-1, interferon-beta, and IL-4 on the production of IL-1 receptor antagonist by human adipose tissue. *J Clin Endocrinol Metab* 89: 2652-2658, 2004.
104. **Kahn BB.** Lilly lecture 1995. Glucose transport: pivotal step in insulin action. *Diabetes* 45: 1644-1654, 1996.
105. **Kamari Y, Shaish A, Vax E, Shemesh S, Kandel-Kfir M, Arbel Y, Olteanu S, Barshack I, Dotan S, Voronov E, Dinarello CA, Apte RN, and Harats D.** Lack of interleukin-1alpha or interleukin-1beta inhibits transformation of steatosis to steatohepatitis and liver fibrosis in hypercholesterolemic mice. *J Hepatol* 55: 1086-1094, 2011.
106. **Kamari Y, Werman-Venkert R, Shaish A, Werman A, Harari A, Gonen A, Voronov E, Grosskopf I, Sharabi Y, Grossman E, Iwakura Y, Dinarello CA, Apte RN, and Harats D.** Differential role and tissue specificity of interleukin-1alpha gene expression in atherogenesis and lipid metabolism. *Atherosclerosis* 195: 31-38, 2007.
107. **Kamei N, Tobe K, Suzuki R, Ohsugi M, Watanabe T, Kubota N, Ohtsuka-Kowatari N, Kumagai K, Sakamoto K, Kobayashi M, Yamauchi T, Ueki K, Oishi Y, Nishimura S, Manabe I, Hashimoto H, Ohnishi Y, Ogata H, Tokuyama K, Tsunoda M, Ide T, Murakami K, Nagai R, and Kadowaki T.** Overexpression of monocyte chemoattractant protein-1 in adipose tissues causes macrophage recruitment and insulin resistance. *J Biol Chem* 281: 26602-26614, 2006.
108. **Kanda H, Tateya S, Tamori Y, Kotani K, Hiasa K, Kitazawa R, Kitazawa S, Miyachi H, Maeda S, Egashira K, and Kasuga M.** MCP-1 contributes to macrophage infiltration into adipose tissue, insulin resistance, and hepatic steatosis in obesity. *J Clin Invest* 116: 1494-1505, 2006.
109. **Kaneto H, Xu G, Fujii N, Kim S, Bonner-Weir S, and Weir GC.** Involvement of c-Jun N-terminal kinase in oxidative stress-mediated suppression of insulin gene expression. *J Biol Chem* 277: 30010-30018, 2002.
110. **Kershaw EE and Flier JS.** Adipose tissue as an endocrine organ. *J Clin Endocrinol Metab* 89: 2548-2556, 2004.
111. **Kersten S.** Mechanisms of nutritional and hormonal regulation of lipogenesis. *EMBO Rep* 2: 282-286, 2001.
112. **Kim JK, Kim YJ, Fillmore JJ, Chen Y, Moore I, Lee J, Yuan M, Li ZW, Karin M, Perret P, Shoelson SE, and Shulman GI.** Prevention of fat-induced insulin resistance by salicylate. *J Clin Invest* 108: 437-446, 2001.

113. **Kim JY, van de Wall E, Laplante M, Azzara A, Trujillo ME, Hofmann SM, Schraw T, Durand JL, Li H, Li G, Jelicks LA, Mehler MF, Hui DY, Deshaies Y, Shulman GI, Schwartz GJ, and Scherer PE.** Obesity-associated improvements in metabolic profile through expansion of adipose tissue. *J Clin Invest* 117: 2621-2637, 2007.
114. **Kinoshita M, Uchida T, Sato A, Nakashima M, Nakashima H, Shono S, Habu Y, Miyazaki H, Hiroi S, and Seki S.** Characterization of two F4/80-positive Kupffer cell subsets by their function and phenotype in mice. *J Hepatol* 53: 903-910, 2010.
115. **Kintscher U, Hartge M, Hess K, Foryst-Ludwig A, Clemenz M, Wabitsch M, Fischer-Posovszky P, Barth TF, Dragun D, Skurk T, Hauner H, Bluher M, Unger T, Wolf AM, Knippschild U, Hombach V, and Marx N.** T-lymphocyte infiltration in visceral adipose tissue: a primary event in adipose tissue inflammation and the development of obesity-mediated insulin resistance. *Arterioscler Thromb Vasc Biol* 28: 1304-1310, 2008.
116. **Kolditz CI and Langin D.** Adipose tissue lipolysis. *Curr Opin Clin Nutr Metab Care* 13: 377-381, 2010.
117. **Kopp E and Ghosh S.** Inhibition of NF-kappa B by sodium salicylate and aspirin. *Science* 265: 956-959, 1994.
118. **Kosteli A, Sugaru E, Haemmerle G, Martin JF, Lei J, Zechner R, and Ferrante AW, Jr.** Weight loss and lipolysis promote a dynamic immune response in murine adipose tissue. *J Clin Invest* 120: 3466-3479, 2010.
119. **Kruger DF, Aronoff SL, and Edelman SV.** Through the looking glass: current and future perspectives on the role of hormonal interplay in glucose homeostasis. *Diabetes Educ* 33 Suppl 2: 32S-46S; quiz 47S-48S, 2007.
120. **Ladyman SR and Grattan DR.** JAK-STAT and feeding. *JAKSTAT* 2: e23675, 2013.
121. **Lafontan M.** Advances in adipose tissue metabolism. *Int J Obes (Lond)* 32 Suppl 7: S39-51, 2008.
122. **Lagathu C, Yvan-Charvet L, Bastard JP, Maachi M, Quignard-Boulange A, Capeau J, and Caron M.** Long-term treatment with interleukin-1beta induces insulin resistance in murine and human adipocytes. *Diabetologia* 49: 2162-2173, 2006.
123. **Lamacchia C, Palmer G, Bischoff L, Rodriguez E, Talabot-Ayer D, and Gabay C.** Distinct roles of hepatocyte- and myeloid cell-derived IL-1 receptor antagonist during endotoxemia and sterile inflammation in mice. *J Immunol* 185: 2516-2524, 2010.
124. **Lanthier N, Molendi-Coste O, Cani PD, van Rooijen N, Horsmans Y, and Leclercq IA.** Kupffer cell depletion prevents but has no therapeutic effect on metabolic and inflammatory changes induced by a high-fat diet. *FASEB J* 25: 4301-4311, 2011.
125. **Larsen CM, Faulenbach M, Vaag A, Ehses JA, Donath MY, and Mandrup-Poulsen T.** Sustained effects of interleukin-1 receptor antagonist treatment in type 2 diabetes. *Diabetes Care* 32: 1663-1668, 2009.
126. **Lee GH, Proenca R, Montez JM, Carroll KM, Darvishzadeh JG, Lee JI, and Friedman JM.** Abnormal splicing of the leptin receptor in diabetic mice. *Nature* 379: 632-635, 1996.
127. **Lee J and Pilch PF.** The insulin receptor: structure, function, and signaling. *Am J Physiol* 266: C319-334, 1994.
128. **Lee YS, Li P, Huh JY, Hwang IJ, Lu M, Kim JI, Ham M, Talukdar S, Chen A, Lu WJ, Bandyopadhyay GK, Schwendener R, Olefsky J, and Kim JB.** Inflammation is necessary for long-term but not short-term high-fat diet-induced insulin resistance. *Diabetes* 60: 2474-2483, 2011.

129. **Leroux A, Ferrere G, Godie V, Cailleux F, Renoud ML, Gaudin F, Naveau S, Prevot S, Makhzami S, Perlemuter G, and Cassard-Doulcier AM.** Toxic lipids stored by Kupffer cells correlates with their pro-inflammatory phenotype at an early stage of steatohepatitis. *J Hepatol* 57: 141-149, 2012.
130. **Li S, Sun Y, Liang CP, Thorp EB, Han S, Jehle AW, Saraswathi V, Pridgen B, Kanter JE, Li R, Welch CL, Hasty AH, Bornfeldt KE, Breslow JL, Tabas I, and Tall AR.** Defective phagocytosis of apoptotic cells by macrophages in atherosclerotic lesions of ob/ob mice and reversal by a fish oil diet. *Circ Res* 105: 1072-1082, 2009.
131. **Liang G, Yang J, Horton JD, Hammer RE, Goldstein JL, and Brown MS.** Diminished hepatic response to fasting/refeeding and liver X receptor agonists in mice with selective deficiency of sterol regulatory element-binding protein-1c. *J Biol Chem* 277: 9520-9528, 2002.
132. **Liu J, Divoux A, Sun J, Zhang J, Clement K, Glickman JN, Sukhova GK, Wolters PJ, Du J, Gorgun CZ, Doria A, Libby P, Blumberg RS, Kahn BB, Hotamisligil GS, and Shi GP.** Genetic deficiency and pharmacological stabilization of mast cells reduce diet-induced obesity and diabetes in mice. *Nat Med* 15: 940-945, 2009.
133. **Lu YC, Yeh WC, and Ohashi PS.** LPS/TLR4 signal transduction pathway. *Cytokine* 42: 145-151, 2008.
134. **Lumeng CN.** Innate immune activation in obesity. *Mol Aspects Med* 34: 12-29, 2013.
135. **Lumeng CN, Bodzin JL, and Saltiel AR.** Obesity induces a phenotypic switch in adipose tissue macrophage polarization. *J Clin Invest* 117: 175-184, 2007.
136. **Lumeng CN, DelProposto JB, Westcott DJ, and Saltiel AR.** Phenotypic switching of adipose tissue macrophages with obesity is generated by spatiotemporal differences in macrophage subtypes. *Diabetes* 57: 3239-3246, 2008.
137. **Lumeng CN, Deyoung SM, Bodzin JL, and Saltiel AR.** Increased inflammatory properties of adipose tissue macrophages recruited during diet-induced obesity. *Diabetes* 56: 16-23, 2007.
138. **MacEwan DJ.** TNF receptor subtype signalling: differences and cellular consequences. *Cell Signal* 14: 477-492, 2002.
139. **Madsen DH and Bugge TH.** Imaging collagen degradation in vivo highlights a key role for M2-polarized macrophages in extracellular matrix degradation. *Oncoimmunology* 2: e27127, 2013.
140. **Mantovani A, Sica A, Sozzani S, Allavena P, Vecchi A, and Locati M.** The chemokine system in diverse forms of macrophage activation and polarization. *Trends Immunol* 25: 677-686, 2004.
141. **Mao J, DeMayo FJ, Li H, Abu-Elheiga L, Gu Z, Shaikenov TE, Kordari P, Chirala SS, Heird WC, and Wakil SJ.** Liver-specific deletion of acetyl-CoA carboxylase 1 reduces hepatic triglyceride accumulation without affecting glucose homeostasis. *Proc Natl Acad Sci U S A* 103: 8552-8557, 2006.
142. **Martinez FO, Sica A, Mantovani A, and Locati M.** Macrophage activation and polarization. *Front Biosci* 13: 453-461, 2008.
143. **McGarry JD.** What if Minkowski had been ageusic? An alternative angle on diabetes. *Science* 258: 766-770, 1992.
144. **McGillicuddy FC, Harford KA, Reynolds CM, Oliver E, Claessens M, Mills KH, and Roche HM.** Lack of interleukin-1 receptor I (IL-1RI) protects mice from high-fat diet-induced adipose tissue inflammation coincident with improved glucose homeostasis. *Diabetes* 60: 1688-1698, 2011.

145. **Meier CA, Bobbioni E, Gabay C, Assimacopoulos-Jeannet F, Golay A, and Dayer JM.** IL-1 receptor antagonist serum levels are increased in human obesity: a possible link to the resistance to leptin? *J Clin Endocrinol Metab* 87: 1184-1188, 2002.
146. **Minokoshi Y, Haque MS, and Shimazu T.** Microinjection of leptin into the ventromedial hypothalamus increases glucose uptake in peripheral tissues in rats. *Diabetes* 48: 287-291, 1999.
147. **Minokoshi Y, Kim YB, Peroni OD, Fryer LG, Muller C, Carling D, and Kahn BB.** Leptin stimulates fatty-acid oxidation by activating AMP-activated protein kinase. *Nature* 415: 339-343, 2002.
148. **Miyazaki M, Flowers MT, Sampath H, Chu K, Otzelberger C, Liu X, and Ntambi JM.** Hepatic stearoyl-CoA desaturase-1 deficiency protects mice from carbohydrate-induced adiposity and hepatic steatosis. *Cell Metab* 6: 484-496, 2007.
149. **Miyazaki Y, Mahankali A, Matsuda M, Mahankali S, Hardies J, Cusi K, Mandarino LJ, and DeFronzo RA.** Effect of pioglitazone on abdominal fat distribution and insulin sensitivity in type 2 diabetic patients. *J Clin Endocrinol Metab* 87: 2784-2791, 2002.
150. **Moitra J, Mason MM, Olive M, Krylov D, Gavrilova O, Marcus-Samuels B, Feigenbaum L, Lee E, Aoyama T, Eckhaus M, Reitman ML, and Vinson C.** Life without white fat: a transgenic mouse. *Genes Dev* 12: 3168-3181, 1998.
151. **Moller DE.** Transgenic approaches to the pathogenesis of NIDDM. *Diabetes* 43: 1394-1401, 1994.
152. **Morioka T, Asilmaz E, Hu J, Dishinger JF, Kurpad AJ, Elias CF, Li H, Elmquist JK, Kennedy RT, and Kulkarni RN.** Disruption of leptin receptor expression in the pancreas directly affects beta cell growth and function in mice. *J Clin Invest* 117: 2860-2868, 2007.
153. **Moschen AR, Molnar C, Enrich B, Geiger S, Ebenbichler CF, and Tilg H.** Adipose and liver expression of interleukin (IL)-1 family members in morbid obesity and effects of weight loss. *Mol Med* 17: 840-845, 2011.
154. **Nakae J, Kitamura T, Kitamura Y, Biggs WH, 3rd, Arden KC, and Accili D.** The forkhead transcription factor Foxo1 regulates adipocyte differentiation. *Dev Cell* 4: 119-129, 2003.
155. **Nakatani Y, Kaneto H, Kawamori D, Hatazaki M, Miyatsuka T, Matsuoka TA, Kajimoto Y, Matsuhisa M, Yamasaki Y, and Hori M.** Modulation of the JNK pathway in liver affects insulin resistance status. *J Biol Chem* 279: 45803-45809, 2004.
156. **Nawrocki AR, Rajala MW, Tomas E, Pajvani UB, Saha AK, Trumbauer ME, Pang Z, Chen AS, Ruderman NB, Chen H, Rossetti L, and Scherer PE.** Mice lacking adiponectin show decreased hepatic insulin sensitivity and reduced responsiveness to peroxisome proliferator-activated receptor gamma agonists. *J Biol Chem* 281: 2654-2660, 2006.
157. **Necela BM, Su W, and Thompson EA.** Toll-like receptor 4 mediates cross-talk between peroxisome proliferator-activated receptor gamma and nuclear factor-kappaB in macrophages. *Immunology* 125: 344-358, 2008.
158. **Neuschwander-Tetri BA, Brunt EM, Wehmeier KR, Oliver D, and Bacon BR.** Improved nonalcoholic steatohepatitis after 48 weeks of treatment with the PPAR-gamma ligand rosiglitazone. *Hepatology* 38: 1008-1017, 2003.
159. **Nguyen MT, Favelyukis S, Nguyen AK, Reichart D, Scott PA, Jenn A, Liu-Bryan R, Glass CK, Neels JG, and Olefsky JM.** A subpopulation of macrophages infiltrates hypertrophic adipose tissue and is activated by free fatty acids via Toll-like receptors 2 and 4 and JNK-dependent pathways. *J Biol Chem* 282: 35279-35292, 2007.

160. **Nguyen MT, Satoh H, Favelyukis S, Babendure JL, Imamura T, Sbodio JI, Zalevsky J, Dahiyat BI, Chi NW, and Olefsky JM.** JNK and tumor necrosis factor-alpha mediate free fatty acid-induced insulin resistance in 3T3-L1 adipocytes. *J Biol Chem* 280: 35361-35371, 2005.
161. **Nielsen S, Guo Z, Johnson CM, Hensrud DD, and Jensen MD.** Splanchnic lipolysis in human obesity. *J Clin Invest* 113: 1582-1588, 2004.
162. **Nishimura S, Manabe I, Nagasaki M, Eto K, Yamashita H, Ohsugi M, Otsu M, Hara K, Ueki K, Sugiura S, Yoshimura K, Kadowaki T, and Nagai R.** CD8+ effector T cells contribute to macrophage recruitment and adipose tissue inflammation in obesity. *Nat Med* 15: 914-920, 2009.
163. **Nishimura S, Manabe I, Takaki S, Nagasaki M, Otsu M, Yamashita H, Sugita J, Yoshimura K, Eto K, Komuro I, Kadowaki T, and Nagai R.** Adipose Natural Regulatory B Cells Negatively Control Adipose Tissue Inflammation. *Cell Metab*, 2013.
164. **Nonogaki K, Fuller GM, Fuentes NL, Moser AH, Staprans I, Grunfeld C, and Feingold KR.** Interleukin-6 stimulates hepatic triglyceride secretion in rats. *Endocrinology* 136: 2143-2149, 1995.
165. **Nov O, Kohl A, Lewis EC, Bashan N, Dvir I, Ben-Shlomo S, Fishman S, Wueest S, Konrad D, and Rudich A.** Interleukin-1beta may mediate insulin resistance in liver-derived cells in response to adipocyte inflammation. *Endocrinology* 151: 4247-4256, 2010.
166. **Obstfeld AE, Sugaru E, Thearle M, Francisco AM, Gayet C, Ginsberg HN, Ables EV, and Ferrante AW, Jr.** C-C chemokine receptor 2 (CCR2) regulates the hepatic recruitment of myeloid cells that promote obesity-induced hepatic steatosis. *Diabetes* 59: 916-925, 2010.
167. **Odegaard JI and Chawla A.** Alternative macrophage activation and metabolism. *Annu Rev Pathol* 6: 275-297, 2011.
168. **Odegaard JI, Ricardo-Gonzalez RR, Goforth MH, Morel CR, Subramanian V, Mukundan L, Red Eagle A, Vats D, Brombacher F, Ferrante AW, and Chawla A.** Macrophage-specific PPARgamma controls alternative activation and improves insulin resistance. *Nature* 447: 1116-1120, 2007.
169. **Ofei F, Hurel S, Newkirk J, Sopwith M, and Taylor R.** Effects of an engineered human anti-TNF-alpha antibody (CDP571) on insulin sensitivity and glycemic control in patients with NIDDM. *Diabetes* 45: 881-885, 1996.
170. **Oh DY, Morinaga H, Talukdar S, Bae EJ, and Olefsky JM.** Increased macrophage migration into adipose tissue in obese mice. *Diabetes* 61: 346-354, 2012.
171. **Oh KJ, Han HS, Kim MJ, and Koo SH.** Transcriptional regulators of hepatic gluconeogenesis. *Arch Pharm Res* 36: 189-200, 2013.
172. **Ohmura K, Ishimori N, Ohmura Y, Tokuhara S, Nozawa A, Horii S, Andoh Y, Fujii S, Iwabuchi K, Onoe K, and Tsutsui H.** Natural killer T cells are involved in adipose tissues inflammation and glucose intolerance in diet-induced obese mice. *Arterioscler Thromb Vasc Biol* 30: 193-199, 2010.
173. **Olefsky JM and Glass CK.** Macrophages, inflammation, and insulin resistance. *Annu Rev Physiol* 72: 219-246, 2010.
174. **Osborn O, Brownell SE, Sanchez-Alavez M, Salomon D, Gram H, and Bartfai T.** Treatment with an Interleukin 1 beta antibody improves glycemic control in diet-induced obesity. *Cytokine* 44: 141-148, 2008.
175. **Osborn O, Sears DD, and Olefsky JM.** Fat-induced inflammation unchecked. *Cell Metab* 12: 553-554, 2010.

176. **Ozcan U, Cao Q, Yilmaz E, Lee AH, Iwakoshi NN, Ozdelen E, Tuncman G, Gorgun C, Glimcher LH, and Hotamisligil GS.** Endoplasmic reticulum stress links obesity, insulin action, and type 2 diabetes. *Science* 306: 457-461, 2004.
177. **Pang C, Gao Z, Yin J, Zhang J, Jia W, and Ye J.** Macrophage infiltration into adipose tissue may promote angiogenesis for adipose tissue remodeling in obesity. *Am J Physiol Endocrinol Metab* 295: E313-322, 2008.
178. **Paquot N, Castillo MJ, Lefebvre PJ, and Scheen AJ.** No increased insulin sensitivity after a single intravenous administration of a recombinant human tumor necrosis factor receptor: Fc fusion protein in obese insulin-resistant patients. *J Clin Endocrinol Metab* 85: 1316-1319, 2000.
179. **Patsouris D, Li PP, Thapar D, Chapman J, Olefsky JM, and Neels JG.** Ablation of CD11c-positive cells normalizes insulin sensitivity in obese insulin resistant animals. *Cell Metab* 8: 301-309, 2008.
180. **Paz K, Hemi R, LeRoith D, Karasik A, Elhanany E, Kanety H, and Zick Y.** A molecular basis for insulin resistance. Elevated serine/threonine phosphorylation of IRS-1 and IRS-2 inhibits their binding to the juxtamembrane region of the insulin receptor and impairs their ability to undergo insulin-induced tyrosine phosphorylation. *J Biol Chem* 272: 29911-29918, 1997.
181. **Petrasek J, Bala S, Csak T, Lippai D, Kodys K, Menashy V, Barrieau M, Min SY, Kurt-Jones EA, and Szabo G.** IL-1 receptor antagonist ameliorates inflammasome-dependent alcoholic steatohepatitis in mice. *J Clin Invest* 122: 3476-3489, 2012.
182. **Pilch PF and Czech MP.** Hormone binding alters the conformation of the insulin receptor. *Science* 210: 1152-1153, 1980.
183. **Pilkis SJ and Granner DK.** Molecular physiology of the regulation of hepatic gluconeogenesis and glycolysis. *Annu Rev Physiol* 54: 885-909, 1992.
184. **Poradzka A, Wronski J, Jasik M, Karnafel W, and Fiedor P.** Insulin replacement therapy in patients with type 1 diabetes by isolated pancreatic islet transplantation. *Acta Pol Pharm* 70: 943-950, 2013.
185. **Postic C, Dentin R, and Girard J.** Role of the liver in the control of carbohydrate and lipid homeostasis. *Diabetes Metab* 30: 398-408, 2004.
186. **Postic C and Girard J.** Contribution of de novo fatty acid synthesis to hepatic steatosis and insulin resistance: lessons from genetically engineered mice. *J Clin Invest* 118: 829-838, 2008.
187. **Powelka AM, Seth A, Virbasius JV, Kiskinis E, Nicoloro SM, Guilherme A, Tang X, Straubhaar J, Cherniack AD, Parker MG, and Czech MP.** Suppression of oxidative metabolism and mitochondrial biogenesis by the transcriptional corepressor RIP140 in mouse adipocytes. *J Clin Invest* 116: 125-136, 2006.
188. **Prieur X, Mok CY, Velagapudi VR, Nunez V, Fuentes L, Montaner D, Ishikawa K, Camacho A, Barbarroja N, O'Rahilly S, Sethi JK, Dopazo J, Oresic M, Ricote M, and Vidal-Puig A.** Differential lipid partitioning between adipocytes and tissue macrophages modulates macrophage lipotoxicity and M2/M1 polarization in obese mice. *Diabetes* 60: 797-809, 2011.
189. **Promrat K, Lutchman G, Uwaifo GI, Freedman RJ, Soza A, Heller T, Doo E, Ghany M, Premkumar A, Park Y, Liang TJ, Yanovski JA, Kleiner DE, and Hoofnagle JH.** A pilot study of pioglitazone treatment for nonalcoholic steatohepatitis. *Hepatology* 39: 188-196, 2004.
190. **Puigserver P, Rhee J, Donovan J, Walkey CJ, Yoon JC, Oriente F, Kitamura Y, Altomonte J, Dong H, Accili D, and Spiegelman BM.** Insulin-regulated hepatic gluconeogenesis through FOXO1-PGC-1alpha interaction. *Nature* 423: 550-555, 2003.

191. **Ramkhelawon B, Hennessy EJ, Menager M, Ray TD, Sheedy FJ, Hutchison S, Wanschel A, Oldebeken S, Geoffrion M, Spiro W, Miller G, McPherson R, Rayner KJ, and Moore KJ.** Netrin-1 promotes adipose tissue macrophage retention and insulin resistance in obesity. *Nat Med*, 2014.
192. **Rangwala SM and Lazar MA.** Peroxisome proliferator-activated receptor gamma in diabetes and metabolism. *Trends Pharmacol Sci* 25: 331-336, 2004.
193. **Richter EA and Hargreaves M.** Exercise, GLUT4, and skeletal muscle glucose uptake. *Physiol Rev* 93: 993-1017, 2013.
194. **Rider P, Carmi Y, Guttman O, Braiman A, Cohen I, Voronov E, White MR, Dinarello CA, and Apte RN.** IL-1alpha and IL-1beta recruit different myeloid cells and promote different stages of sterile inflammation. *J Immunol* 187: 4835-4843, 2011.
195. **Rodriguez-Hernandez H, Simental-Mendia LE, Rodriguez-Ramirez G, and Reyes-Romero MA.** Obesity and inflammation: epidemiology, risk factors, and markers of inflammation. *Int J Endocrinol* 2013: 678159, 2013.
196. **Romeo GR, Lee J, and Shoelson SE.** Metabolic syndrome, insulin resistance, and roles of inflammation--mechanisms and therapeutic targets. *Arterioscler Thromb Vasc Biol* 32: 1771-1776, 2012.
197. **Rosen ED and Spiegelman BM.** Adipocytes as regulators of energy balance and glucose homeostasis. *Nature* 444: 847-853, 2006.
198. **Ross SE, Erickson RL, Gerin I, DeRose PM, Bajnok L, Longo KA, Misek DE, Kuick R, Hanash SM, Atkins KB, Andresen SM, Nebb HI, Madsen L, Kristiansen K, and MacDougald OA.** Microarray analyses during adipogenesis: understanding the effects of Wnt signaling on adipogenesis and the roles of liver X receptor alpha in adipocyte metabolism. *Mol Cell Biol* 22: 5989-5999, 2002.
199. **Roth Flach RJ, Matevossian A, Akie TE, Negrin KA, Paul MT, and Czech MP.** beta3-Adrenergic receptor stimulation induces E-selectin-mediated adipose tissue inflammation. *J Biol Chem* 288: 2882-2892, 2013.
200. **Sabio G and Davis RJ.** cJun NH2-terminal kinase 1 (JNK1): roles in metabolic regulation of insulin resistance. *Trends Biochem Sci* 35: 490-496, 2010.
201. **Saleh J, Sniderman AD, and Cianflone K.** Regulation of Plasma fatty acid metabolism. *Clin Chim Acta* 286: 163-180, 1999.
202. **Saltiel AR.** You are what you secrete. *Nat Med* 7: 887-888, 2001.
203. **Saltiel AR and Kahn CR.** Insulin signalling and the regulation of glucose and lipid metabolism. *Nature* 414: 799-806, 2001.
204. **Sartipy P and Loskutoff DJ.** Monocyte chemoattractant protein 1 in obesity and insulin resistance. *Proc Natl Acad Sci U S A* 100: 7265-7270, 2003.
205. **Sauter NS, Schulthess FT, Galasso R, Castellani LW, and Maedler K.** The antiinflammatory cytokine interleukin-1 receptor antagonist protects from high-fat diet-induced hyperglycemia. *Endocrinology* 149: 2208-2218, 2008.
206. **Savage DB, Choi CS, Samuel VT, Liu ZX, Zhang D, Wang A, Zhang XM, Cline GW, Yu XX, Geisler JG, Bhanot S, Monia BP, and Shulman GI.** Reversal of diet-induced hepatic steatosis and hepatic insulin resistance by antisense oligonucleotide inhibitors of acetyl-CoA carboxylases 1 and 2. *J Clin Invest* 116: 817-824, 2006.
207. **Schaffer JE.** Lipotoxicity: when tissues overeat. *Curr Opin Lipidol* 14: 281-287, 2003.

208. **Schmidt AM.** Insulin resistance and metabolic syndrome: mechanisms and consequences. *Arterioscler Thromb Vasc Biol* 32: 1753, 2012.
209. **Semenkovich CF.** TZDs and diabetes: testing the waters. *Nat Med* 11: 822-824, 2005.
210. **Shaul ME, Bennett G, Strissel KJ, Greenberg AS, and Obin MS.** Dynamic, M2-like remodeling phenotypes of CD11c+ adipose tissue macrophages during high-fat diet--induced obesity in mice. *Diabetes* 59: 1171-1181, 2010.
211. **Shi H, Kokoeva MV, Inouye K, Tzameli I, Yin H, and Flier JS.** TLR4 links innate immunity and fatty acid-induced insulin resistance. *J Clin Invest* 116: 3015-3025, 2006.
212. **Shimabukuro M, Zhou YT, Levi M, and Unger RH.** Fatty acid-induced beta cell apoptosis: a link between obesity and diabetes. *Proc Natl Acad Sci U S A* 95: 2498-2502, 1998.
213. **Shimomura I, Shimano H, Korn BS, Bashmakov Y, and Horton JD.** Nuclear sterol regulatory element-binding proteins activate genes responsible for the entire program of unsaturated fatty acid biosynthesis in transgenic mouse liver. *J Biol Chem* 273: 35299-35306, 1998.
214. **Shoelson SE, Herrero L, and Naaz A.** Obesity, inflammation, and insulin resistance. *Gastroenterology* 132: 2169-2180, 2007.
215. **Shoelson SE, Lee J, and Goldfine AB.** Inflammation and insulin resistance. *J Clin Invest* 116: 1793-1801, 2006.
216. **Shoelson SE, Lee J, and Yuan M.** Inflammation and the IKK beta/I kappa B/NF-kappa B axis in obesity- and diet-induced insulin resistance. *Int J Obes Relat Metab Disord* 27 Suppl 3: S49-52, 2003.
217. **Smith CM, Marks AD, Lieberman MA, and Marks DB.** *Marks' basic medical biochemistry : a clinical approach*. Philadelphia: Lippincott Williams & Wilkins, 2005.
218. **Snijder MB, Visser M, Dekker JM, Goodpaster BH, Harris TB, Kritchevsky SB, De Rekeneire N, Kanaya AM, Newman AB, Tylavsky FA, and Seidell JC.** Low subcutaneous thigh fat is a risk factor for unfavourable glucose and lipid levels, independently of high abdominal fat. The Health ABC Study. *Diabetologia* 48: 301-308, 2005.
219. **Solinas G, Vilcu C, Neels JG, Bandyopadhyay GK, Luo JL, Naugler W, Grivennikov S, Wynshaw-Boris A, Scadeng M, Olefsky JM, and Karin M.** JNK1 in hematopoietically derived cells contributes to diet-induced inflammation and insulin resistance without affecting obesity. *Cell Metab* 6: 386-397, 2007.
220. **Somm E, Cettour-Rose P, Asensio C, Charollais A, Klein M, Theander-Carrillo C, Juge-Aubry CE, Dayer JM, Nicklin MJ, Meda P, Rohner-Jeanrenaud F, and Meier CA.** Interleukin-1 receptor antagonist is upregulated during diet-induced obesity and regulates insulin sensitivity in rodents. *Diabetologia* 49: 387-393, 2006.
221. **Souza SC, Palmer HJ, Kang YH, Yamamoto MT, Muliro KV, Paulson KE, and Greenberg AS.** TNF-alpha induction of lipolysis is mediated through activation of the extracellular signal related kinase pathway in 3T3-L1 adipocytes. *J Cell Biochem* 89: 1077-1086, 2003.
222. **Spranger J, Kroke A, Mohlig M, Hoffmann K, Bergmann MM, Ristow M, Boeing H, and Pfeiffer AF.** Inflammatory cytokines and the risk to develop type 2 diabetes: results of the prospective population-based European Prospective Investigation into Cancer and Nutrition (EPIC)-Potsdam Study. *Diabetes* 52: 812-817, 2003.
223. **Stienstra R, Joosten LA, Koenen T, van Tits B, van Diepen JA, van den Berg SA, Rensen PC, Voshol PJ, Fantuzzi G, Hijmans A, Kersten S, Muller M, van den Berg WB, van Rooijen N, Wabitsch M, Kullberg BJ, van der Meer JW, Kanneganti T, Tack CJ, and Netea MG.** The

inflammasome-mediated caspase-1 activation controls adipocyte differentiation and insulin sensitivity. *Cell Metab* 12: 593-605, 2010.

224. **Stienstra R, Saudale F, Duval C, Keshtkar S, Groener JE, van Rooijen N, Staels B, Kersten S, and Muller M.** Kupffer cells promote hepatic steatosis via interleukin-1beta-dependent suppression of peroxisome proliferator-activated receptor alpha activity. *Hepatology* 51: 511-522, 2010.

225. **Suganami T, Nishida J, and Ogawa Y.** A paracrine loop between adipocytes and macrophages aggravates inflammatory changes: role of free fatty acids and tumor necrosis factor alpha. *Arterioscler Thromb Vasc Biol* 25: 2062-2068, 2005.

226. **Summers SA.** Ceramides in insulin resistance and lipotoxicity. *Prog Lipid Res* 45: 42-72, 2006.

227. **Sun K, Kusminski CM, and Scherer PE.** Adipose tissue remodeling and obesity. *J Clin Invest* 121: 2094-2101, 2011.

228. **Sutherland C, O'Brien RM, and Granner DK.** New connections in the regulation of PEPCK gene expression by insulin. *Philos Trans R Soc Lond B Biol Sci* 351: 191-199, 1996.

229. **Szabo G and Csak T.** Inflammasomes in liver diseases. *J Hepatol* 57: 642-654, 2012.

230. **Tang X, Guilherme A, Chakladar A, Powelka AM, Konda S, Virbasius JV, Nicoloro SM, Straubhaar J, and Czech MP.** An RNA interference-based screen identifies MAP4K4/NIK as a negative regulator of PPARgamma, adipogenesis, and insulin-responsive hexose transport. *Proc Natl Acad Sci U S A* 103: 2087-2092, 2006.

231. **Taniguchi CM, Emanuelli B, and Kahn CR.** Critical nodes in signalling pathways: insights into insulin action. *Nat Rev Mol Cell Biol* 7: 85-96, 2006.

232. **Targher G, Bertolini L, Padovani R, Rodella S, Tessari R, Zenari L, Day C, and Arcaro G.** Prevalence of nonalcoholic fatty liver disease and its association with cardiovascular disease among type 2 diabetic patients. *Diabetes Care* 30: 1212-1218, 2007.

233. **Tesz GJ, Guilherme A, Guntur KV, Hubbard AC, Tang X, Chawla A, and Czech MP.** Tumor necrosis factor alpha (TNFalpha) stimulates Map4k4 expression through TNFalpha receptor 1 signaling to c-Jun and activating transcription factor 2. *J Biol Chem* 282: 19302-19312, 2007.

234. **Thorne A, Lonnqvist F, Apelman J, Hellers G, and Arner P.** A pilot study of long-term effects of a novel obesity treatment: omentectomy in connection with adjustable gastric banding. *Int J Obes Relat Metab Disord* 26: 193-199, 2002.

235. **Tran TT and Kahn CR.** Transplantation of adipose tissue and stem cells: role in metabolism and disease. *Nat Rev Endocrinol* 6: 195-213, 2010.

236. **Unger RH.** Lipotoxicity in the pathogenesis of obesity-dependent NIDDM. Genetic and clinical implications. *Diabetes* 44: 863-870, 1995.

237. **Uysal KT, Wiesbrock SM, Marino MW, and Hotamisligil GS.** Protection from obesity-induced insulin resistance in mice lacking TNF-alpha function. *Nature* 389: 610-614, 1997.

238. **Valasek MA and Repa JJ.** The power of real-time PCR. *Adv Physiol Educ* 29: 151-159, 2005.

239. **Van Rooijen N and Sanders A.** Liposome mediated depletion of macrophages: mechanism of action, preparation of liposomes and applications. *J Immunol Methods* 174: 83-93, 1994.

240. **Vane JR.** Inhibition of prostaglandin synthesis as a mechanism of action for aspirin-like drugs. *Nat New Biol* 231: 232-235, 1971.

241. **Ventre J, Doebber T, Wu M, MacNaul K, Stevens K, Pasparakis M, Kollias G, and Moller DE.** Targeted disruption of the tumor necrosis factor-alpha gene: metabolic consequences in obese and nonobese mice. *Diabetes* 46: 1526-1531, 1997.
242. **Vernia S, Cavanagh-Kyros J, Barrett T, Jung DY, Kim JK, and Davis RJ.** Diet-induced obesity mediated by the JNK/DIO2 signal transduction pathway. *Genes Dev* 27: 2345-2355, 2013.
243. **Virtue S and Vidal-Puig A.** Adipose tissue expandability, lipotoxicity and the Metabolic Syndrome--an allostatic perspective. *Biochim Biophys Acta* 1801: 338-349, 2010.
244. **Virtue S and Vidal-Puig A.** Assessment of brown adipose tissue function. *Front Physiol* 4: 128, 2013.
245. **Visser M, Bouter LM, McQuillan GM, Wener MH, and Harris TB.** Elevated C-reactive protein levels in overweight and obese adults. *JAMA* 282: 2131-2135, 1999.
246. **Waki H and Tontonoz P.** Endocrine functions of adipose tissue. *Annu Rev Pathol* 2: 31-56, 2007.
247. **Walther TC and Farese RV, Jr.** Lipid droplets and cellular lipid metabolism. *Annu Rev Biochem* 81: 687-714, 2012.
248. **Wang SP, Laurin N, Himms-Hagen J, Rudnicki MA, Levy E, Robert MF, Pan L, Oligny L, and Mitchell GA.** The adipose tissue phenotype of hormone-sensitive lipase deficiency in mice. *Obes Res* 9: 119-128, 2001.
249. **Wang Y, Beydoun MA, Liang L, Caballero B, and Kumanyika SK.** Will all Americans become overweight or obese? estimating the progression and cost of the US obesity epidemic. *Obesity (Silver Spring)* 16: 2323-2330, 2008.
250. **Weber A, Wasiliew P, and Kracht M.** Interleukin-1beta (IL-1beta) processing pathway. *Sci Signal* 3: cm2, 2010.
251. **Weisberg SP, Hunter D, Huber R, Lemieux J, Slaymaker S, Vaddi K, Charo I, Leibel RL, and Ferrante AW, Jr.** CCR2 modulates inflammatory and metabolic effects of high-fat feeding. *J Clin Invest* 116: 115-124, 2006.
252. **Weisberg SP, McCann D, Desai M, Rosenbaum M, Leibel RL, and Ferrante AW, Jr.** Obesity is associated with macrophage accumulation in adipose tissue. *J Clin Invest* 112: 1796-1808, 2003.
253. **Wellen KE and Hotamisligil GS.** Inflammation, stress, and diabetes. *J Clin Invest* 115: 1111-1119, 2005.
254. **Wen H, Gris D, Lei Y, Jha S, Zhang L, Huang MT, Brickey WJ, and Ting JP.** Fatty acid-induced NLRP3-ASC inflammasome activation interferes with insulin signaling. *Nat Immunol* 12: 408-415, 2011.
255. **Wentworth JM, Naselli G, Brown WA, Doyle L, Phipson B, Smyth GK, Wabitsch M, O'Brien PE, and Harrison LC.** Pro-inflammatory CD11c+CD206+ adipose tissue macrophages are associated with insulin resistance in human obesity. *Diabetes* 59: 1648-1656, 2010.
256. **White MF.** The IRS-signalling system: a network of docking proteins that mediate insulin action. *Mol Cell Biochem* 182: 3-11, 1998.
257. **White MF.** IRS proteins and the common path to diabetes. *Am J Physiol Endocrinol Metab* 283: E413-422, 2002.
258. **Williamson RT.** On the Treatment of Glycosuria and Diabetes Mellitus with Sodium Salicylate. *Br Med J* 1: 760-762, 1901.

259. **Winer S, Chan Y, Paltser G, Truong D, Tsui H, Bahrami J, Dorfman R, Wang Y, Zielenski J, Mastronardi F, Maezawa Y, Drucker DJ, Engleman E, Winer D, and Dosch HM.** Normalization of obesity-associated insulin resistance through immunotherapy. *Nat Med* 15: 921-929, 2009.
260. **Wu D, Molofsky AB, Liang HE, Ricardo-Gonzalez RR, Jouihan HA, Bando JK, Chawla A, and Locksley RM.** Eosinophils sustain adipose alternatively activated macrophages associated with glucose homeostasis. *Science* 332: 243-247, 2011.
261. **Xu H, Barnes GT, Yang Q, Tan G, Yang D, Chou CJ, Sole J, Nichols A, Ross JS, Tartaglia LA, and Chen H.** Chronic inflammation in fat plays a crucial role in the development of obesity-related insulin resistance. *J Clin Invest* 112: 1821-1830, 2003.
262. **Xu X, Grijalva A, Skowronski A, van Eijk M, Serlie MJ, and Ferrante AW, Jr.** Obesity activates a program of lysosomal-dependent lipid metabolism in adipose tissue macrophages independently of classic activation. *Cell Metab* 18: 816-830, 2013.
263. **Yao J, Mackman N, Edgington TS, and Fan ST.** Lipopolysaccharide induction of the tumor necrosis factor-alpha promoter in human monocytic cells. Regulation by Egr-1, c-Jun, and NF-kappaB transcription factors. *J Biol Chem* 272: 17795-17801, 1997.
264. **Yin MJ, Yamamoto Y, and Gaynor RB.** The anti-inflammatory agents aspirin and salicylate inhibit the activity of I(kappa)B kinase-beta. *Nature* 396: 77-80, 1998.
265. **Young JL, Mora A, Cerny A, Czech MP, Woda B, Kurt-Jones EA, Finberg RW, and Corvera S.** CD14 deficiency impacts glucose homeostasis in mice through altered adrenal tone. *PLoS One* 7: e29688, 2012.
266. **Yuan M, Konstantopoulos N, Lee J, Hansen L, Li ZW, Karin M, and Shoelson SE.** Reversal of obesity- and diet-induced insulin resistance with salicylates or targeted disruption of Ikkbeta. *Science* 293: 1673-1677, 2001.
267. **Zeyda M and Stulnig TM.** Obesity, inflammation, and insulin resistance--a mini-review. *Gerontology* 55: 379-386, 2009.
268. **Zhang HH, Halbleib M, Ahmad F, Manganiello VC, and Greenberg AS.** Tumor necrosis factor-alpha stimulates lipolysis in differentiated human adipocytes through activation of extracellular signal-related kinase and elevation of intracellular cAMP. *Diabetes* 51: 2929-2935, 2002.
269. **Zhang Y, Proenca R, Maffei M, Barone M, Leopold L, and Friedman JM.** Positional cloning of the mouse obese gene and its human homologue. *Nature* 372: 425-432, 1994.
270. **Zimmermann R, Lass A, Haemmerle G, and Zechner R.** Fate of fat: the role of adipose triglyceride lipase in lipolysis. *Biochim Biophys Acta* 1791: 494-500, 2009.